ROLE OF ENDOGENOUS IGFBP-3 IN MAMMARY EPITHELIAL CELL APOPTOSIS

By

ALLYSON M. AGOSTINI-DREYER

A Dissertation submitted to the

Graduate School - New Brunswick

Rutgers, The State University of New Jersey

in partial fulfillment of the requirements

for the degree of

Doctor of Philosophy

Graduate Program in Nutritional Sciences

written under the direction of

Dr. Wendie S. Cohick

and approved by

_____

_____

_____

_____

_____

New Brunswick, New Jersey

May 2014

ABSTRACT OF THE DISSERTATION

Role of Endogenous IGFBP-3 in Mammary Epithelial Cell Apoptosis

by ALLYSON M. AGOSTINI-DREYER

Dissertation Director:

Dr. Wendie S. Cohick

The overall goal of this work was to investigate a role for endogenous insulin-like growth factor binding protein-3 (IGFBP-3) in intrinsic apoptosis in non-transformed bovine mammary epithelial cells (MEC). IGFBP-3 was produced and secreted in response to anisomycin (ANS), an activator of the intrinsic apoptotic pathway. Knock-down of IGFBP-3 with small interfering (si)RNA attenuated ANS-induced apoptosis, establishing a role for IGFBP-3 in MEC apoptosis. A nuclear function for IGFBP-3 was suggested by findings from cell fractionation experiments showing that ANS induced nuclear accumulation of IGFBP-3. In MECs, knock-down of IGFBP-3 attenuated ANS-induced phosphorylation and nuclear export of the orphan nuclear receptor Nur77. Co-immunoprecipitation experiments revealed an association between IGFBP-3 and Nur77 in ANS-treated cells, but not in untreated controls, suggesting that IGFBP-3 exerts its nuclear effects through physical association with Nur77. A second goal of the thesis was to determine the mechanism by which IGFBP-3 localizes to the nucleus in bovine MEC. An inhibitor of endocytosis had no effect on nuclear localization of IGFBP-3 while an inhibitor of secretion enhanced nuclear IGFBP-3. Together these data indicate that nuclear IGFBP-3 does not arise from secreted IGFBP-3 that is re-internalized. Since the molecular weight of glycosylated IGFBP-3 is near the cut-off for passive diffusion through nuclear pores, IGFBP-3 was tagged with GFP in

order to determine if transport was a regulated process. ANS treatment of cells transfected with IGFBP-3-GFP increased the protein in the nucleus, indicating that nuclear import of IGFBP-3 is a regulated event. An antibody specific to bovine IGFBP-3 was generated to enable co-immunoprecipitation experiments. An association between IGFBP-3 and nuclear transport protein importin-β was found only in ANS-treated cells. Inhibition of importin-β attenuated nuclear import of IGFBP-3-GFP, establishing a role for importin-β in nuclear transport of IGFBP-3. In summary, these data indicate that nuclear localization of IGFBP-3 plays a role in intrinsic apoptosis in MEC and are the first to establish a mechanism for nuclear transport of *endogenous* IGFBP-3.

Acknowledgments

I have many people to thank for support and mentorship throughout my education. First, I would like thank my advisor and mentor Dr. Wendie Cohick who has provided countless hours of guidance and encouragement.

My committee members have provided thoughtful insight in the development and analysis of this work. I would like to thank Dr. Dawn Brasaemle, Dr. T.J. Thomas, Dr. Carol Bagnell, and Dr. Nicholas Bello for serving on my committee.

The members of the Cohick laboratory have provided me with scientific and moral support. I would especially like to thank Dr. Amanda E. Jetzt for her technical assistance and general laboratory expertise.

Finally I would like thank my family and friends for supporting me in all of my educational endeavors.

The work in this thesis was supported by National Research Initiative Competitive Grant no. 2009-35206-05210 from the USDA National Institute of Food and Agriculture.

Acknowledgment of previously published work

Chapter 2 of this dissertation, entitled "IGF binding protein-3 mediates stress-induced apoptosis in non-transformed mammary epithelial cells", was originally published in *Journal of Cellular Physiology* in April 2013. Allyson Agostini-Dreyer contributed figures 3, 7-9, and ½ each of figures 1, 2, 4, 5, 9. Allyson also contributed to editing and revisions of the manuscript.

The original article is reprinted with permission from:

> Leibowitz BJ, Agostini-Dreyer A, Jetzt AE, Krumm CS, Cohick WS. IGF binding protein-3 mediates stress-induced apoptosis in non-transformed mammary epithelial cells. *Journal of Cellular Physiology* 2013;228(4):734-742.

Table of Contents

List of Tables

List of Figures

List of abbreviations

Apaf-1	apoptotic protease activating factor-1
ANS	anisomycin
Bcl	B-cell lymphoma
BH	Bcl-homology
C2	ceramide
CHO	Chinese hamster ovary
CK-2	casein kinase-2
DISC	death-inducing signaling complex
DD	death domain
DED	death effector domain
DNAPK	DNA-dependent protein kinase
EGF	epidermal growth factor
Endo-H	endoglycosidase-H_f
ESCC	esophageal squamous cell carcinoma
FADD	Fas-associated death domain
GFP	green fluorescent protein
IGF-I	insulin-like growth factor-I
IGF-IR	IGF-I receptor
IGFBP	insulin-like growth factor binding protein
IHC	immunohistochemistry
IP	immunoprecipitation
MEC	mammary epithelial cell
MMP	matrix metalloproteinase
MOMP	mitochondrial outer membrane permeabilization
NES	nuclear export sequence
NLS	nuclear localization sequence
OVA	ovalbumin
PARP	poly ADP ribose polymerase
PC-3	prostate cancer cells
PC-12	pheochromocytoma cells
RXRα	retinoid-x-receptor-α
siRNA	small-interfering ribonucleic acid
SMAC/DIABLO	second-mitochondria-derived activator of caspase/direct IAP-binding protein with low PI
Tf/R	transferrin/transferrin receptor
TGF	transforming growth factor
TNF	tumor necrosis factor
TRAIL	TNF-related apoptosis-inducing ligand
U2-OS	osteosarcoma cell line
VEGF	vascular endothelial growth factor
VSMC	vascular smooth muscle cells
XIAP	x-linked inhibitor of apoptosis

Chapter 1.

Introduction and review of the literature

Introduction and significance

In the dairy cow, lactational output is a function of mammary epithelial cell number. Lactation peaks approximately 3-6 weeks after calving when secretory cell number and milk yield per cell have reached their peak (1). After peak yield is reached, yield per cell remains unchanged, however milk-secreting mammary epithelial cells begin to die off and milk output gradually declines (1). These data indicate that the decline in milk yield is attributed to decreased secretory cell number and not due to a change in output per cell. The period marking the rise in cell death and start of mammary gland remodeling is termed involution. During involution milk secreting cells gradually die off and the mammary gland returns to its pre-lactation state. In the case of the dairy cow, the animal is bred back and the mammary gland prepares for the next lactation period. The balance between survival and apoptotic signals determines lactation persistency, and altering this balance in favor of cellular survival has the potential to delay involution and increase total lactational yield.

Once milk production drops below a certain daily output, costs associated with animal maintenance outweigh profit from sale of the milk. This necessitates breeding the cow back at a certain time point so that she calves and reinitiates the lactation cycle before the loss in productivity is realized. Calving is associated with significant metabolic health issues that require costly veterinary care, therefore, practices that lead to enhanced lactation persistency will increase productive efficiency in dairy cows. Understanding basic mechanisms that delay apoptosis in the mammary gland will ultimately lead to practices that increase persistency and increase total lactation yield by prolonging secretory cell survival.

One factor known to positively affect cellular survival in the mammary gland is the mitogen insulin-like growth factor-I (IGF-I). IGF-I promotes proliferation in the mammary gland, warranting an investigation of the role of the IGF-axis in lactation and involution.

The IGF family consists of IGF-I, IGF-II, the IGF-IR, and six IGF binding proteins (IGFBPs). IGF-II functions primarily during gestation, while IGF-I exerts its effects pre- and post-natally (2,3). IGF-I binds its receptor at the cell surface to stimulate proliferation, differentiation, and cellular survival (4). The majority of circulating IGF-I is bound to IGFBP-3, which functions as a carrier protein, protecting IGF-I from serum proteases and preventing insulin-like effects of free IGF-I. The most abundant binding protein, IGFBP-3, functions to facilitate the proliferative effects of IGF-I by sequestering IGF-I in the bloodstream and releasing it to the IGF-I receptor (IGFR) in target tissues. At the cell surface IGFBP-3 can either enhance or inhibit the mitogenic effects of IGF-I. Interestingly, IGFBP-3 has been reported to bind cell surfaces to potentiate IGF-I signaling (5,6). However, an excess of IGFBP-3 in culture medium has also been shown to inhibit IGF-I-induced proliferation (7,8). This effect was initially attributed to the ability of IGFBP-3 to bind IGF-I and sequester it from its receptor, however, mutants of IGFBP-3 that do not bind IGF-I or IGF-II retain this anti-proliferative effect, supporting a role for IGFBP-3 in apoptosis that is independent of IGF-I (reviewed by Firth and Baxter (9)). The objective of this work is to examine the IGF-independent functions of IGFBP-3 in mammary epithelial cell (MEC) apoptosis.

Mechanisms of apoptosis

The balance between cellular survival and death is an important point of control in tissue development and homeostasis. Dysregulation of apoptosis can have pathological consequences. Resistance to apoptosis contributes to tumorigenesis as cells divide unchecked, while elevated rates of apoptosis are implicated in autoimmune and degenerative diseases (10).

The two primary pathways of apoptosis are extrinsic and intrinsic apoptosis. Extrinsic, or ligand-mediated, apoptosis is triggered by a ligand such as Fas-L binding its receptor at the cell surface, activating intracellular signaling to initiate cell death (11,12). Alternatively, intrinsic apoptosis is activated by a range of cell stressors that induce cytochrome-c release from the mitochondria (13,14). As demonstrated in Fig. 1, the two pathways converge on activation of caspases, which initiate the final stages of cell death. While intrinsic and extrinsic apoptosis are distinct pathways, there is evidence that crosstalk occurs and that the extrinsic pathway can activate the mitochondrial pathway to enhance the apoptotic response. Given the complexity of cell signaling in vivo it is probable that overlap occurs between intrinsic and extrinsic apoptosis during tissue remodeling. In MECs, IGFBP-3 is primarily indicated in intrinsic apoptosis so this work focuses on the intrinsic pathway.

Intrinsic pathway of apoptosis

Cellular stressors that induce the intrinsic pathway of apoptosis include growth factor withdrawal, UV-irradiation, heat shock, or chemical stressors such as chemotherapeutic agents. These stimuli promote mitochondrial permeabilization, facilitating the release of pro-apoptotic proteins basally sequestered in the mitochondria. Cytochrome-c release from the mitochondria

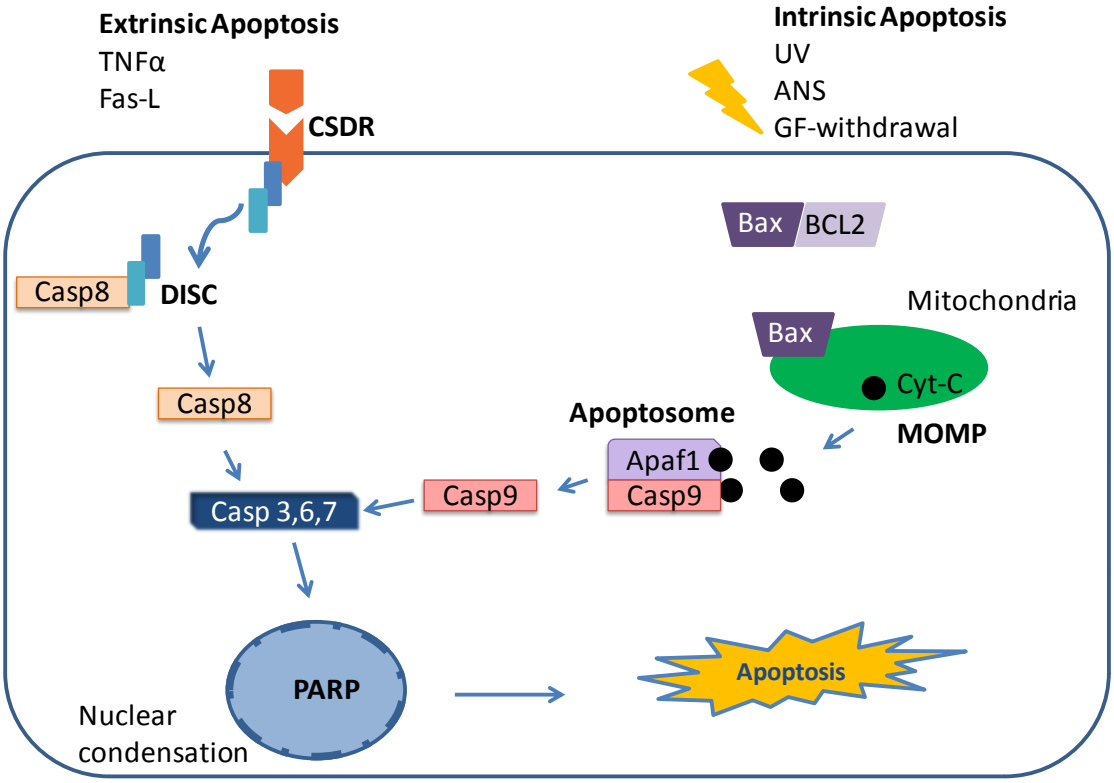

Fig. 1. Mechanisms of extrinsic and intrinsic apoptosis. Extrinsic apoptosis: Ligand binding activates cell surface death receptors (CSDR), initiating formation of a death induced signaling complex (DISC), composed of the receptor's death domain and caspase-8. Intrinsic apoptosis: Cellular stressors induce release of Bax from Bcl-2. Bax inserts into the outer mitochondrial membrane, causing mitochondrial outer membrane permeabilization (MOMP), and cytochrome c (Cyt-C) release. Cytochrome c associates with Apaf1 and caspase-9, forming the apoptosome. The two mechanisms converge on activation of effector caspases 3&7, which go on to cleave other intracellular proteins, including poly ADP ribose polymerase (PARP) and structural proteins, to promote apoptosis.

activates cysteine-dependent aspartate-directed proteases (caspases), which induce the final stages of cell death.

The Bcl-2 family of proteins contains over 20 members that function to regulate cell survival and apoptosis by regulating mitochondrial permeability and cytochrome-c release (15,16). These proteins contain between one and four Bcl-2 homology (BH) domains. Anti-apoptotic Bcl-2

members, including Bcl-2 and Bcl-X_L, and Mcl-1, typically have all four conserved Bcl-2 homology domains (BH1-4). Bcl-2 and Bcl-X_L inhibit apoptosis by inhibiting mitochondrial membrane pore formation. Pro-apoptotic members such as Bax and Bak have domains BH1-3. BH-3-only members such as Bid, Bim, and Bad simply possess the BH3 domain. BH-3-only proteins exert their effects indirectly by activating the pro-apoptotic Bcl-2 proteins and binding and sequestering pro-survival members.

In the absence of stress, mitogens exert their pro-survival effects in part through up-regulation of Bcl-2 and Bcl-X_L. IGF-I protects cells from apoptosis by up-regulating Bcl-2 and Bcl-X_L (17,18). Over-expression of these survival proteins results in resistance to apoptosis, and is associated with tumor progression, making the Bcl-2 family the target of chemotherapy treatments (19,20). In MCF-7 breast cancer cells IGF-II induces Bcl-2 and Bcl-X_L, and their expression is inhibited with the anti-tumor agent resveratrol (21). IGF-signaling also inhibits the pro-apoptotic protein Bad by inducing its phosphorylation so it can no longer bind and antagonize Bcl-2 or Bcl-X_L (19).

In response to stressors that activate the intrinsic apoptotic pathway, the survival Bcl-2 proteins are inhibited or down-regulated. Multiple stressors induce phosphorylation of Bcl-2 to inhibit its survival functions (22,23). The intrinsic stressor anisomycin (ANS) can also inhibit production of Bcl-2 to sensitize cells to apoptosis (24,25).

In contrast, the pro-apoptotic Bcl-2 members are activated by cellular stress. Bax localizes to the mitochondrial membrane where it oligomerizes with Bak to form mitochondrial pores, resulting in mitochondrial outer membrane permeabilization (MOMP). MOMP facilitates release of cytochrome-c and second mitochondria-derived activator of caspase (Smac/DIABLO)

(15,26-28). In the cytosol, Smac/DIABLO binds X-linked inhibitor of apoptosis (XIAP) to disrupt XIAP-caspase interactions and permit activation of caspases (29,30). Concurrently, cytochrome-c associates with apoptotic protease activating factor-1 (Apaf1) and pro-caspase-9, forming a complex titled the apoptosome (31). The association of these proteins converts caspase-9 to its active form, which then recruits and activates caspase-3 to initiate the final stages of apoptosis (32).

Caspases cleave a wide range of target proteins to execute the final stages of cell death. In the absence of stress caspases exist in their inactive zymogen forms. Cleavage of a pro-domain of the zymogen results in activation of their protease activity. Caspases 8 and 9 are initiator caspases and can auto-catalyze their own activation, first cleaving their pro-domains then cleaving and activating effector caspases (13,33). Caspases 3, 6, and 7 are classified as effector or executioner caspases for their roles in destruction of the cell. Protease activity of these active caspases includes cleavage of nuclear membrane proteins, DNA-repair enzymes, and the cytoskeleton, resulting in nuclear fragmentation and cell death. Effector caspases also cleave Bcl-2 and Bcl-X_L to inhibit their survival activity, and cleave and activate pro-apoptotic Bid and Bax to further shift the ratio of survival to apoptotic Bcl-2-family proteins in favor of cell death (12). Activation of the effector caspases marks the irreversible phase of apoptosis, as there is no mechanism to re-ligate proteins modified by these proteases.

Extrinsic pathway of apoptosis

The extrinsic pathway of apoptosis is initiated when cell surface death receptors are activated by their ligands. Fas-ligand (FasL), tumor necrosis factor (TNF), and TNF-related apoptosis-inducing ligand (TRAIL) bind Fas, TNFR, and TRAIL-R1-2, respectively (34). Each of the receptors

has an intracellular death domain (DD). Ligand binding results in recruitment of Fas-associated death domain (FADD) to the receptor DD (35). Pro-caspase-8 then uses its death effector domain (DED) to bind FADD. This DD-FADD-caspase-8 complex is termed the death-inducing signaling complex (DISC) (12,31). The DISC acts as a scaffold to facilitate dimerization and auto-activation of caspase-8. Active caspase-8 is released to cleave and activate effector caspases 3, 6, and 7. The effector caspases then effect nuclear membrane degradation, DNA fragmentation, and cell death. Interestingly, caspase-8 can also recruit the mitochondria at this stage by cleaving Bid to its active form, truncated Bid (tBid). tBid activates Bax, resulting in MOMP and eventual recruitment of the apoptosome (12,28). In TRAIL-induced apoptosis, recruitment of Bax for initiation of MOMP is also crucial for release of Smac/DIABLO (36). Smac/DIABLO disrupts XIAP inhibition of caspase-3 activation, and when Bax is knocked down caspase-3 remains inhibited and apoptosis is attenuated (36).

Apoptosis in the mammary gland

In the lactating mammary gland, net loss of milk secreting cells begins after peak yield is reached. While the apoptotic mechanisms leading to loss of MECs during mid to late lactation have not been investigated per se, the apoptotic process has been extensively studied during involution. At the local level, milk stasis contributes to initiation of apoptosis (37-39). Cessation of suckling leads to engorgement of the mammary gland with milk and causes structural changes in the milk-producing epithelial cells (37,39). These local events are thought to trigger the initial phases of involution. During late lactation the rate of apoptosis exceeds the rate of proliferation, resulting in a net loss of cells and a gradual return to a gland resembling a pre-pregnancy state (1).

Evidence of both apoptosis and autophagy is detected in the involuting mammary gland (40). It is hypothesized that there is a stress threshold that once reached signals cells to abandon the autophagic survival response in favor of cell death (41). Evidence for apoptosis in the involuting mammary gland includes increased expression of caspase-3, Bax, and Bak (42-45), and detection of cleaved PARP. Interestingly, pro-survival Bcl-2 is also up-regulated, however the ratio of apoptotic to survival proteins rises, favoring apoptosis (45). Initiation of apoptosis is accompanied by infiltration of macrophages for removal of dead cells and associated cellular debris. While epithelial cells can be shed into the milk, this accounts for removal of less than 2% of perished cells (1).

These data clearly indicate that apoptosis is occurring in the mammary gland. The molecular mechanisms that result in increased apoptotic Bcl-2 proteins and caspase activity remain unclear. Induction of involution clearly begins at the local level as milk stasis triggers functional and morphological changes in the gland. We propose that IGFBP-3 produced in the mammary gland has an apoptotic role and contributes to local regulation of cellular death.

IGFBP-3 and cellular fate

IGFBP-3 is a multi-faceted protein with functions in both proliferation and apoptosis. In circulation IGFBP-3 functions as a carrier protein, facilitating transport of IGF-I to its cell-surface receptor. However, IGFBP-3 is produced by most tissues and can act locally, exerting its effects directly or by modulating external stimuli. IGFBP-3 can either enhance or inhibit mitogenic stimuli to influence cellular proliferation. Additionally, IGFBP-3 functions in cell death by either directly inducing apoptosis or through indirect mechanisms by enhancing other cellular stressors. Multiple potential mechanisms, including binding IGF-I, caspase activation, and cellular localization are proposed to determine the biological function of IGFBP-3. While a role for IGFBP-3 is established in both proliferation and apoptosis, the molecular switch controlling the physiological function of IGFBP-3 remains unknown. Multiple potential mechanisms, including binding IGF-I, caspase activation, and cellular localization are proposed to influence the biological function of IGFBP-3.

Growth stimulatory effects of IGFBP-3

IGFBP-3 can promote survival by enhancing IGF-I signaling. Bovine MECs basally express low levels of IGFBP-3, however when transfected to over-express IGFBP-3 their sensitivity to IGF-I is enhanced (46,47). IGF-signaling induced by an IGF-I analogue with reduced affinity for IGFBPs is also enhanced by IGFBP-3 expression, indicating that IGFBP-3 potentiates IGF-I signaling independent of IGF-binding (46). In breast cancer cells, membrane-bound IGFBP-3 has an increased affinity for IGF-I that potentially helps tether IGF-I at the cell surface to promote IGF-IR binding (48). IGFBP-3 can also positively affect IGF-IR activation, which could contribute to survival of cancer cells and might explain the positive correlation between IGFBP-3 expression and cancer metastasis. In human embryonic vascular endothelial cells (HUVECs) IGFBP-3

induces expression and secretion of IGF-I, resulting in IGF-IR activation and angiogenesis (49). IGFBP-3 also enhances IGF-IR activation in IGF-I-treated breast epithelial cells (5,50). As in bovine MECs, IGFBP-3 potentiates IGF-IR activation induced by an IGF-I analogue with reduced affinity for IGFBPs, indicating this effect is independent of an association between IGFBP-3 and IGF-I (5,50). Interestingly, the mitogenic effects of IGFBP-3 were reversed when cells were plated on fibronectin to simulate a tumor microenviroment, suggesting that the function of IGFBP-3 is influenced by cellular environment (50). Involvement of sphingosine signaling elucidates a mechanism for IGFBP-3-mediated growth factor signaling independent of an interaction with IGF-I. IGFBP-3 indirectly enhances IGF-signaling and promotes cellular survival in HUVECs by activating sphingosine kinase-1, resulting in production of sphingosine-1-phosphate (S1P) (6,49). Work in the breast epithelial cell line MCF10-A shows that S1P can transactivate the IGF-IR, enhancing growth factor-induced proliferation (5). Thus, IGFBP-3 exerts its IGF-independent effects at least in part through up-regulation of S1P, resulting in transactivation of IGF-R.

IGFBP-3 also potentiates activation of the epidermal growth factor receptor (EGFR). In MCF10A normal human MECs, IGFBP-3 potentiates activation of EGFR by multiple ligands, including EGF, transforming growth factor (TGF) –α, and heregulin (51). Potentiation of EGF signaling results in enhanced proliferation of MCF10A cells (51). Pre-treatment with IGFBP-3 potentiates activation of ERK and AKT by EGFR ligands. This indicates that IGFBP-3 exerts its effects independent of binding to the ligands, but instead primes the EGFR for ligand-induced activation. IGFBP-3-induced S1P can transactivate both IGF-IR and EGFR, supporting a mechanism for EGFR priming by IGFBP-3 (5).

Apoptotic and growth inhibitory effects of IGFBP-3

Binding of IGFBP-3 to IGF-I can also have an antagonistic effect. In MCF10A cells, IGFBP-3 binds IGF-I to inhibit IGF-IR activation and prevent IGF-I-induced proliferation (8). In HUVECs, IGFBP-3 has similar anti-proliferative effects dependent on an N-terminal region containing the IGF-binding domain, suggesting that IGFBP-3 binds IGF-I to inhibit its mitogenic functions (52). IGFBP-3 also attenuates activation of IGF-IR by IGF-I in MCF-7 cells and inhibits IGF-I-stimulated proliferation in non-malignant human and bovine MECs (53-55). Induction of IGFBP-3 expression results in reduced activation of AKT by IGF-I, suggesting that IGFBP-3 binds IGF-I to prevent IGF-IR activation.

In addition to binding IGF-I, IGFBP-3 can modulate IGF-I expression and IGF-IR activation. Transgenic mice over-expressing IGFBP-3 show decreased prostate tumorigenesis (56). In these animals IGFBP-3 expression is associated with down-regulation of IGF-IR, EGFR, and increased apoptosis. Work in rats indicates that IGFBP-3 expression in non-small cell lung cancer xenografts attenuates IGF-signaling by inhibiting Bcl-2 expression, resulting in caspase activation, PARP cleavage, and apoptosis (57).

While IGFBP-3 can exert its anti-proliferative and pro-apoptotic effects by inhibiting IGF-I, effects independent of IGF-binding also exist. Interestingly, the IGF-independent effects of IGFBP-3 all tend to be growth inhibitory (58). Transfection with IGFBP-3 induces apoptosis in multiple cell lines (59-61). Transfection of U2-OS cells with IGFBP-3 induces caspase-dependent apoptosis even when it is mutated to prevent secretion, indicating a role for intracellular IGFBP-3 (60). IGFBP-3 induces changes in cell morphology and apoptosis when expressed in MCF-7 breast cancer cells (62). Another group found similar results in MCF-7 and MDB-231 cells where

IGFBP-3 transfection induces caspase activation and inhibits DNA synthesis (59,61). In addition, IGFBP-3 mutated to have reduced affinity for IGF-I induced the same effects, indicating that the apoptotic effects of IGFBP-3 are independent of IGF-I signaling and demonstrating that the effects of IGFBP-3 extend beyond inhibition of IGF-I-induced survival signaling (61).

Transfection experiments show that IGFBP-3 expression induces apoptosis and serve as a tool to examine the function of locally produced IGFBP-3. Interestingly, addition of exogenous IGFBP-3 can have similar apoptotic effects suggesting the apoptotic role of IGFBP-3 might extend beyond paracrine effects in these cells. Treatment of cells with exogenous IGFBP-3 induces apoptosis in a number of cell systems. In prostate cancer cells, treatment with IGFBP-3 or an IGFBP-3-mutant that does not bind IGF-I inhibits DNA synthesis and induces apoptosis (63). IGFBP-3 is able to induce apoptosis in IGFR-negative fibroblasts, and this effect is not reduced when cells are co-incubated with IGF-I, indicating that IGFBP-3 can induce apoptosis independent of IGF-binding or IGF-IR signaling (64).

Other groups show that endogenous or exogenous IGFBP-3 has no direct apoptotic effect but potentiates death induced by other apoptotic compounds (50,65-68). IGFBP-3 is expressed at low levels in bovine MECs and expression is induced by an intrinsic pathway-activating stressor anisomycin (ANS) (65). Over-expression of IGFBP-3 does not induce apoptosis however knock-down of endogenous IGFBP-3 attenuates ANS-induced apoptosis, supporting a role for IGFBP-3 in modulating external stressors (65). IGFBP-3 also enhances the apoptotic effects of TNF-α in prostate cancer cells and normal MECs (66,67). In HS578T breast cancer cells, IGFBP-3 treatment has no effect alone but potentiates the apoptotic effect of the ceramide analogue C2 (68). The HS578T cells are not responsive to IGF-I, and a non-IGF-binding mutant IGFBP-3

retains its ability to enhance C2-induced death, indicating that these effects are independent of both IGF-binding and IGF-IR activation.

IGFBP-3 is implicated in chemo-sensitivity of multiple cancers, leading to an investigation into the role of IGFBP-3 expression in modulation of tumor progression. Adenoviral expression of IGFBP-3 in MCF-7-derived LCC9 tamoxifen-resistant breast cancer cells directly induces apoptosis and sensitizes cells to chemotherapeutic drugs (69). MCF-7 cells and human MECs express endogenous IGFBP-3, with expression up-regulated by apoptotic stressors including 1,25-dihydroxyvitamin D (1,25,D_3) and the chemotherapeutic agent celecoxib (53,54). This newly synthesized and secreted IGFBP-3 inhibits IGF-I induced activation of AKT, suggesting IGFBP-3 could act to sequester the circulating IGF-I to prevent IGF-IR activation, effectively inhibiting proliferation (53,54). The chemotherapeutic agent trastuzumab also induces expression of IGFBP-3, resulting in reduced IGF and EGF survival signaling to induce growth inhibition (70). Breast cancer cells expressing low levels of IGFBP-3 show increased resistance to trastuzumab treatment, further supporting a role for IGFBP-3 in tumor cell growth inhibition (70). In osteosarcoma cells, IGFBP-3 is produced in response to transforming growth factor-β (TGF-β) and acts to attenuate TGF-β-induced proliferation by antagonizing IGF-IR signaling (71). In prostate cancer cells adenoviral expression of IGFBP-3 disinhibits NF-κB activation, reduces production of VEGF and adhesion molecules ICAM-1 and VCAM-1. Together, these effects result in sensitization of prostate cancer cells to doxorubicin-induced apoptosis (72). Recombinant IGFBP-3 can also act alone to inhibit proliferation of breast and prostate cancer cells when added to the growth media indicating that circulating, as opposed to endogenous, IGFBP-3 may also play a role in chemo-sensitivity (73). These data support an apoptotic role for IGFBP-3 and suggest that impaired secretion of IGFBP-3 could contribute to enhanced growth signaling and

tumorigenesis of malignant cells. However, data investigating the role of circulating IGFBP-3 in regulating the local tumor environment are conflicting, with data supporting both positive and inverse correlations between circulating IGFBP-3 and breast cancer prognosis (74). Therefore whether in vitro data support in vivo data remains to be determined.

The apoptotic functions of IGFBP-3 make up-regulation of IGFBP-3 expression a potential chemotherapeutic approach for cancer. In patients with esophageal squamous cell carcinoma (ESCC), low tumor expression of IGFBP-3 is associated with increased tumor aggressiveness and reduced patient survival (75). These data suggest that resistance to apoptosis correlates with reduced expression of IGFBP-3. In vitro experiments suggest this effect is likely due to the ability of IGFBP-3 to sensitize ESCC to chemotherapeutic agents (76). Data in senescent fibroblasts support this hypothesis. With increasing passage number, intracellular IGFBP-3 is reduced, and resistance to apoptosis increases (77). One group found that IGFBP-3 expression is reduced in prostate tumor cells relative to normal prostate epithelial cells, further supporting autocrine or paracrine effects of endogenous IGFBP-3 in tumor growth (72).

Interestingly, the growth factor-inhibitory and apoptotic effects of IGFBP-3 have a protective effect against inflammation, making IGFBP-3 expression a therapeutic target for asthma treatment. In a murine model of allergen-induced airway disease, treatment with IGFBP-3 inhibits production of IGF-I and VEGF in ovalbumin (OVA) -treated mice, and reduces inflammatory cytokines (78). These molecular effects culminate in reduced airway inflammation and improved pathological outcomes in OVA-treated mice (78). Another group found similar anti-inflammatory effects for IGFBP-3. Mice over-expressing IGFBP-3 show reduction of both inflammatory markers and asthma-induced hyper-proliferation in sectioned lung tissues from

OVA-treated animals (79). Both groups found that IGFBP-3 activates caspases and that the caspase activation is responsible for degradation of IκBα and p65-NF-κB. Interestingly, Kim and colleagues found that IGFBP-3 alone induces apoptosis (78), while Lee and colleagues showed that IGFBP-3 expression does not induce apoptosis but instead sensitizes cells to the death effects of pro-inflammatory cytokine TNF-α (79).

In summary, IGFBP-3 influences cellular survival and death through both direct and indirect effects. While it is clear that IGFBP-3 has a role in apoptosis, a number of questions remain. First, a molecular switch that determines whether IGFBP-3 is growth-stimulatory or apoptotic has not been identified. Second, no clear mechanism exists detailing how IGFBP-3 induces or mediates apoptosis. Further, the range of physiological effects IGFBP-3 exerts implicates that IGFBP-3 acts through multiple mechanisms with its function being influenced by the cellular environment.

IGFBP-3 and caspase activation

Regardless of whether IGFBP-3 modulates apoptosis through direct or indirect mechanisms, caspase activation is required to initiate the final stages of cell death. IGFBP-3-induced apoptosis involves activation of caspases -3 and -7 in multiple cell lines (60,61,69,80,81). One group found that IGFBP-3 over-expression activates caspase-8, and identified a putative IGFBP-3 receptor (IGFBP-3R), demonstrating mRNA expression of the IGFBP-3R in a number of human tissues, including prostate, heart, and lung but no data from breast tissue (82). These experiments involved transfection of IGFBP-3R into cell types that do not naturally express the receptor or IGFBP-3 so the importance of endogenous IGFBP-3 and IGFBP-3R are still unknown. Conflicting data regarding activation of caspase 8 versus caspase 9 in different cell lines could be

accounted for by cell-type specific expression of an IGFBP-3R, which could also influence cellular uptake and compartmentalization of IGFBP-3. However, the presence of a specific IGFBP-3R has not been confirmed by other groups to date. Treatment of MECs with IGFBP-3 is not anti-proliferative, making it unlikely that IGFBP-3 acts through a cell surface receptor in these cells (46). In addition, expression of IGFBP-3 with a mutated secretion signal induces activation of both caspases 8 and 9 in PC-3 prostate cancer cells, indicating that IGFBP-3 does not have to be secreted to induce apoptosis (83). In summary, while caspase activation is clearly part of the apoptotic function of IGFBP-3, how IGFBP-3 mediates caspase activation is still unclear.

IGFBP-3 and Bcl-2 proteins

The balance between Bcl-2 proteins that promote survival versus apoptosis contributes to regulation of MOMP and caspase activation. Expression of IGFBP-3 in non-small cell lung cancer (NSCLC) tumor xenografts results in decreased Bcl-2 protein, activation of caspase-3, and PARP cleavage (57). These molecular events triggered by IGFBP-3 expression slow the progression of the xenograft tumors. Treatment of PC-3 prostate cancer cells with TNFα induces expression and secretion of IGFBP-3; therefore a role for IGFBP-3 in TNFα-induced apoptosis was examined (67). In PC-3 cells IGFBP-3 induces apoptosis singularly and has an additive effect with TNFα. Either treatment induces phosphorylation and inactivation of Bcl-2. In addition, knock-down of IGFBP-3 attenuates TNFα-induced Bcl-2 phosphorylation (67). These data indicate that endogenous IGFBP-3 acts upstream of the mitochondria to inhibit survival proteins.

Further evidence indicates that in addition to inhibiting the Bcl-2 survival proteins IGFBP-3 activates the apoptotic members of the Bcl-2 family. In breast cancer cells, IGFBP-3 expression induces apoptosis by up-regulating Bax and Bad mRNA and protein, while simultaneously down-

regulating Bcl-2 expression (84). This shift in the ratio of survival to apoptotic Bcl-2 proteins results in increased sensitivity to radiation-induced apoptosis. Few data exist in normal, non-cancerous cells, however one group found that IGFBP-3 and Bax associate in testes isolated from rats treated with IGFBP-3 (85). In vivo experiments suggest the association between IGFBP-3 and Bax contributes to induction of apoptosis by facilitating mitochondrial release of cytochrome-c and Smac/DIABLO (85). Interestingly, while treatment of MDA-MB-231 breast cancer cells with IGFBP-3 induces cleavage of both caspases 8 and 9, IGFBP-3 cannot enhance activation of Bid by TNFα, suggesting the effects of IGFBP-3 are primarily through the intrinsic apoptotic pathway (59). These data indicate that IGFBP-3 can affect expression and activation of both survival and apoptotic Bcl-2 proteins to shift their balance in favor of apoptosis.

Nuclear localization of IGFBP-3

Cellular localization is reported to influence the function of IGFBP-3. While IGFBP-3 is a secreted protein, it also contains a nuclear localization sequence (NLS) and has been found in the nucleus (86). However, whether nuclear localization is necessary for apoptosis remains controversial. Under basal conditions, IGFBP-3 is present in the nucleus of actively dividing opossum kidney and human breast cancer cells which is hard to reconcile with a role in apoptosis (86,87). In porcine embryonic myogenic cells IGFBP-3 is expressed basally in proliferating cells and localizes to the nucleus after treatment with TGF-β, a growth-inhibitor (7). These data suggest IGFBP-3 is directed to the nucleus in response to cellular conditions. However, over-expression of IGFBP-3 in osteosarcoma cells leads to increased nuclear IGFBP-3 and cell death in the absence of a cell stressor suggesting that in cells where IGFBP-3 directly induces apoptosis no external stimuli is needed to direct IGFBP-3 to the nucleus (60,88). Interestingly, human senescent fibroblasts lack nuclear IGFBP-3 and are resistant to cell death, supporting a role for nuclear IGFBP-3 in

apoptosis (77). However expression of IGFBP-3 with a mutated NLS was still able to induce apoptosis in breast and prostate cancer cells suggesting that IGFBP-3 may also interact with cytoplasmic proteins to regulate cell death (80,83). In contrast, IGFBP-3 requires an intact NLS to inhibit proliferation in myoblasts, suggesting a requirement for nuclear localization in these cells (89). These data indicate that the function of endogenous, nuclear IGFBP-3 could be specific to both cell-type and extracellular stimuli. More work in normal (non-cancerous) cells is needed to determine the function of nuclear IGFBP-3 in these cells.

Nuclear interactions

Several studies suggest that IGFBP-3 has intracellular binding partners. In prostate cancer cells treated with exogenous IGFBP-3, IGFBP-3 localizes to the nucleus where it interacts with the nuclear receptor retinoid X receptor-α (RXRα) (90). In these cells, IGFBP-3 facilitates the association of RXRα with orphan nuclear receptor Nur77, then the RXRα/Nur77-complex translocates from the nucleus to the cytoplasm to ultimately cause caspase activation and induce apoptosis (91). In addition, siRNA knock-down of either RXR-α or Nur77 inhibits the stress-induced movement of the other in prostate cancer cells (92). A potential nuclear export sequence (NES) has been identified in IGFBP-3 and mutation of this sequence inhibits nuclear export not just of IGFBP-3, but also of the RXRα/Nur77-complex in prostate cancer cells (93). Nur77 has been shown to be required for apoptosis in breast cancer cells, pancreatic cancer cells, and murine epithelial fibroblasts (94-96). While the association between IGFBP-3 and Nur77 is well studied in prostate cancer cells, little data exist in other cell types.

Mechanism for nuclear import

Clear evidence exists for nuclear binding partners of IGFBP-3, however the mechanism of nuclear import remains controversial. Secreted IGFBP-3 is reportedly re-internalized then directed to the nucleus in multiple cell lines. In prostate cancer cells, IGFBP-3 production and nuclear localization are induced as part of TGF-β-induced extrinsic apoptosis (81). Addition of anti-IGFBP-3 antibody to treatment medium attenuates nuclear localization of IGFBP-3 and apoptosis in these cells, indicating that IGFBP-3 is secreted then re-internalized as part of the apoptotic response. Extracellular IGFBP-3 is reported to bind transferrin (Tf) to form a ternary complex with Tf and its receptor (TfR), this complex then gets internalized and IGFBP-3 is released inside the cell (81,97,98). In addition, inhibition of either clathrin or caveolin can reduce uptake of IGFBP-3 added to extracellular medium, however these studies do not address the cellular trafficking of endogenous IGFBP-3 (88,98).

Detection of non-secreted IGFBP-3 in the nucleus calls into question whether secretion and re-internalization are required for nuclear import of IGFBP-3. IGFBP-3 with a mutated secretion signal can still localize to the nucleus and induce apoptosis in osteosarcoma cells or prostate cancer cells (60,83). While it remains possible that secreted IGFBP-3 could be internalized, this seems like a major inefficiency in the tightly controlled apoptotic process.

Once directed to the nucleus IGFBP-3 is proposed to be actively transported across the nuclear pore, utilizing a NLS. Mutation of the NLS of IGFBP-3 attenuates nuclear import (60,89,99). Affinity studies show that IGFBP-3 can bind importins-α and -β via its NLS, with a stronger affinity for importin-β (99,100). In permeabilized breast cancer cells an importin-β immuno-neutralizing antibody prevents nuclear accumulation of IGFBP-3, indicating that IGFBP-3 can

bind importin-β in live cells. A role for importin-β in transport of endogenous IGFBP-3 in intact cells has not been investigated.

Post-translational modifications of IGFBP-3

Glycosylation

IGFBP-3 circulates as a glycoprotein with a molecular weight of approximately 40-45 kDa in human serum and is reported to be N-glycosylated at Asn89, Asn109, and Asn172 (101). Glycosylation is not required for IGFBP-3 to bind IGF-I, however, under-glycosylated IGFBP-3 has a lower affinity for IGF-I and shows increased cell surface binding (101-103). Glycosylated IGFBP-3 has a greater effect on potentiation of IGF signaling than non-glycosylated IGFBP-3, possibly due to decreased stability of the non-glycosylated form (104). The recombinant IGFBP-3 used to investigate the apoptotic functions of IGFBP-3 is generally produced in mammalian cells, which are able to fully glycosylate IGFBP-3 (87,88,93,105). However, one group compared the ability of glycosylated and non-glycosylated IGFBP-3 to enhance C2-induced apoptosis and found that non-glycosylated IGFBP-3 retained its apoptotic effect (106).

The most compelling evidence supporting the influence of glycosylation status on determining the biological role of IGFBP-3 is in breast cancer cells undergoing the unfolded protein response (UPR). In chemotherapy-resistant cells IGFBP-3 enhanced survival by promoting autophagy in cells treated with anti-tumor agents that induce UPR (107). IGFBP-3 bound GRP78 to induce autophagy, but did not affect progression of the UPR (108). Under-glycosylated IGFBP-3 had higher affinity for GRP78 than its partially or fully glycosylated counterparts, supporting a role for glycosylation status in modulating cellular function of IGFBP-3 (108).

In summary, little definitive data exist describing the functional significance of glycosylation of IGFBP-3. The literature currently supports a role for glycosylation in stability of secreted IGFBP-3. Glycosylation status does not affect the ability of IGFBP-3 to mediate apoptosis in human MECs, evidenced by equal apoptotic effects of IGFBP-3 regardless of glycosylation status (106). In contrast, under-glycosylated IGFBP-3 may be a signal for onset of autophagy, pushing the cell into a survival rather than apoptotic state (108). These data further implicate cellular environment in determination of biological function of IGFBP-3. The type and degree of stress influence whether the cell proliferates, dies, or enters autophagy. IGFBP-3 has a role in each of these responses and serves as a mediator of cellular homeostasis.

Phosphorylation

Another form of post-translational modification known to regulate function of IGFBP-3 is phosphorylation. Phosphorylation of IGFBP-3 by an unidentified membrane associated kinase at the cell surface increases its affinity for IGF-I (48). The functional significance of this effect is unclear but may assist in localization of IGF-I near its receptor at the cell surface. In addition, the fraction of IGFBP-3 that is phosphorylated increases when breast cancer cells are treated with either mitogenic or apoptotic stimuli, suggesting the involvement of multiple kinases that are differentially regulated (109).

Two intracellular kinases are known to phosphorylate IGFBP-3 under opposing conditions. The first, casein kinase-2 (CK2) is a constitutively active kinase located in the nuclear and cytosolic cellular compartments (110). CK2 has a basal anti-apoptotic function, and exerts this survival effect in part through inhibition of the apoptotic effects of IGFBP-3 (111). IGFBP-3-induced apoptosis in prostate cancer cells is enhanced when CK2 activity is inhibited (111). CK2-

phosphorylation of IGFBP-3 at Ser167 has no effect on the affinity of IGFBP-3 for the cell surface or for IGF-I but does enhance the ability of IGFBP-3 to potentiate IGF-I-induced DNA synthesis (111,112). These data show that CK2 promotes cellular survival by phosphorylating IGFBP-3 to inhibit its apoptotic functions and enhance its mitogenic role.

While phosphorylation by CK2 enhances the mitogenic effects of IGFBP-3, phosphorylation by DNA-dependent protein kinase (DNAPK) at Ser156 activates the apoptotic functions of IGFBP-3 (113). IGFBP-3 phosphorylated by DNAPK has decreased affinity for IGF-I and increased nuclear retention in permeabilized nuclei (114). Nuclear retention of IGFBP-3 suggests the presence of a nuclear binding partner. In prostate cancer cells, inhibition of DNAPK attenuates the apoptotic effects of IGFBP-3 and IGFBP-3 is unable to associate with RXRα as part of the apoptotic response (113). Together, these data show that phosphorylation of IGFBP-3 by DNAPK promotes apoptosis, possibly through regulation of the association between IGFBP-3 and RXRα. These data are especially interesting because DNAPK acts in the nucleus to facilitate repair of DNA double strand breaks and maintain cellular homeostasis (115). In the absence of cellular stress DNAPK has a role in cellular survival, however under cases of extreme DNA-damage, DNAPK is implicated in the initiation of apoptosis (116).

Proteolysis

Proteolytic fragmentation of IGFBP-3 offers another level of functional control for this protein. IGFBP-3 proteolyzed by human pregnancy serum retains its ability to bind IGF-I but with a lower affinity, and is unable to inhibit IGF-I-induced IGF-IR activation in HUVECs (102). In this scenario, fragmentation of IGFBP-3 serves to increase bio-availability of IGF-I and enhance IGF-IR activation.

Fragmentation of IGFBP-3 also has a role in pathological states. IGFBP-3 is proteolyzed at two sites by matrix metalloprotein-7 (MMP-7), an enzyme expressed in cancer cells but absent in normal stromal cells (105). In colon cancer cells, proteolyzed IGFBP-3 has reduced affinity for IGF-I and loses its ability to sequester IGF-I from its receptor (105). These data indicate that proteolysis of circulating IGFBP-3 increases local IGF-signaling in cancer cells.

Fragmented IGFBP-3 shows reduced ability to bind the cell surface of Hs578T breast cancer cells (106). However, proteolyzed IGFBP-3 retains its ability to potentiate C2-induced apoptosis (106). A non-secreted N-terminal fragment of IGFBP-3 that is unable to bind IGF-I directly induces caspase-dependent apoptosis as efficiently as the intact protein in PC3 prostate cancer cells (117). These data indicate that IGFBP-3 exerts its apoptotic effects independent of secretion or IGF-binding.

Interestingly, in obese persons, total circulating IGFBP-3 is reduced and detection of fragmented IGFBP-3 is increased (118). In vitro experiments show that intact IGFBP-3 protects against insulin resistance in primary human adipocytes and reduces inflammation in vascular endothelial cells, but that proteolyzed IGFBP-3 loses this protective effect (118). These data indicate a role for IGFBP-3 in protection against the metabolic changes associated with obesity.

Together these data indicate that while fragmentation of IGFBP-3 does not enhance its apoptotic effects the fragments do retain their apoptotic potential. However, proteolysis has differential effects on survival of cancer and endothelial cells suggesting that the biological function of IGFBP-3 is regulated locally in response to cellular environment.

Nur77 in apoptosis

Like IGFBP-3, Nur77 is a multi-functional protein with dual roles in apoptosis and survival. Also known as NGF1B, NAK1, or TR3, Nur77 is classified as an orphan nuclear receptor with no ligand identified to date. Expression of Nur77 is induced by serum and growth factors, and functions in the nucleus to induce transcription of pro-survival and anti-apoptotic proteins (119,120). Endogenous Nur77 is required for growth factor-induced proliferation, and Nur77 over-expression results in increased proliferation of lung cancer cells (121). Consistent with a role in survival, Nur77 is over-expressed in many cancers, including cancers of the breast, lung, prostate and colon (122). Knock-down of Nur77 in pancreatic cancer cells reduces Bcl-2 protein and increases activation of caspases, supporting a pro-survival function for Nur77 in these cells (95). In addition to its direct role promoting tumor cell proliferation, Nur77 also enhances angiogenesis to support tumor vascularization (120). Data in non-cancer cells show Nur77 has a role in neuronal survival, and reduced Nur77 expression is associated with Parkinson's disease (96).

Induction of Nur77 message and protein also occurs in response to apoptotic stimuli and Nur77 is implicated in altering the Bcl-2 family proteins in favor of apoptosis (120). Expression of Nur77 is up-regulated in T-cells as part of the negative selection process and promotes apoptosis to prevent auto-immune reactions (123,124). In cancer cells, Nur77 protein is induced by chemotherapy drugs and contributes to their apoptotic effects (125,126). Over-expression of Nur77 in cancer cells or T-cells results in caspase activation and cytochrome c release, implicating a role for Nur77 in intrinsic apoptosis (126,127).

Translocation of Nur77 out of the nucleus is specific to death stimuli, offering one mechanism governing the role of Nur77 in cell fate (122). In the absence of stress, Nur77 resides predominantly in the nucleus where it acts as a transcription factor (121,128). Upon exposure to cellular stress Nur77 translocates from the nucleus to the cytoplasm, shutting off its transcriptional role in survival and enhancing its apoptotic potential (129,130).

Phosphorylation is a key regulator of nuclear export of Nur77. Cellular stress induces phosphorylation of Nur77, resulting in reduced DNA-binding and enhanced nuclear export. AKT phosphorylates Nur77 at Ser350, resulting in reduced transcriptional activity (131,132). Mutation of Nur77 at Ser350 attenuates the apoptotic effects of Nur77 in T-cells and rat fibroblasts, indicating that phosphorylation is required for the apoptotic potential of Nur77 (131,132). In lung cancer cells treated with ANS, JNK phosphorylates Nur77, inhibiting its transcriptional activity (121,130,133). In addition, phosphorylation of Nur77 by JNK promotes its nuclear export and mitochondrial targeting (121).

Nur77 is found in the mitochondria of multiple cell types exposed to cellular stressors (91,124,125,134). Treatment of T-cells with PMA induces mitochondrial localization of Nur77 where it associates with Bcl-2 (124). This association induces a conformational change in Bcl-2, converting Bcl-2 into an apoptotic protein. In contrast, Wang et al. found in T-cells that while Nur77 localizes to the mitochondria it does not associate with Bcl-2 (127). Expression of Nur77 was sufficient to induce apoptosis in Wang et al. so no additional stressor was used for their experiment, indicating that association between Nur77 and Bcl-2 could be a response to specific cell stressors. In prostate cancer cells, mitochondrial Nur77 is reported to associate with Bcl-2 (125,134). As in T-cells, this association is thought to induce a conformational change in Bcl-2,

converting it to an apoptotic protein (134). Work in vascular smooth muscle cells (VSMCs) shows that Nur77 localizes to the mitochondria and associates with Bcl-2 in response to treatment with alpha-lipoic acid, resulting in apoptosis and reduced inflammation (129). Interestingly, one group found that Nur77 localizes to the mitochondria of prostate cancer cells but not colon cancer cells, suggesting that cellular localization is differentially regulated across cell types (126).

As previously discussed, IGFBP-3 is reported to have a role in nuclear export of Nur77 in prostate cancer cells (91,93). In these cells, IGFBP-3 facilitates the association between Nur77 and RXRα. RXRα has a nuclear export sequence (NES) that this Nur77-RXRα complex utilizes for nucleo-cytoplasmic transport (92). Nur77 and RXRα are both phosphorylated by JNK, suggesting that phosphorylation of these proteins may also contribute to modulation of their interaction and cellular localization (130,133,135,136).

Together, these data suggest that Nur77 acts through multiple mechanisms to promote apoptosis. Much of the literature is in cancer cell lines transfected to over-express Nur77. Additionally, much of the work examining the role of mitochondrial Nur77 has come from a single lab working in prostate cancer cells. More work is needed to determine the role of endogenous Nur77 in apoptosis of normal epithelial cells and to establish the role of IGFBP-3 in modulating the cellular localization and function of Nur77.

MAC-Ts as a model for intrinsic apoptosis in the mammary gland

This work utilizes bovine mammary alveolar cells (MAC-T) immortalized with SV-40 large-T antigen, as described in Huynh et al. (137). Isolated from primary bovine alveolar cells, MAC-T cells retain the morphology of epithelial cells and differentiation can be induced to produce milk proteins, mimicking lactation. We previously established that these cells produce IGFBPs 2-6 and are responsive to IGF-I (138). MAC-T cells produce a low level of IGFBP-3 under basal conditions, evidenced by accumulation of IGFBP-3 in conditioned media.

Much of the research focusing on IGFBP-3 in apoptosis has been done in cancer cells that are transfected with IGFBP-3 or treated with exogenous IGFBP-3. It remains to be determined how the cellular function (survival vs. apoptosis) of endogenous IGFBP-3 is determined in the bovine mammary gland and how IGFBP-3 signals the cell to survive or perish. Based on their morphological similarity to primary cells, IGF-responsiveness, and production of IGFBP-3, MAC-T cells serve as an appropriate in vitro model to study the role of IGFBP-3 in bovine mammary gland apoptosis.

Specific aims

A requirement for IGFBP-3 in the apoptotic pathway has been established in both normal and transformed epithelial cells, including bovine mammary epithelial cells (MECs) (66), mink lung cells (139), and breast (80,140), and prostate cancer epithelial cells (63,79). The literature suggests that during apoptosis IGFBP-3 shifts the ratio of Bcl-2 family member proteins in favor of those that promote apoptosis. IGFBP-3 has also been found in the nucleus where it promotes translocation of Nur77 and retinoid X receptor-alpha (RXRα) out of the nucleus to sustain the mitochondrial-mediated intrinsic apoptotic pathway (91).

It remains unclear how exogenous stress stimuli mediate the apoptotic role of endogenous IGFBP-3 in cell death in normal epithelial cells. Bovine MECS produce endogenous IGFBP-3 at low levels basally, but production increases in response to the cell stressor anisomycin (ANS). The objective of this thesis was to determine how nuclear IGFBP-3 mediates the pathway of stress-induced apoptosis. The overall goal of this work is to address how IGFBP-3 is directed to the nucleus in ANS-induced cellular stress and how IGFBP-3 modulates nuclear proteins to modulate cell stress. The mechanisms described in the following aims are illustrated in Fig. 2.

The first aim establishes a role for IGFBP-3 in intrinsic apoptosis. IGFBP-3 mRNA and protein are regulated by ANS, so we hypothesized that IGFBP-3 is required for ANS-induced apoptosis (Chapter 2). IGFBP-3 has been detected in the nucleus of cells exposed to cellular stress so we hypothesized that ANS directs IGFBP-3 to the nucleus as part of the apoptotic response. Small interfering (si) RNA was used to knock-down IGFBP-3 then ANS-induced cleavage of caspases and PARP were measured as indicators of apoptosis. Treated cells were also fractionated to examine localization of IGFBP-3 in cells treated ± ANS.

Nuclear IGFBP-3 is reported to associate with nuclear receptors Nur77 and RXRα to facilitate nuclear export and mitochondrial targeting of Nur77. The second aim investigates a role for IGFBP-3 in modulation of ANS-induced activation and nuclear export of Nur77 (Chapter 3). Knock-down of Nur77 was used to determine if Nur77 is required for ANS-induced apoptosis. Next, knock-down of IGFBP-3 was used to determine if IGFBP-3 is required for ANS to activate and induce nuclear export of Nur77.

The mechanism for nuclear localization of IGFBP-3 remains controversial. Conflicting data exist debating whether IGFBP-3 is secreted then re-internalized before being directed to the nucleus. The third aim used inhibitors of secretion and endocytosis to determine if nuclear IGFBP-3 is derived from intra- or extra-cellular IGFBP-3, and if nuclear transport protein importin-β facilitates transport into the nucleus (Chapter 4).

Working in a bovine MEC model provides a unique set of challenges due to the limited availability of commercial antibodies that cross-react with bovine proteins. The final aim was to purify recombinant bovine IGFBP-3 and use it as an antigen to generate a primary antibody recognizing bovine IGFBP-3 (Chapter 5).

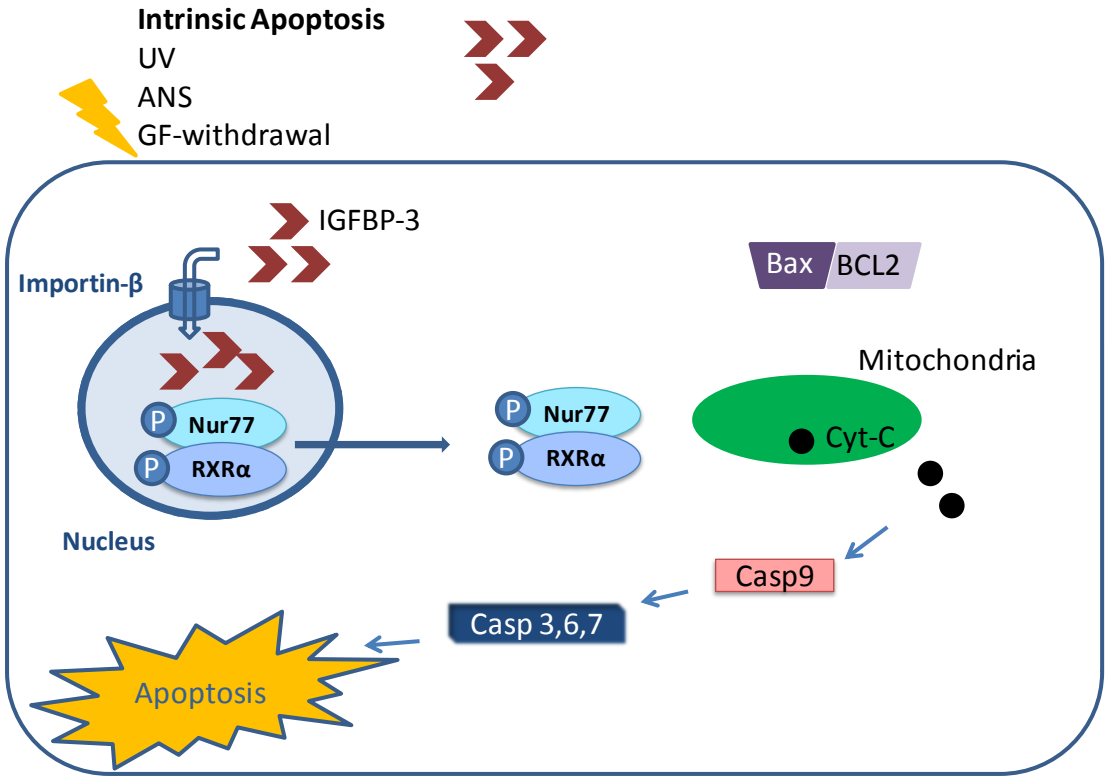

Fig. 2. Proposed mechanism for IGFBP-3 in MEC apoptosis. Intrinsic stressors induce production, secretion and nuclear localization of IGFBP-3. Nuclear IGFBP-3 is imported into the nucleus by importin-β, then facilitates phosphorylation and nuclear export of Nur77 and RXRα. Nur77 acts in the cytoplasm or mitochondria to induce cytochrome c (Cyt-C) release, caspase activation, and eventual apoptosis.

Chapter 2.

IGF binding protein-3 mediates stress-induced apoptosis in non-transformed mammary epithelial cells

Abstract

Mammary epithelial cell (MEC) number is an important determinant of milk production in lactating dairy cows. IGF-I increases IGF binding protein-3 (IGFBP-3) production in these cells, which plays a role in its ability to enhance proliferation. In the present study, we show that the apoptotic factor anisomycin (ANS) also increases IGFBP-3 mRNA and protein in a dose and concentration-dependent manner that mirrors activation of caspase-3 and -7, with significant increases in both IGFBP-3 protein and caspase activation observed by 3 h. Knock-down of IGFBP-3 with small interfering (si) RNA attenuated the ability of ANS to induce apoptosis, while knock-down of IGFBP-2, the other major IGFBP made by bovine MEC, had no effect. Reducing IGFBP-3 also decreased the ability of ANS to induce mitochondrial cytochrome c release, indicating its involvement in the intrinsic apoptotic pathway. In contrast, transfection with IGFBP-3 in the absence of ANS failed to induce apoptosis. Since both the mitogen IGF-I and the apoptotic inducer ANS increase IGFBP-3 production in MEC, we proposed that cellular localization might determine IGFBP-3 action. While both IGF-I and ANS stimulated the release of IGFBP-3 into conditioned media, only ANS induced nuclear localization of IGFBP-3. A pan-caspase inhibitor had no effect on ANS-induced nuclear localization of IGFBP-3, indicating that nuclear entry of IGFBP-3 precedes caspase activation. Treatment with IGF-I had no effect on ANS-induced nuclear localization, but did block ANS-induced apoptosis. In summary, our data indicate that IGFBP-3 plays a role in stress-induced apoptosis that may require nuclear localization in non-transformed MEC.

Introduction

The amount of milk a lactating dairy cow produces over a lactation cycle is determined by the number of secretory mammary epithelial cells (MEC) present in the gland over time (141). The decline in milk yield following peak lactation is associated with loss of MECs by apoptosis. In addition, loss of MECs occurs during involution following cessation of milking (142,143). A number of management practices including bovine somatotropin administration, continuous milking, increased frequency of milking, photoperiod manipulation, or a combination of these treatments have been explored in attempts to increase overall lactation yield and persistency (142-146). While the IGF system has been proposed to play an important role in maintaining MEC numbers in response to these treatments, the molecular mechanisms that underlie these effects are not well-delineated.

The balance between cell survival and death is regulated by opposing factors that promote and inhibit the apoptotic process. At the cellular level, IGF-I and IGFBP-3 each interact with intracellular proteins or signaling cascades that regulate apoptosis, and thus may represent the yin and yang of apoptotic regulation (147,148). IGFBP-3 can modulate cell death through diverse mechanisms, including IGF-independent effects (149). These pro-apoptotic effects may occur as a result of its association with a cell surface receptor (82), presence in the cytosol (150), localization to the nucleus (91,151), or transport between cellular compartments (93), suggesting that IGFBP-3 actions are both complex and dependent on cellular context.

Studies across multiple cell types have indicated that promitogenic and prosurvival factors as well as growth inhibitory and proapoptotic factors increase IGFBP-3 synthesis. We have previously reported that the mitogenic and pro-survival factor IGF-I increases IGFBP-3 mRNA

and protein in the non-transformed bovine MEC line MAC-T and primary bovine MEC (152,153). We recently reported that the pro-inflammatory cytokine TNF-α also increases IGFBP-3 mRNA and protein in MAC-T cells, however, TNF-α does not induce apoptosis (154). The antibiotic anisomycin activates the JNK and p38 pathways and induces apoptosis in multiple cell types (reviewed in (155)). Therefore, in the present study we sought to determine if ANS would have similar effects on IGFBP-3 mRNA and protein and if these increases play a role in its ability to activate apoptosis. Furthermore, since IGFBP-3 contains a nuclear localization sequence (NLS) in its carboxy-terminal domain that facilitates its transport to the nucleus (99), we hypothesized that cellular localization of IGFBP-3 may be important in determining its biological role within the cell.

Materials and Methods

Chemical reagents

Phenol red-free (PRF) DMEM-low glucose media, gentamycin, bovine insulin, ANS and fetal bovine serum (FBS) were purchased from Sigma (St. Louis MO). Recombinant human IGF-I (100% identical to bovine IGF-I) was obtained from Peprotech (Princeton, NJ). DMEM with high glucose, penicillin and streptomycin were purchased from Invitrogen (Carlsbad, CA). Antibodies against the following proteins were purchased as indicated: Akt, PARP and cleaved caspase 3 and -7 (Cell Signaling Technology, Inc., Danvers, MA), actin (EMD-Calbiochem, La Jolla, CA), HSP60 (Abcam, Cambridge, MA), cytochrome c (BD Pharmingen, San Diego, CA), porin (MitoSciences, Eugene, OR), and lamin A/C (Santa Cruz, Dallas, TX). Polyclonal antibodies specific for bovine IGFBP-3 and IGFBP-2 were kindly provided by Dr. David Clemmons, University of North Carolina at Chapel Hill. Hoechst 33342 dye was supplied by Invitrogen. Bovine siRNA IGFBP-2 oligonucleotides were purchased from Sigma. A custom SmartPool siRNA for bovine IGFBP-3 and scramble siRNA control were purchased from Dharmacon Inc. (Lafayette, CO). The pan caspase inhibitor Z-VAD-FMK was purchased from BD Pharmingen.

Cell culture

The bovine MEC line MAC-T (156) was routinely maintained in complete media consisting of DMEM containing 4.5 g/liter D-glucose (i.e. DMEM-H), 20 U/ml penicillin, 20 μg/ml streptomycin, 50 μg/ml gentamicin, 10% FBS, and 5 μg/ml insulin. For experiments, cells were plated and grown to confluence in phenol-red free DMEM-H containing 10% fetal bovine serum (FBS) and antibiotics and without insulin. Cells were rinsed with phosphate buffered saline (PBS), and incubated in serum-free (SF) DMEM-H with 0.2% BSA and 30 nM sodium selenite overnight prior to exposure to treatments in SF DMEM-H without additives.

Western immunoblotting and ligand blotting

Cells were lysed or conditioned media were collected as previously described (157). Cell fractionations were prepared with either the Nuclear Fractionation Kit or the Mitochondrial Fractionation Kit from Active Motif (Cambridge MA) according to manufacturer's instructions. Total protein content of lysates or fractions was determined using the Bio-Rad Protein Assay (Bio-Rad, Hercules, CA). Proteins were separated by SDS polyacrylamide gel electrophoresis (PAGE) on 10 or 12.5% gels and transferred to nitrocellulose (0.2 µm; Bio-Rad) or PVDF (0.45 µM; Millipore, Bedford, MA) membranes. Western immunoblots and ^{125}I-IGF-I ligand blotting assays were performed as previously described (154)

siRNA experiments

MAC-T cells were plated in complete media at 3.0 x 10^4 cells/cm^2. The following day, subconfluent cells were transfected with 50 nM IGFBP-3 or IGFBP-2 siRNA oligos, as well as a corresponding concentration of scrambled control siRNA, using Mirus Transit TKO Transfection Reagent (Stratagene, La Jolla, CA) according to manufacturer's instructions. After 48 h, cells were washed and incubated overnight in serum-free media, then treated for analysis of gene knockdown or ANS-induced apoptosis. Gene knockdown of IGFBP-3 and IGFBP-2 was verified by western ligand blotting and immunoblotting as described above.

Transient transfection of IGFBP-3

MAC-T cells were plated in complete media at 3.5 x 10^4 cells/cm^2. The next day subconfluent cells were transfected with a plasmid encoding cDNA for bovine IGFBP-3 or plasmid alone (157). Plasmids were prepared using the EndoFree plasmid Maxi Kit (Qiagen, Valencia CA). Cells were transfected using SuperFect (Qiagen) combined with plasmid in a 1:5 ratio for 60 x 15 mm dishes

and in a 1:10 ratio for 96 well plates. The transfection mixture was prepared in DMEM-H with no additives, vortexed for 10 sec, and incubated at RT for 10 min. Spent media were removed from cells and replaced with fresh complete media and the transfection mixture. After 3 h, media were removed and replaced with fresh complete media. Following a 24 h recovery in serum-containing media, cells were rinsed twice in PBS and incubated with fresh serum-free media containing sodium selenite and BSA. After 22 h, conditioned media and whole cell lysates were collected and caspase activation was determined.

Measurements of apoptosis

Nucleosome accumulation was measured using the Cell Death Detection ELISA^{PLUS} Assay (Roche Diagnostics, Indianapolis IN). Caspase-3/7 activation was measured with the Sensolyte Homogenous AMC Caspase-3/7 Assay and activation of individual caspases 3, -8 and -9 was determined with the fluorometric SensoLyte AMC Caspase Substrate Sampler Kit (AnaSpec, Inc., Freemont, CA). PARP and caspase-3 and -7 cleavage were measured by Western immunoblot. Terminal deoxynucleotidyl transferase-mediated dUTP nick-end labeling (TUNEL) staining was determined by plating cells on glass chamber slides (BD Falcon). Following treatment, cells were fixed with 4% paraformaldehyde, permeabilized using 0.1% sodium citrate and 0.1% Triton X-100, and stained using the In Situ Cell Death Detection kit (Roche). After counterstaining with Hoechst 33342 (Invitrogen), slides were examined under a Nikon Eclipse E800 fluorescent microscope. Images were captured with ACT-1 software.

Reverse transcription quantitative PCR (RT-qPCR)

Cells were lysed with Trizol (Invitrogen) and RNA was isolated using an RNeasy kit (Qiagen). RNA integrity was assessed by visualization of 28 and 18S ribosomal bands after agarose gel

electrophoresis. RNA (2 μg) was reverse transcribed with the High Capacity Reverse Transcriptase kit (Applied Biosystems, Foster City, CA). For qPCR, primer sets were developed using PrimerQuest (IDT, Coralville, IA) and purchased from Sigma-Aldrich. For IGFBP-3, primers were Forward, 5' CAGAGGAGACACCCAGAA 3'; Reverse; 5' GGAACTTGAGGTGGTTAGC 3'. For cyclophilin, primers were Forward, 5' GAGCACTGGAGAGAAAGGATTTGG 3'; Reverse, 5' TGAAGTCACCACCCTGGCACATAA 3'. To validate each primer set, individual standard curves were established using serial dilutions (1:2 through 1:20,000) of a common pool of RNA. Samples were diluted 1:4 and 5 μl were amplified in a 20 μl reaction containing 10 μl Power SYBR Green (Applied Biosystems), 4 μl H_2O and 0.5 μl (0.25 μM IGFBP-3, 0.125 μM cyclophilin) of each gene specific primer. Reactions were run on the ABI 7300 system using cycle parameters of 95°C for 10 min, followed by 40 cycles of 95°C for 15 sec and 60°C for 1 min. The amplification efficiencies for the primers were 99.8 ± 0.3% for IGFBP-3 and 100 ± 0.01% for cyclophilin (mean ± SD for three independent curves). Data were analyzed using the relative $\Delta\Delta C_T$ method with cyclophilin as the housekeeping gene. PCR products were verified by gel electrophoresis and melting curve analysis.

Statistical analysis

Data from experiments were analyzed by ANOVA with differences considered significant for $P < 0.05$. Tukey or SNK post-hoc tests were utilized for pair-wise comparisons. Analyses were performed with SigmaStat (2.03) software (SPSS Inc., Chicago, IL).

Results

ANS induces apoptosis and IGFBP-3 production in a concentration- and time-dependent manner

To determine if ANS induces apoptosis in MAC-T cells as described in other cell types, cells were exposed to ANS at concentrations of 0.001 to 0.1 μM for 6 h. Twofold to fourfold increases in nucleosome accumulation were observed (Fig. 1A). Since 0.1 μM ANS induced the greatest response, we examined caspase 3/7 activation over time and found that caspases were significantly activated by 3 h of treatment, with greater increases observed after 6 h in response to this concentration of ANS (Fig. 1B). Time course analysis indicated that the increase observed at 6 h represented the maximal response and that this was sustained through 16 h (data not shown). ANS activated the intrinsic pathway as shown by the finding that treatment with 0.1 μM ANS for 6 h activated caspase 9 but not caspase 8 (Fig. 1C).

IGFBP-3 mRNA levels followed a similar concentration and time-dependent pattern in response to ANS (Fig. 2A and B). Significant increases in IGFBP-3 mRNA were observed following 6 h of treatment with 0.025 to 0.1 μM ANS, respectively (Fig. 2A). Following exposure to 0.1 μM ANS, significant increases in IGFBP-3 mRNA levels were detected by 3 h with greater increases observed by 6 h of treatment (Fig. 2B). As shown in Fig. 3A, increases in IGFBP-3 protein in whole cell lysates were detected as early as 3 h following ANS treatment with maximal increases observed at 8 h. Increases in IGFBP-3 protein in cell lysates were sustained through 24 h. IGFBP-3 was also secreted by the cell as evidenced by its increase in conditioned media (Fig. 3B). IGFBP-3 protein was present as a doublet in both whole cell lysates and conditioned media, as shown by others (77,158), representing glycosylated forms of the protein (101). IGFBP-2 is the major IGFBP synthesized by these cells under basal conditions (152). As shown in Fig. 3A and

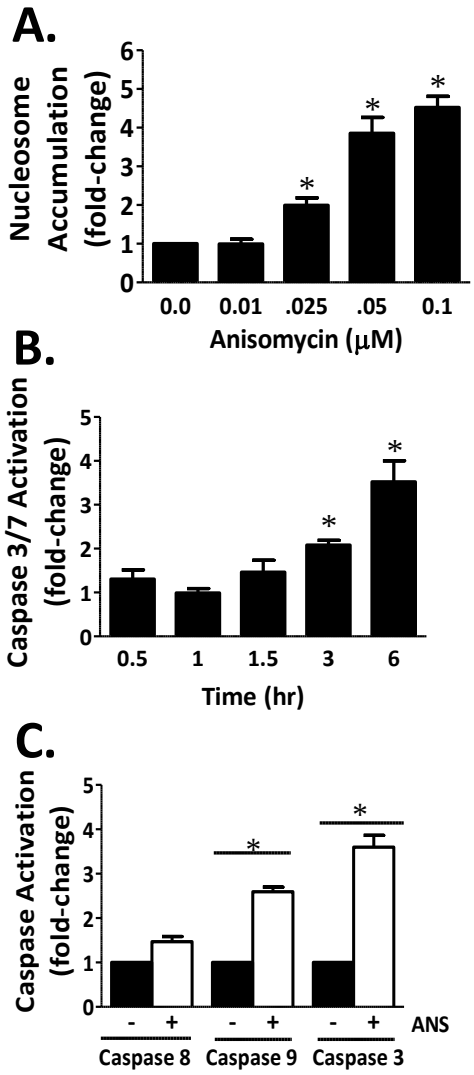

Fig. 1. Anisomycin (ANS) induces the intrinsic apoptotic pathway in a concentration- and time-dependent manner. Confluent MAC-T cells were serum-starved overnight and treated with ANS. (A) After 6 h of treatment apoptosis was measured by nucleosome accumulation with the Cell Death Detection ELISA^{PLUS} Assay (Roche). (B) Caspase 3/7 activation was measured by the Sensolyte Homogenous AMC Caspase-3/7 Caspase Assay (AnaSpec) after treatment with 0.1 μM ANS for the indicated times. (C) Cells were treated with ANS for 6 h. Caspase activity was measured by fluorescence using SensoLyte kits for individual caspases. Bars represent mean ± SEM of 3 independent experiments, with each treatment performed in triplicate within experiments. * indicates $P < 0.05$.

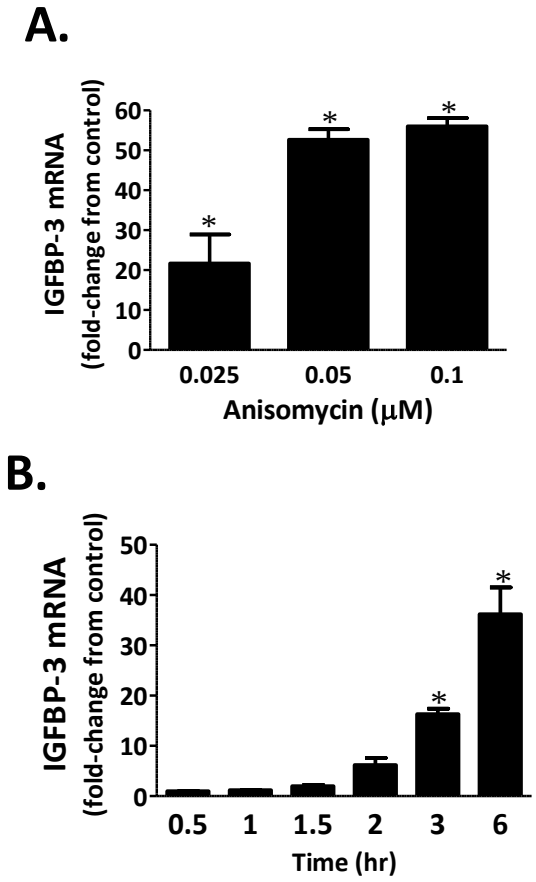

Fig. 2. Anisomycin (ANS) induces IGFBP-3 mRNA in a concentration and time-dependent manner. (A) Confluent MAC-T cells were serum-starved overnight and treated with ANS for 6 h or (B) with 0.1 μM ANS for increasing periods of time. Total RNA was collected and IGFBP-3 mRNA levels were analyzed by qRT-PCR, with data corrected for cyclophilin levels. Bars represent mean ± SEM of at least 3 independent experiments, with each treatment measured in triplicate within experiments. * indicates $P < 0.05$.

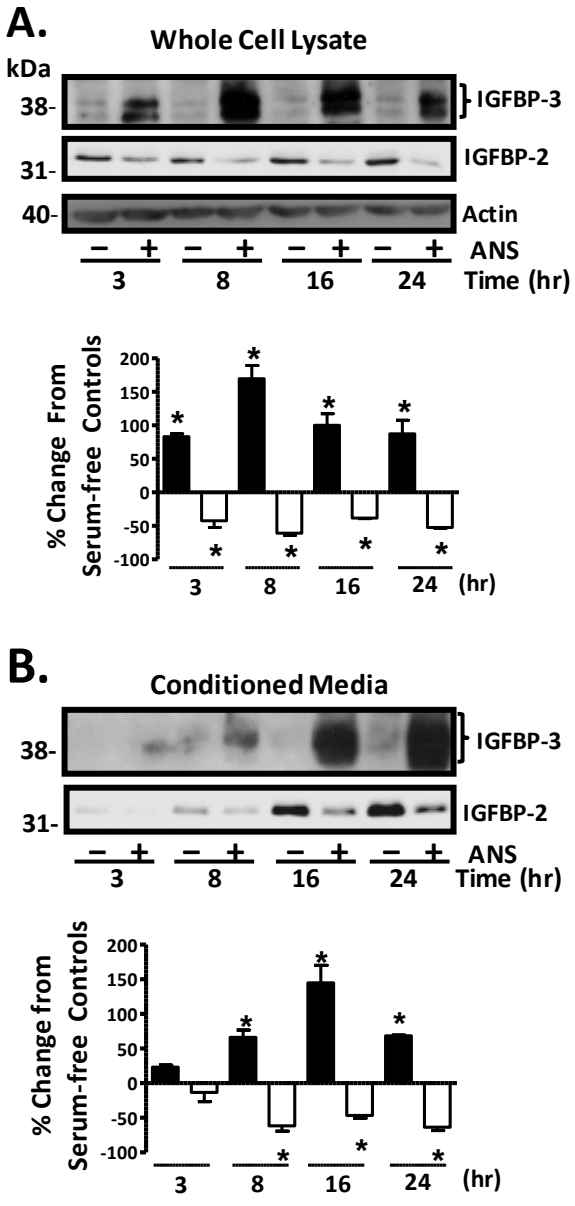

Fig. 3. Anisomycin (ANS) induces IGFBP-3 protein production in a time-dependent manner. Confluent MAC-T cells were serum-starved overnight and treated with ANS (0.1 μM) for the indicated times. Conditioned media were collected prior to cell lysis. (A) Total protein from whole cell lysates (50 μg) or (B) equal volumes of conditioned media were analyzed by SDS PAGE and immunoblotted with antibodies against IGFBP-3 and IGFBP-2. Immunoblots are representative of three independent experiments. Data were quantified by densitometry. IGFBP-3 and IGFBP-2 in whole cell lysates were corrected for loading using actin. Black bars represent IGFBP-3 and white bars represent IGFBP-2. Bars represent mean ± SEM of three experiments. * indicates $P < 0.05$ compared to serum-free control at each time point.

B, the abundance of IGFBP-2 in whole cell lysates and conditioned media from ANS-treated cells decreased over time relative to serum-free controls at each time point, indicating that the stimulatory effect of ANS on IGFBP-3 was specific to this form of IGFBP. ANS did not cause a change in the levels of any other form of IGFBP (data not shown).

IGFBP-3 plays a role in ANS-induced apoptosis

To determine if IGFBP-3 was required for ANS-induced apoptosis, IGFBP-3 was knocked down with siRNA. Knock-down of IGFBP-2 was also conducted to assess if the response was specific for IGFBP-3. As shown in Fig. 4A and B, treatment with siRNA for IGFBP-3 and IGFBP-2 effectively reduced ANS-induced IGFBP-3 and basal IGFBP-2, respectively, in both conditioned media and whole cell lysates. Knock-down of IGFBP-3 did not affect the ability of ANS to reduce IGFBP-2 levels while conversely, IGFBP-2 knock-down did not affect the ability of ANS to induce IGFBP-3 levels (Fig. 4B). Interestingly, knock-down of IGFBP-3 with or without ANS led to an increase in IGFBP-2 relative to the respective scramble controls. TUNEL staining (Fig. 4C) and PARP cleavage (Fig. 5B) were used to determine the effect of IGFBP-3 or -2 knock-down on ANS-induced apoptosis. In IGFBP-3 knock-down cells, the ability of ANS to induce apoptosis was reduced, while knock-down of IGFBP-2 had no effect on this response. This was associated with reductions in caspase 3/7 activation in cells treated with IGFBP-3 siRNA relative to cells treated with IGFBP-2 or control siRNA (Fig. 5A). Western immunoblotting with antibodies that recognize the cleaved forms of caspase 3 and -7 showed that cleavage of both caspases was attenuated when IGFBP-3 was knocked down (Fig. 5B). Knock-down of IGFBP-3 also attenuated the release of mitochondrial cytochrome C, a hallmark of the intrinsic apoptotic pathway induced by ANS (Fig. 5C).

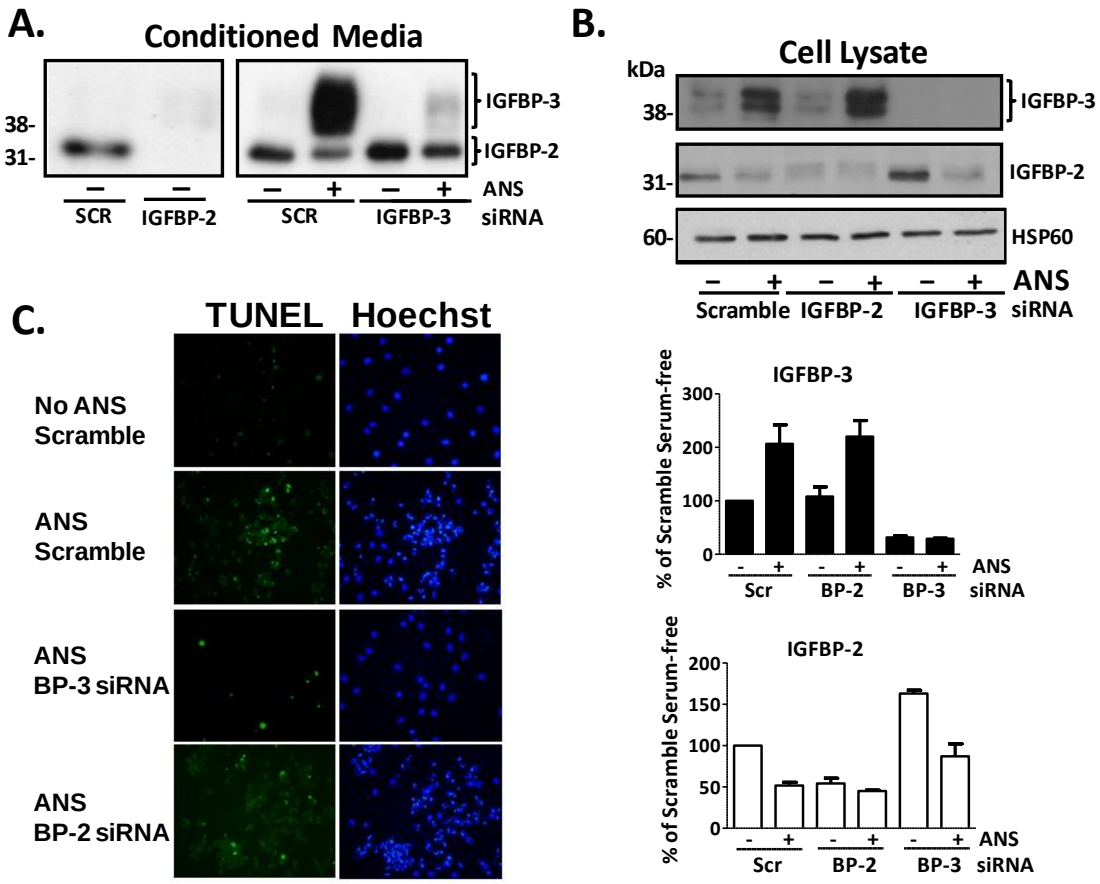

Fig. 4. Knock-down of IGFBP-3 attenuates anisomycin (ANS)-induced apoptosis. MAC-T cells were transfected with 50 nM IGFBP-3, IGFBP-2 or scramble siRNA for 48 h, serum-starved overnight, and treated with ANS (0.1 µM). (A) Equal volumes of conditioned media collected after 24 h exposure to ANS were analyzed by western ligand blotting with [^{125}I]-IGF-I. The knock-downs of IGFBP-3 and IGFBP-2 were performed in separate experiments. (B) Cell lysates collected after 6 h exposure to ANS were immunoblotted with IGFBP-3, IGFBP-2 and actin. Knock-downs of IGFBP-3 and -2 were performed in the same experiments. Data were quantified by densitometry. IGFBP-3 and IGFBP-2 in whole cell lysates were corrected for loading using HSP60. Black bars (■) represent IGFBP-3 and white bars (□) represent IGFBP-2. Bars represent mean ± SEM of three experiments. (C) Apoptosis was measured after 6 h exposure to ANS by TUNEL staining with the In Situ Cell Death Detection Kit, Fluorescein (Roche). Immunoblots and cell staining are representative of three independent experiments.

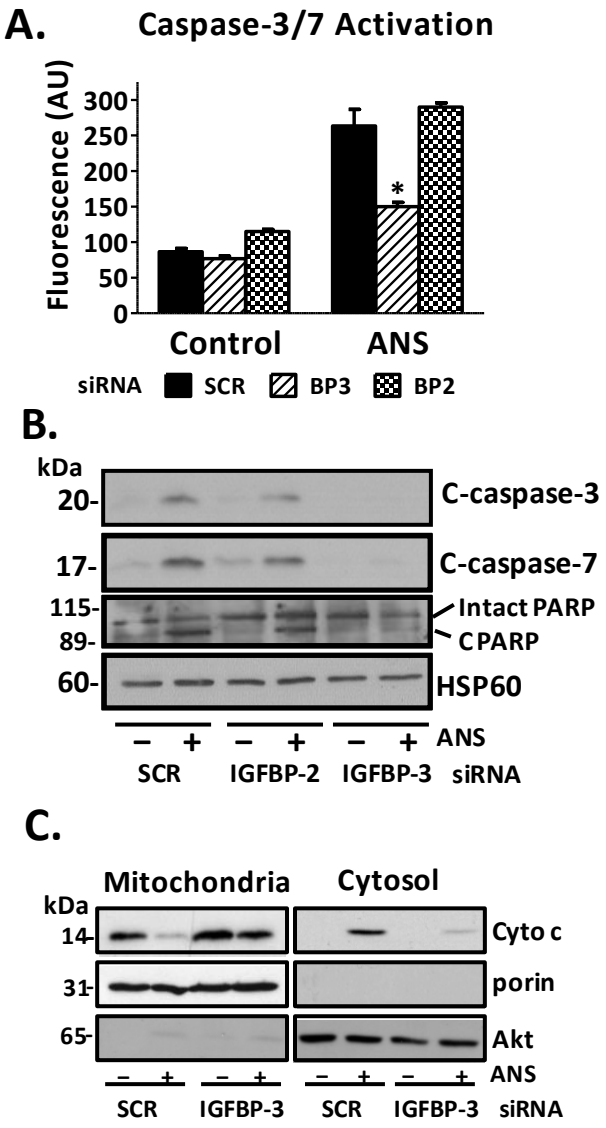

Fig. 5. Knock-down of IGFBP-3 attenuates anisomycin (ANS)-induced caspase activation, PARP cleavage and release of mitochondrial cytochrome C. MAC-T cells were transfected with 50 nM siRNA for 48 h, serum-starved overnight, and treated with 0.1 µM ANS for 6 h. (A) Caspase activation was measured with the Sensolyte Homogenous AMC Caspase-3/7 Assay (AnaSpec). Bars represent mean ± SEM of at least 3 independent experiments. * $P < 0.05$; Different from scramble siRNA + ANS and IGFBP-2 siRNA + ANS. (B) Cell lysates were immunoblotted with antibodies that recognize cleaved caspase 3 or -7 and PARP. HSP60 was used as a loading control. (C) Cells were fractionated into mitochondrial and cytosolic protein fractions and immunoblotted for cytochrome C. Porin and Akt were used as mitochondrial and cytoplasmic markers, respectively. Blots are representative of three independent experiments.

Transfection with IGFBP-3 does not induce apoptosis

To determine if IGFBP-3 could induce apoptosis independent of ANS, MAC-T cells were transfected with a mammalian expression vector containing bovine IGFBP-3 cDNA. As shown in Fig. 6, transfection with IGFBP-3 resulted in expression of IGFBP-3 in both whole cell lysates and conditioned media. However, there was no effect of transfection on caspase 3/7 activation. Untransfected cells treated with or without ANS for 6 h were included as positive controls.

IGFBP-3 localizes to the nucleus in cells treated with ANS but not IGF-I

Similar to ANS, IGF-I is also a potent inducer of IGFBP-3 secretion in MAC-T cells as well as primary bovine MEC (152,153). However, ANS and IGF-I produce opposite physiological outcomes i.e., apoptosis versus cell proliferation and survival, respectively. Since nuclear localization of IGFBP-3 has been proposed to play a role in IGFBP-3 induced apoptosis, we hypothesized that ANS and IGF-I may differ in their ability to induce nuclear localization of IGFBP-3. To test this hypothesis, cells were treated with ANS or IGF-I and fractionated into nuclear and cytosolic compartments (Fig. 7A). Under serum-free conditions, IGFBP-3 was low to undetectable in both the cytosol and the nucleus. When cells were treated with ANS, IGFBP-3 was detected in the nucleus by 3 h of treatment, with even larger increases observed by 8 h. In contrast, IGFBP-3 was not detectable in the nucleus between 3 and 8 h (data not shown) or between 16 and 24 h (Fig. 7B), even though considerable IGFBP-3 was present in the media conditioned by cells treated with IGF-I (Fig. 7C). Similar IGFBP-3 levels were observed in media conditioned by either ANS or IGF-I between 16 and 24 h (Fig. 7C).

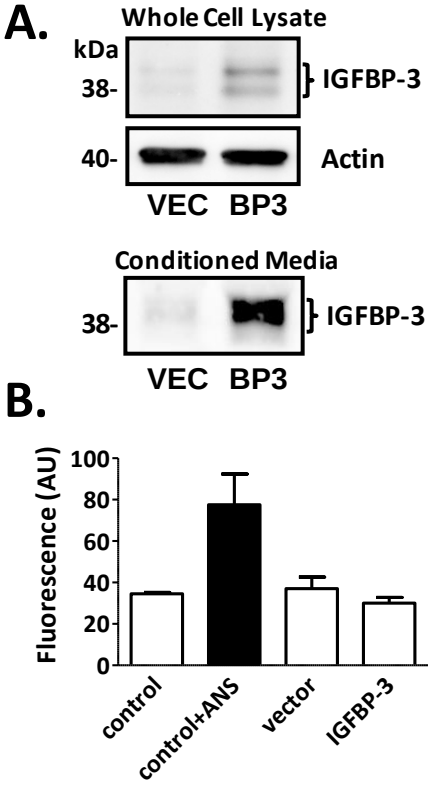

Fig. 6. Transfection with IGFBP-3 does not induce caspase activation. MAC-T cells were transfected with empty vector (vec) or IGFBP-3 expression plasmid. (A) Whole cell lysates and conditioned media were collected and immunoblotted for IGFBP-3 and actin. Blots are representative of three independent experiments. (B) Caspase activity was measured by fluorescence using the Sensolyte Homogenous AMC Caspase-3/7 Fluorometric Assay (AnaSpec). Untransfected cells treated ± 0.1 µM ANS for the last 6 h were included as positive controls. Bars represent mean ± SD of 2 independent experiments, with each treatment performed in triplicate within experiments.

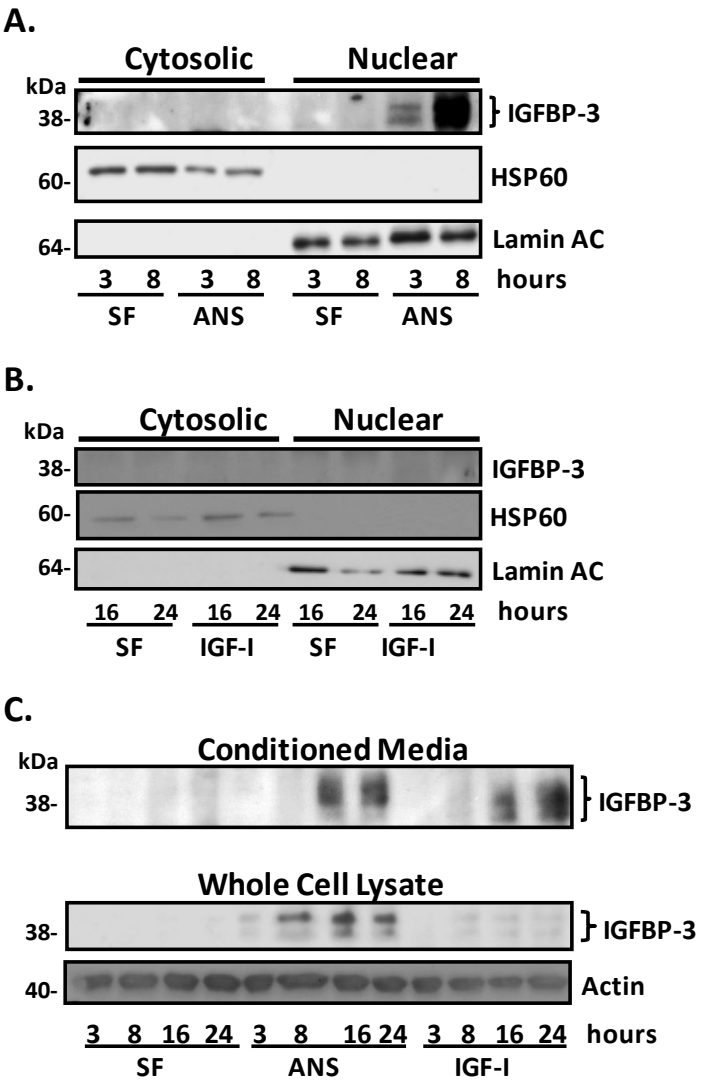

Fig. 7. Anisomycin (ANS) but not IGF-I directs IGFBP-3 to the nucleus. MAC-T cells were serum-starved overnight and treated with IGF-I (100 ng/ml) or ANS (0.1 µM) for the indicated times. (A-B) Cytosolic (50 µg) and nuclear (30 µg) fractions were isolated and immunoblotted for IGFBP-3, HSP60 and lamin AC. (C) Equal concentrations of conditioned media (100 µl) or whole cell lysates (30 µg) were immunoblotted for IGFBP-3. Actin was used as a loading control. Blots are representative of four independent experiments.

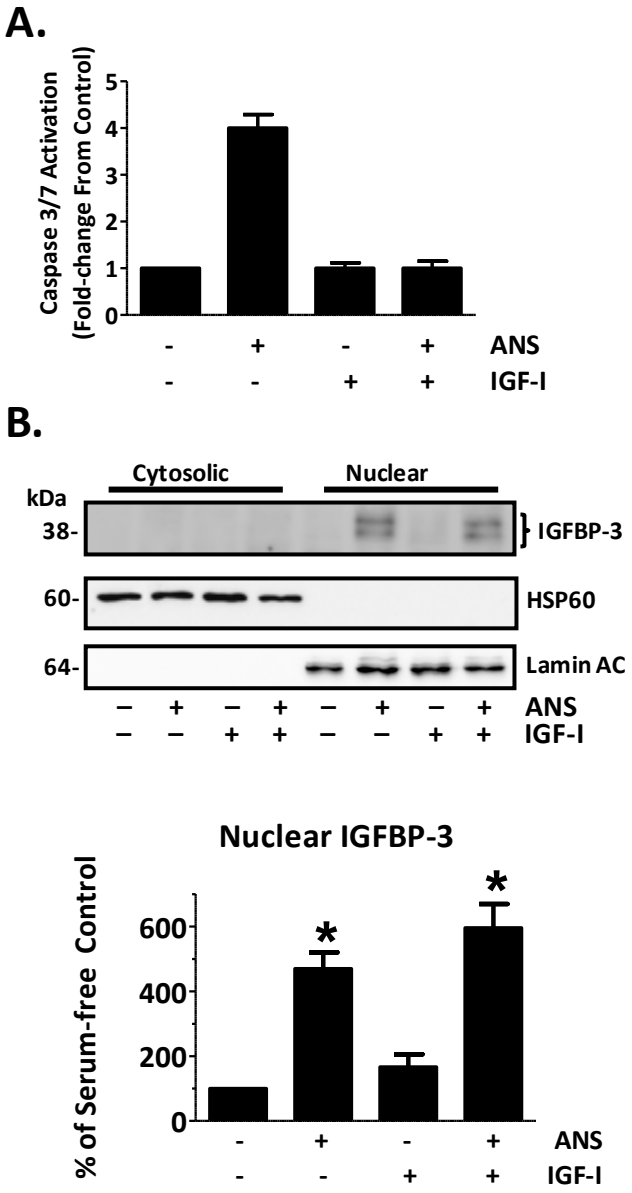

Fig. 8. IGF-I prevents ANS-induced apoptosis but not nuclear localization of IGFBP-3. MAC-T cells were serum-starved overnight and treated ± ANS (0.1 µM), IGF-I (100 ng/ml), or IGF-I + ANS for 8 h. (A) Caspase activity was measured by fluorescence using the Sensolyte Homogenous AMC Caspase-3/7 Fluorometric Assay (AnaSpec). Bars represent mean ± SEM of 3 independent experiments, with each treatment performed in triplicate within experiments. (B) Cytosolic (50 µg) and nuclear (30 µg) fractions were isolated and immunoblotted for IGFBP-3, HSP60 and lamin AC. Blots are representative of three independent experiments. Data were quantified by densitometry. Nuclear IGFBP-3 was corrected for loading using lamin AC. Bars represent meant ± SEM of three experiments. * indicates $P < 0.05$ compared to serum-free control. Nuclear IGFBP-3 was not different between ANS and ANS + IGF-I.

IGF-I prevents ANS-induced apoptosis but not nuclear localization of IGFBP-3

Since IGF-I and ANS have divergent effects on both apoptosis and nuclear localization of IGFBP-3 we determined the effect of treating cells with a combination of these agents. As shown in Fig. 8A, the addition of IGF-I completely blocked the ability of ANS to induce caspase activation. However, ANS-induced nuclear localization of IGFBP-3 still occurred.

IGFBP-3 is directed to the nucleus in ANS-treated cells in the absence of caspase activation

In order to determine if nuclear localization of IGFBP-3 occurs upstream of caspase activation, cells were treated with a caspase 3/7 inhibitor to block ANS-induced apoptosis. As shown in Fig. 9A, the pan caspase inhibitor Z-VAD-FMK completely blocked caspase 3/7 activation. However, cell fractionation experiments showed that IGFBP-3 still localized to the nucleus (Fig. 9B), indicating that nuclear localization occurs upstream of caspase 3/7 activation in the apoptotic cascade.

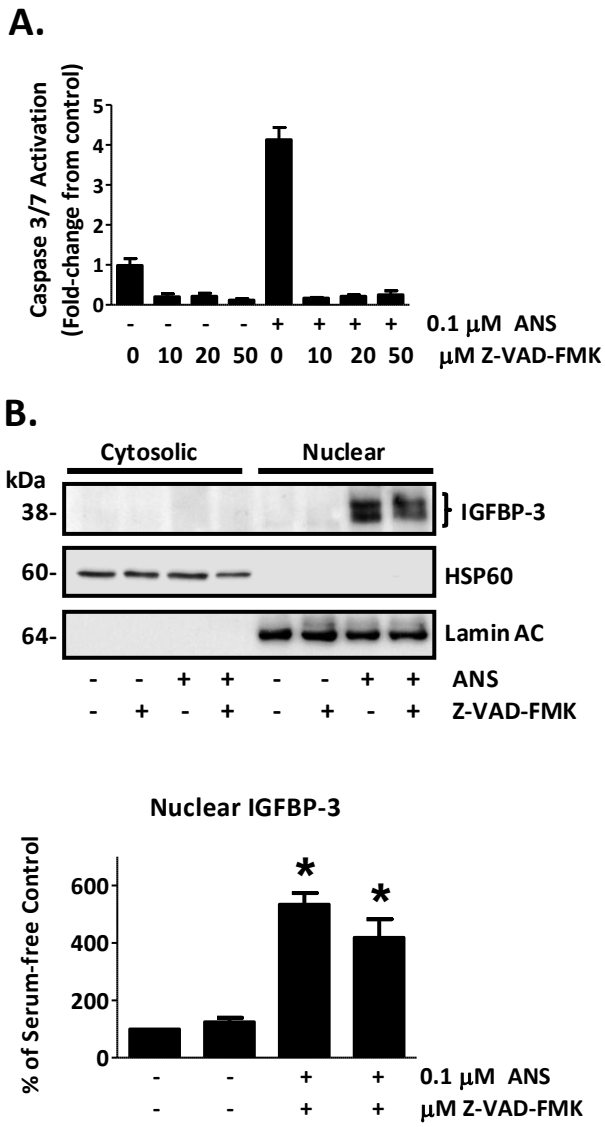

Fig. 9. IGFBP-3 is directed to the nucleus in the absence of caspase activation. Confluent MAC-T cells were serum-starved overnight and treated ± 0.1 μM ANS ± the pan-caspase-inhibitor Z-VAD-FMK for 6 h. (A) Caspase activity was measured by fluorescence using the Sensolyte Homogenous AMC Caspase-3/7 Fluorometric Assay (AnaSpec). A representative experiment is shown. Bars indicate mean ± SD of 3 triplicate wells per treatment. (B) Cells were treated ± 10 μM Z-VAD-FMK. Cytosolic (50 μg) and nuclear (30 μg) fractions were isolated and immunoblotted for IGFBP-3, HSP60 and lamin AC. Immunoblots are representative of four independent experiments. Data were quantified by densitometry. Nuclear IGFBP-3 was corrected for loading using lamin AC. Bars represent mean ± SEMof three experiments. * indicates $P < 0.05$ compared to serum-free control. Nuclear IGFBP-3 was not different between ANS and ANS + Z-VAD-FMK.

Discussion

Multiple molecules that are growth inhibitory, proapoptotic or both induce IGFBP-3 in vitro and reduction of IGFBP-3 in these systems often abrogates the ability of these factors to elicit growth inhibition or apoptosis (reviewed in (9)). The majority of these studies have focused on growth inhibition and the few that have examined apoptosis have used cancer cell lines (67,159,160). In the present study, we show that activating the intrinsic apoptotic pathway with ANS induces both IGFBP-3 production and apoptosis in non-transformed MEC. Knockdown of IGFBP-3 with siRNA significantly reduces the apoptotic response by attenuating ANS-induced release of mitochondrial cytochrome c and subsequent caspase activation, demonstrating a role for IGFBP-3 in the intrinsic apoptotic pathway. Interestingly, increasing intracellular IGFBP-3 via transient transfection alone does not induce caspase activation in MAC-T cells.

While IGFBP-3 is a secreted protein, it contains a bipartite nuclear localization signal in its conserved C-terminal domain and can localize to the nucleus where it may play a role in IGFBP-3-induced apoptosis. Since IGF-I also increases IGFBP-3 production in bovine MECs (152) and knock-down of IGFBP-3 attenuates both basal and IGF-I-stimulated proliferation (154), we hypothesized that differences in cellular localization of IGFBP-3 might be observed with IGF-I and ANS. The idea that IGFBP-3 may have a nuclear mode of action originated with studies that detected fluorescently labeled IGFBP-3 in the nucleus following its addition to cell culture supernatants (86,87,161,162). Interestingly, in most of these studies nuclear uptake was observed in cells that appeared to be actively dividing**.** Later studies went on to show that exogenous IGFBP-3 localizes to the nucleus and induces apoptosis (60,81,151). Fewer studies have examined the ability of exogenous apoptotic or growth inhibitory agents to induce nuclear localization of endogenously produced IGFBP-3. Nuclear localization is induced by TNF-α in

insulin-secreting tumor cell lines (160) and by TGF-β in PC3 prostate cancer cells (81). Following treatment of porcine embryonic myogenic cells with TGF-β, IGFBP-3 is detectable in almost all nuclei compared with 50% of untreated cells (7). In the present study we show that IGFBP-3 is low to undetectable in the nuclear fraction of untreated MECs. Treatment with ANS induces relatively rapid production and nuclear localization of IGFBP-3 (within three h) that corresponds with caspase activation. While IGFBP-3 accumulates in the conditioned media following exposure to either ANS or IGF-I, nuclear localization of IGFBP-3 is only observed with ANS, supporting our hypothesis that cellular localization of IGFBP-3 may determine its function. Inhibiting caspase activation with a pan caspase inhibitor did not affect nuclear localization of IGFBP-3, indicating that this occurs upstream of mitochondrial cytochrome c release and subsequent caspase activation. We have reported that the IGFBP profile in untreated and IGF-I-treated cells is similar between MAC-T cells and primary bovine MEC, with very low levels of IGFBP-3 detected in untreated primary cells similar to MAC-T cells (153). Anisomycin also induces apoptosis and IGFBP-3 mRNA levels in primary bovine MEC (our unpublished data). Therefore it will be important to determine if nuclear IGFBP-3 is also detected when primary bovine MEC are treated with ANS.

IGFBP-3 still localized to the nucleus in cells treated with a combination of IGF-I and ANS even though ANS-induced caspase activation was prevented. ANS exerts its effects on apoptosis through activation of the JNK signaling pathway (25,154,155,163) while IGF-I exerts many of its pro-survival effects through activation of AKT (148). Both signaling pathways affect multiple control points in the apoptotic machinery to regulate apoptosis, including transcriptional activation of pro- or anti-apoptotic genes and post-translational modifications that affect protein-protein interactions to control mitochondrial membrane permeability and subsequent

caspase activation (148,164). Regulation of the Bcl-2 family of proteins represents a major focal point of these regulatory pathways (16,148,164). To our knowledge, the ability of IGF-I to block ANS-induced apoptosis has not been examined. However, IGF-I has been shown to block activation of the intrinsic apoptotic pathway by other stressors via the regulation of Bcl-2 proteins through multiple mechanisms (20,165-167). Work in breast cancer cells has shown that IGFBP-3 transfection increases the ratio of pro-apoptotic to anti-apoptotic members of the Bcl-2 family (84) and increases levels of the inactive, serine phosphorylated form of Bcl-2 in prostate cancer cells (67). Interestingly, Bax has recently been shown to interact with IGFBP-3 at the level of the mitochondria to trigger the intrinsic apoptotic pathway (85). Studies are presently in progress to determine if ANS and IGF-I mediate apoptosis and survival, respectively, by affecting Bcl-2 proteins in MAC-T cells and if IGFBP-3 is required for these responses.

In the present work, levels of IGFBP-3 and IGFBP-2 were found to be inversely regulated by ANS. In addition, knock-down of IGFBP-3 with siRNA increased IGFBP-2 levels in the absence or presence of ANS relative to their respective scramble control. However, IGFBP-2 levels were still inhibited with ANS treatment in IGFBP-3 knockdown cells. Similar to IGFBP-3, IGFBP-2 exerts both IGF-dependent as well as IGF-independent effects to either stimulate or inhibit multiple cellular processes depending on cell type and physiological condition (9,168). Of relevance to the present study, overexpression of IGFBP-2 in lung adenocarcinoma cells decreased procaspase 3 expression and inhibited camptothecin-induced apoptosis. Opposite effects were observed with siRNA knock-down of IGFBP-2 (169). Thus it is possible that IGFBP-2 has a pro-survival effect in MAC-T cells and that inhibition of IGFBP-2 by either ANS or IGFBP-3 might play a role in ANS-induced apoptosis.

In studies with TGF-β-treated PC3 cells, nuclear localization of IGFBP-3 was dramatically reduced by addition of an IGFBP-3 neutralizing antibody to the conditioned media, suggesting that secreted IGFBP-3 was being internalized and directed to the nucleus (81). They also found that addition of exogenous IGFBP-3 together with IGF-I or Leu60 IGF-I, which binds IGFBP-3 but not the IGF receptor, reduces nuclear IGFBP-3, while this effect is not observed with an IGF-I analogue that does not bind IGFBPs, suggesting that binding to IGF-I prevented internalization of IGFBP-3. Recent work using electron and confocal microscopy of intact living osteosarcoma cells confirms that exogenous IGFBP-3 is internalized via three major endocytic pathways (170), confirming earlier work by Lee and coworkers (81). In our study, IGFBP-3 produced in response to ANS may first be secreted, then re-internalized and directed to the nucleus, while IGFBP-3 produced in response to IGF-I may fail to be internalized because it binds IGF-I in the conditioned media.

Several mechanisms have been proposed for how nuclear IGFBP-3 may play a role in apoptosis. Exogenous IGFBP-3 has been shown to mediate apoptosis by binding to RXRα in the nucleus and affecting transcription of retinoid-responsive genes (151,171). In contrast, Lee et al. proposed a mechanism whereby IGFBP-3 can interact with RXRα in the nucleus and facilitate interaction with Nur77, causing the RXRα/Nur77 complex to translocate to the mitochondria to induce apoptosis (91). However, others have used mutational analysis to show that IGFBP-3 can induce apoptosis in prostate and breast cancer cells in an IGF-independent manner without either binding RXR-α or localizing to the nucleus (80,90). The recent report that a specific IGFBP-3 receptor may mediate the effects of exogenous IGFBP-3 through a death receptor-mediated pathway provides a mechanism by which IGFBP-3 could induce apoptosis independent of nuclear localization (82). However, our data do not support a role for an IGFBP-3 receptor in

MAC-T cells. Collectively, these studies have led to the idea that IGFBP-3 can promote apoptosis through multiple mechanisms. It should be noted that the preponderance of these studies have been conducted with either addition of exogenous IGFBP-3 or genetically engineered overexpression of IGFBP-3, with the goal of using IGFBP-3 as a therapeutic tool to inhibit cancer progression. However, how endogenous IGFBP-3 is involved in the ability of physiological stimuli to induce apoptosis in noncancerous cells is relatively unexplored.

Activation of the intrinsic apoptotic pathway can be induced by many stressors, including withdrawal of growth factors (172). The factors that cause apoptosis of mammary epithelial cells during the declining phase of the lactation curve in dairy cattle or during involution following cessation of milking is unknown, but could be related to withdrawal of growth factors such as IGF-I. Further studies will be aimed at determining how nuclear IGFBP-3 plays a role in this apoptotic pathway in non-transformed cells.

Chapter 3.

IGFBP-3 mediates intrinsic apoptosis through modulation of Nur77 phosphorylation and nuclear export

Abstract

While IGFBP-3 localizes to the nucleus during apoptosis, its nuclear function remains unclear. We previously reported that in the non-transformed bovine mammary epithelial cell line MAC-T the intrinsic apoptosis inducer anisomycin (ANS) activates production and nuclear localization of IGFBP-3, and that IGFBP-3 knock-down attenuates ANS-induced apoptosis. Exogenous IGFBP-3 has been shown to induce apoptosis by facilitating nuclear export of the orphan receptor Nur77 in prostate cancer cells. Therefore the goal of the present work was to determine if Nur77 plays an IGFBP-3-dependent role in intrinsic apoptosis. Knock-down of Nur77 with siRNA decreased ANS-induced cleavage of caspases 3 & 7 and their downstream target PARP, indicating a role for Nur77 in ANS-induced apoptosis. Cellular fractionation and immunofluorescence showed that ANS induced phosphorylation and nuclear export of Nur77. These effects were attenuated by knock-down of IGFBP-3. Knock-down of Jun-N-terminal kinase (JNK) with siRNA also reduced ANS-induced Nur77 phosphorylation and nuclear export. Co-immunoprecipitation experiments showed that ANS induces association of IGFBP-3 with Nur77, suggesting that IGFBP-3 may bind Nur77 in the nucleus and facilitate its activation by JNK, which is required for its nuclear export. These data indicate for the first time that endogenous IGFBP-3 may play a role in intrinsic apoptosis by interacting with Nur77 to facilitate its nuclear export.

Introduction

A role for IGFBP-3 in apoptosis is well-accepted. Addition of IGFBP-3 to cell culture supernatant or expression of IGFBP-3 induces apoptosis in breast and prostate cancer cells, and osteosarcoma cells (59,60,81,83). Alternatively, in other studies IGFBP-3 does not induce apoptosis directly but instead augments the effects of other apoptotic stressors (65,66,106). While several potential mechanisms have been proposed, a complete understanding of how IGFBP-3 induces or potentiates apoptosis is lacking.

IGFBP-3 is found in the nucleus of multiple cell types during apoptosis (7,60,81). Nuclear IGFBP-3 is reported to bind nuclear transcription factors Nur77 and RXRα. In prostate cancer cells treated with exogenous IGFBP-3, IGFBP-3 is found in the nucleus where it interacts with nuclear receptor retinoid X receptor-α (RXRα) (90). Nuclear IGFBP-3 facilitates the association of RXRα with orphan nuclear receptor Nur77. This RXRα/Nur77 complex translocates from the nucleus to the cytoplasm, ultimately causing caspase activation and inducing apoptosis (91). In addition, siRNA knock-down of either RXRα or Nur77 inhibits the stress-induced movement of the other in prostate cancer cells (92). A potential nuclear export sequence (NES) has been identified in IGFBP-3 and mutation of this sequence inhibits nuclear export of not just IGFBP-3, but also of the RXRα/Nur77-complex in prostate cancer cells (93).

Nur77 is an orphan nuclear receptor that is transcriptionally active in the nucleus of proliferating cells (121,128). Upon phosphorylation Nur77 is exported out of the nucleus, inhibiting its nuclear function and permitting its apoptotic functions in the cytoplasm (128,131-133). Nur77 is required for apoptosis in breast cancer cells, pancreatic cancer cells, and murine epithelial fibroblasts (91,95,96). Treatment of prostate cancer cells with IGFBP-3 induces activation of JNK

and nuclear export of phosphorylated Nur77 suggesting that these two proteins could co-regulate activation and localization of Nur77 (94).

Anisomycin (ANS) induces intrinsic apoptosis in MAC-T cells (Chapter 2), and has been used to study the apoptotic response in multiple cell types, including HEK293T cells (133) and human hepatoma HuH7 cells (135). We found previously that ANS also induces IGFBP-3 mRNA and protein, and siRNA knock-down of IGFBP-3 attenuates ANS-induced apoptosis, indicated by absence of mitochondrial cytochrome c release and reduced caspase 3&7 activation (Chapter 2). These data established a role for IGFBP-3 in ANS-induced intrinsic apoptosis in MAC-T cells. JNK2 is also activated by ANS in a number of cell lines (66,130,135,173) and is reported to play a role in intrinsic apoptosis (173,174). In contrast to prostate cancer cells, IGFBP-3 does not contribute to activation of JNK in MAC-T cells (66). However, JNK is reported to phosphorylate Nur77 so it is likely that IGFBP-3 acts downstream of JNK activation (130,133). The objective of this study was to determine if IGFBP-3 and JNK exert their apoptotic effects by modulating activation and localization of Nur77 in non-transformed mammary epithelial cells.

Materials and Methods

Chemical reagents

Phenol red-free (PRF) DMEM-low glucose media, gentamicin, bovine insulin, ANS, and fetal bovine serum (FBS) were purchased from Sigma (St. Louis MO). DMEM with high glucose, penicillin and streptomycin were purchased from Invitrogen (Carlsbad, CA). Anisomycin was purchased from Sigma. Antibodies against the following proteins were purchased as indicated: PARP, JNK, and cleaved caspase 3 and -7 (Cell Signaling Technology, Inc., Danvers, MA), actin (EMD-Calbiochem, La Jolla, CA), HSP60 (Abcam, Cambridge, MA), Nur77 (Active Motif, Carlsbad, CA), phospho-Nur77, phospho-JNK, RXRα, Bax and lamin AC (Santa Cruz, Dallas, TX), AKT (Upstate, Billerica, MA), porin (MitoSciences, Eugene, OR), anti-His (Genscript, Piscataway, NJ) anti-rabbit IgG (GE, Pittsburgh, PA), Alexafluor415 anti-rabbit IgG (Invitrogen). A polyclonal antibody against bovine IGFBP-3 was kindly provided by Dr. David Clemmons, University of North Carolina at Chapel Hill. Custom SmartPool siRNA for bovine IGFBP-3, JNK2, and scramble siRNA control were purchased from Dharmacon, Inc (Lafayette, CO). Custom siRNA for bovine Nur77 was purchased from Sigma (St. Louis, MO). Mirus Transit TKO transfection reagent was purchased from Stratagene (La Jolla, Ca).

Cell culture

The bovine MEC line MAC-T (137) was routinely maintained in complete media consisting of DMEM containing 4.5 g/liter D-glucose (i.e., DMEM-H), 20 U/ml penicillin, 20 μg/ml streptomycin, 50 μg/ml gentamicin, 10% FBS, and 5mg/ml insulin. For experiments, cells were plated and grown to confluence in phenol red-free DMEM-H containing 10% FBS and antibiotics and without insulin. Cells were rinsed with phosphate-buffered saline (PBS), and incubated in

serum-free (SF) DMEM-H with 0.2% BSA and 30 nM sodium selenite overnight prior to exposure to treatments in SF DMEM-H without additives.

Cell fractionation and Western immunoblotting

Whole cell lysates were collected in lysis buffer (1% Triton-X 100, 50 mM HEPES, 80 mM β-glycerophosphate, 2 mM EDTA, 2 mM EGTA, 10 mM NaF, 0.1% SDS, supplemented with 0.1 mM PMSF, 1 µg/ml each of aprotinin, leupeptin, and trypsin inhibitor, 10 mM NaF and 2 mM NaO) or in lysis buffer AM1 (Active Motif) supplemented with protease inhibitors. Cells collected with lysis buffer were incubated 30 min on ice then centrifuged 10,000 x g for 10 min. Cells collected in AM1 were collected according to manufacturer's instructions. For nuclear and cytosolic extraction, cytosolic extracts were obtained by lysing cells in hypertonic buffer (20 mM Hepes pH 7, 10 mM KCL, 0.1% Triton, 20% glycerol supplemented with 1 mM DTT, 1 mM PMSF, 1 µg/ml each of aprotinin, leupeptin, and trypsin inhibitor, 10 mM NaF and 2 mM NaO) with 10 strokes of the dounce homogenizer followed by centrifugation for 5 min at 1000 x g. Pellets were resuspended in buffer C (20 mM Hepes pH 7.9, 0.42 M NaCl, 1.5 mM $MgCl_2$, 0.2 mM EDTA, 25% glycerol, supplemented with 0.1 mM DTT, 0.1 mM PMSF, 1 µg/ml each of aprotinin, leupeptin, and trypsin inhibitor, 10 mM NaF and 2 mM NaO), incubated on ice 30 min, then centrifuged at 13,250 RPM for 10 min and the supernatant was saved as the nuclear fraction.

To obtain the mitochondrial fraction cells were suspended in homogenization buffer (10 mM HEPES pH 7.4, 0.25 M sucrose, 1 mM EGTA, supplemented with 1 mM PMSF, 1 µg/ml each of aprotinin, leupeptin, and trypsin inhibitor, 10 mM NaF and 2 mM NaO) then subjected to 40 strokes of the dounce homogenizer. Nuclei and intact cells were pelleted by centrifuging lysates 15 min at 1000 x g. The supernatant was transferred to a fresh tube then centrifuged 15 min at

10,000 x g. The resulting supernatant was saved as the cytosolic fraction and the pellet was resuspended in homogenization buffer to obtain the mitochondrial pellet. Lysates were assayed for protein with the BioRad Protein Assay (BioRad, Hercules, Ca). Proteins were separated by SDS polyacrylamide gel electrophoresis (PAGE) on 10 or 15% gels and transferred to nitrocellulose (0.2 μm; Bio-Rad) or PVDF (0.45 μM; Millipore, Billerica, MA) membranes. Membranes were blocked for 1 h at room temperature in Tris–buffered saline + 0.05% Tween-20 (v/v) (TBS-T) and 5% non-fat dried milk (w/v), and incubated with primary antisera at 4°C overnight with gentle agitation. Membranes were then washed in TBS-T and incubated for 1 h at room temperature with appropriate HRP-conjugated secondary antibodies. Peroxidase activity was detected with ECL Prime (GE, Pittsburgh, PA). Chemiluminescence was detected with the Fluorchem FC2 (Protein Simple, Santa Clara, CA).

Indirect immunofluorescence

Cells were plated on 8-well Ibidi (Martinsried, Germany) μ-slides for fluorescent imaging. To examine localization of endogenous Nur77, cells were grown to confluence then serum-starved overnight, treated ± ANS, then fixed with 10% neutral buffered formalin for 20 min, permeabilized with 0.1% Triton for 10 min, blocked 30 min with phosphate buffered saline (PBS) + 5% BSA. After blocking cells were incubated with 1:400 Nur77 (Active Motif) or phospho-Nur77 (Santa Cruz) in PBS + 5% BSA for 90 min, washed 3x with PBS and 2x with PBS + 5% BSA, followed by incubation with 1:500 AlexaFluor514 goat anti-rabbit (Invitrogen) in PBS + 5% BSA for 60 min, then washed 3x with PBS. Nuclei were stained with Hoechst (Invitrogen). Cells were stored in mounting media (Ibidi) and imaged with an Olympus FSX100 microscope. Nur77 and Hoechst signal were acquired each acquired separately, then an image overlaying both

wavelengths was acquired. Acquisition times were held constant for each antibody or stain to ensure differences in signal strength were not due to exposure time.

Construction of His-tagged IGFBP-3 (IGFBP3-His)

A PCR reaction was used to add a 6x-His tag to the C terminus of bovine IGFBP-3. *Xho*I and *Not*I restriction sites were added to the 5' and 3' ends, respectively, to flank the IGFBP-His sequence, producing a 923 bp IGFBP3-His fragment. The 50 µl PCR reaction contained 20 ng DNA template (pRc/RSV IGFBP3, Grill and Cohick, 2000), 20 pmol forward primer 5'-ATATTACTCGAG TAATGCTGCGGGCACGCCCCGCGCTC-3', 20 pmol reverse primer 5'-ATAGTTTAGCGGCCGCTCAATGGTGATGGTGATGATGCTTGCTCTCCATGCTGTAGCAGT-3', 2 mM Mg SO_4, 0.2 mM of each dNTP, 5% DMSO and 1 unit Platinum *Taq* High Fidelity DNA Polymerase (Life Technologies, Carlsbad, CA). The cycling parameters were 94˚C 2 min; 30 cycles of 94˚C 1 min, 55˚C 1 min, 68˚C 1 min; 68˚C 10 min. The IGFBP-3-His fragment was purified using Nucleospin Gel and PCR Clean-up kit (Macherey-Nagel, Bethlehem, PA). IGFBP3-His (insert) and pEGFP-N1 (vector) were digested with *Xho*I and *Not*I. This digestion excises EGFP from the plasmid. After vector dephosphorylation with Anarctic Phosphatase (New England Biolabs) both insert (902 bp) and vector (3945 bp) were purified as described above and ligated using T4 DNA Ligase (Invitrogen, Carlsbad, CA). The ligation reaction was used to transform One Shot TOP 10 competent cells (Invitrogen). After miniprep, colonies were screened for positive clones by restriction digestion. Bovine IGFBP3-His construction was confirmed by sequencing.

Transient transfection of IGFBP-3

MAC-T cells were plated in complete media at 3.5 x 10^4 cells/cm^2. The next day subconfluent cells were transfected with a plasmid encoding cDNA for IGFBP-3-His. Plasmids were prepared

using the EndoFree plasmid Maxi Kit (Qiagen, Valencia CA). Cells were transfected using SuperFect combined with plasmid in a 1:5 ratio for 100 x 25 mm^2 dishes. The transfection mixture was prepared in DMEM-H with no additives, vortexed for 10 sec, and incubated at RT for 10 min. Spent media were removed from cells and replaced with fresh complete media and the transfection mixture. After 3 h, media were removed and replaced with fresh complete media. Following a 24 h recovery in serum-containing media, cells were rinsed twice in PBS and incubated with fresh SF DMEM-H for 30 min, then treated as indicated in the figure legends.

Transient transfection of Nur77 and fluorescence microscopy

GFP-TR3 (Nur77) plasmid expressing human Nur77 was generously provided by Dr. X-K Zhang at the Sanford-Burnham Medical Research Institute, La Jolla, CA. Cells were plated on 8-well Ibidi μ-slides. When cells reached ~80% confluency they were transfected with plasmids encoding EGFP or GFP-TR3. After 24 h cells were washed with PBS, and incubated in serum-free media for 30 min. Media were aspirated and replaced with serum-free media + MitoTracker Red for 15 min. Spent media were aspirated and cells were treated ± ANS for 60 min prior to fixation and Hoechst nuclear staining. Cells were stored in mounting media (Ibidi) and imaged with an Olympus FSX100 microscope. Nur77, MitoTracker Red, and Hoechst signal were each acquired separately, then an image overlaying all three wavelengths was acquired.

siRNA experiments

MAC-T cells were plated in complete media at $3x10^4$ cells/cm^2. The following day, subconfluent cells were transfected with 50 nM IGFBP-3, JNK2, Nur77 or scrambled control siRNA, using Mirus Transit TKO Transfection Reagent (Stratagene, La Jolla, CA) according to manufacturer's instructions. Confluent cells were washed and incubated overnight in SF media, then treated for

analysis of gene knock-down or ANS-induced apoptosis. Cells plated for knock-down experiments for indirect immunofluorescence were incubated overnight in serum-free media, treated with ANS then fixed and stained as detailed above. Gene knock-down of Nur77 was verified by Western immunoblotting as described above and by mRNA analysis. IGFBP-3 and JNK knock-downs were verified in previous publications (65,66).

Apoptosis assay

Cells were treated ± ANS then assayed for Caspase 3 and 7 cleavage with the Sensolyte Homogenous AMC Caspase-3/7 Caspase Assay (AnaSpec) according to manufacturer's instructions.

Reverse transcription quantitative PCR (RT-qPCR)

Cells were lysed with Trizol (Invitrogen) and RNA was isolated using the NucleoSpin RNA isolation kit (Machery Nagel, Bethlehem PA). RNA integrity was assessed by visualization of 28 and 18s ribosomal bands after agarose gel electrophoresis. RNA (2 µg) was reverse transcribed with the High Capacity Reverse Transcriptase kit (Applied Biosystems, Foster City, CA). qPCR primer sets were developed using PrimerQuest (IDT, Coralville, IA) and purchased from Sigma-Aldrich. For Nur77 primers were forward, 5'-TTCCTCTACCAACTGTCAGGCACA-3', reverse, 5'-TCGAACTTGAAGGAAGCAGAGGCT. For cyclophilin primers were forward, 5'-GAGCACTGGAGAGAAAGGATTTGG-3'; reverse, 5'-TGAAGTCACCACCCTGGCACATAA-3'. To validate each primer set individual standard curves were established using serial dilutions (1:2 through 1:20,000) of a common pool of RNA. The slope and amplification efficiency for the standard curve generated with each primer set was determined with efficiencies between 90% and 110% considered acceptable. Melt curves were evaluated to ensure that a single product

was amplified. To use the $2^{-\Delta\Delta Ct}$ method for calculating treatment effects, the efficiencies of the primers for the target and housekeeping genes must amplify at the same rate. To determine this, ΔC_t ($C_{t\ target} - C_{t\ reference}$) was plotted for each dilution of the standard curve. As per the Applied Biosystems guidelines, if the absolute value of the slope for ΔC_t vs. log input amount of RNA is less than 0.1, then the primers for the target and housekeeping genes amplify at the same rate and the $2^{-\Delta\Delta Ct}$ method can be used to analyze the data. Samples were diluted 1:4 and 5 µl were amplified in a 20 µl reaction containing 10 µl SYBR green (Applied Biosystems), 4 µl water, and 0.5 µl (0.25 µm Nur77, 0.125 µm cyclophilin) of each gene-specific primer. Reactions were run on the ABI 7300 system using cycle parameters of 95°C for 10 min, followed by 40 cycles of 95°C for 15 sec and 60°C for 1 min. Data were analyzed using the relative $\Delta\Delta C_T$ method with cyclophilin as the housekeeping gene. PCR products were verified by melt curve analysis.

Statistical analysis

Data from experiments were analyzed by two-way ANOVA with Bonferonni post-tests, with differences considered significant for $P<0.05$. Analyses were performed with GraphPad Prism (La Jolla, CA).

Results

Nur77 plays a role in ANS-induced apoptosis

To investigate if Nur77 plays a role in IGFBP-3-dependent intrinsic apoptosis, we first used siRNA to knock-down Nur77 to determine if Nur77 contributes to ANS-induced apoptosis in MECs. Knock-down of Nur77 resulted in reduction of ANS-induced PARP cleavage, measured by Western immunoblotting (Fig. 1A). Cleavage of caspase 3&7 was also attenuated (Fig. 1B and C). These data indicate a role for Nur77 in intrinsic apoptosis. Analysis of protein (Fig. 1A) and mRNA (Fig. 1D) confirms successful knock-down of Nur77 expression.

ANS induces phosphorylation of Nur77

Phosphoryation of Nur77 is reported to inhibit its transcriptional activity and favor its apoptotic role (128,131-133). To examine the effects of ANS on Nur77 expression and phosphorylation, cells were treated with ANS for 1, 1.5, or 3 h then whole cell lysates were collected. As shown in the middle panel of Fig. 2A, Nur77 was detected in whole cell lysates under basal conditions, and levels were not increased by ANS. However, while some phosphorylated Nur77 was detected under basal conditions, ANS induced further phosphorylation which peaked around 60 min (top panel of Fig. 2A). The phospho-Nur77 band was the same molecular weight as the upper band detected by the total-Nur77 antibody. To confirm that the band detected by the phospho-specific antibody was specific to phosphorylated Nur77, lysates were treated with lambda protein phosphatase (LPP) to remove all phosphate groups (Fig. 2B). As expected, LPP digestion completely reduced detection of phospho-Nur77.

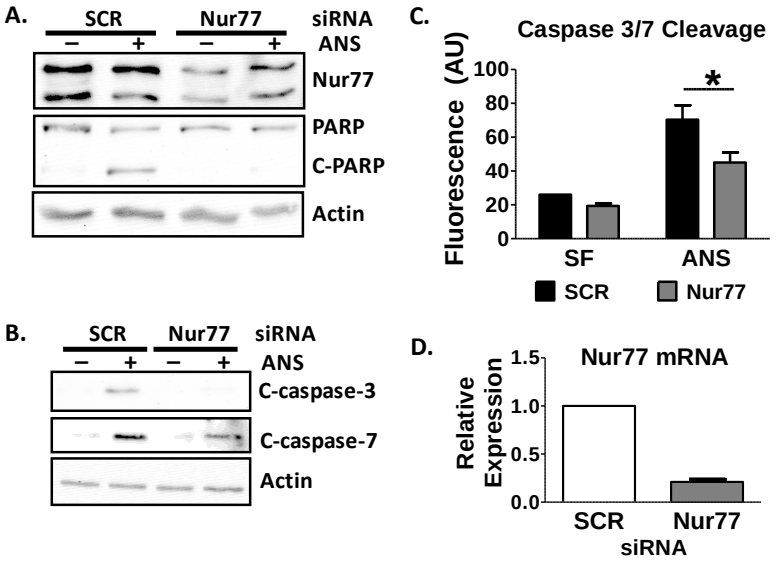

Fig. 1. Nur77 is required for ANS-induced apoptosis. Cells transfected for 48 h (A,B) or 72 h (C) with scramble (SCR) or Nur77 siRNA were serum-starved overnight then treated with 0.1 µM ANS for 6 h. (A, B) Whole cell lysates were immunoblotted for Nur77, cleavage of PARP and caspases 3-7. Actin served as a loading control. Blots are representative of three independent experiments. (C) Caspase 3 and 7 cleavage was measured by the Sensolyte Homogenous AMC Caspase-3/7 Caspase Assay (AnaSpec). Bars represent mean ± SE of three experiments, with each treatment performed in triplicate within an experiment. * indicates significant difference between indicated treatments ($p < 0.05$). (D) Total RNA was collected from untreated cells 48 h after transfection and Nur77 message was analyzed by RT-qPCR. Data were corrected for cyclophilin levels. Error bars represent mean ± SE of three experiments.

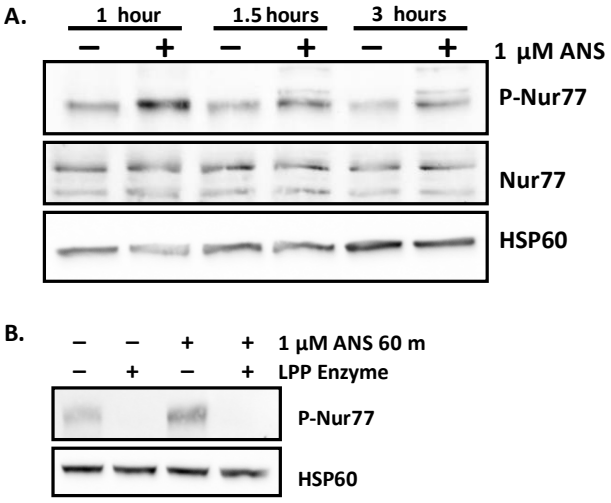

Fig. 2. ANS induces phosphorylation of Nur77. Cells were serum-starved overnight then treated ± 1 µM ANS for the indicated times. (A) Whole cell lysates were immunoblotted for total or phospho Nur77. HSP60 served as a loading control. (B) Lysates collected in phosphatase-free lysis buffer were incubated ± Lambda protein phosphatase to dephosphorylate all proteins. Samples were then immunoblotted for phospho-Nur77. HSP60 served as a loading control. Blots are representative of three independent experiments.

Nur77 and P-Nur77 are exported from the nucleus to the cytoplasm in response to ANS

Phosphorylated Nur77 is reported to be exported from the nucleus to either the cytoplasm or the mitochondria. Fractionation experiments indicated that Nur77 resides in the nucleus of untreated cells (Fig. 3). Upon addition of ANS, phosphorylated Nur77 was exported from the nucleus to the cytoplasm (Fig. 3A), however neither total nor phospho-Nur77 were detected in the mitochondria under treatment or control conditions (Fig. 3B). Bax localizes to the mitochondria in MECs in response to intrinsic stressors so we used Bax as a positive control to confirm that our mitochondrial isolation technique was valid (26,175,176). As expected, mitochondria isolated from cells treated with ANS had more Bax than serum-free controls (Fig. 3C).

To confirm fractionation data, cells were transfected with GFP-Nur77 and microscopy was used to track the fluorescent signal. Cells transfected with GFP-Nur77 were treated for 1 h with 1.0 μM ANS (Fig. 3D). Similar to fractionation data, ANS induced nuclear export of Nur77. Nuclei were stained with Hoechst and mitochondria were stained with MitoTracker Red. In the absence of treatment, Nur77 resided predominantly in the nucleus but moved to the cytoplasm following ANS-treatment. The cytoplasmic Nur77-GFP was diffuse throughout the cell, but no yellow hue was detected. Absence of the yellow color indicating overlay of GFP-Nur77 with MitoTracker Red supports the fractionation data showing an absence of mitochondrial Nur77. Even with enhanced production of Nur77 in transfected cells we are unable to detect Nur77 in the mitochondria, indicating that Nur77 does not localize to the mitochondria in detectable quantities in this system.

JNK knock-down attenuates ANS-induced apoptosis

To determine if JNK is activated by ANS and required for ANS-induced apoptosis cells were transfected with siRNA targeting JNK then treated with ANS. As shown in Fig. 4A, JNK was activated by ANS treatment and siRNA knock-down of JNK2 attenuated ANS-induced cleavage of caspases 3&7 and their downstream target PARP. Immunoblot data are supported by data from fluorescent caspase-activation assay data demonstrating that JNK2 siRNA significantly attenuated ANS-induced activation of caspases 3&7 (Fig. 4B, $p<0.05$). These data indicate that JNK is involved in intrinsic apoptosis in normal MECs.

Fig. 3. ANS increases cytoplasmic but not mitochondrial Nur77. (A) Cells were treated for 90 min ± 1.0 µM ANS. 50 µg cytoplasmic and 30 µg nuclear fractions were immunoblotted for Nur77 and p-Nur77. HSP60 served as a cytoplasmic marker and lamin AC served as a nuclear marker. (B) Cells were treated for 90 min or (C) 4 h ± 1.0 µM ANS then fractionated into cytosolic and mitochondrial fractions. Blots are representative of two independent experiments. Data shown in (C) were quantified by densitometry and Bax was normalized to porin. (D) Cells transfected with GFP-Nur77 or eGFP were treated for 90 min ± 1.0 µM ANS then cells were fixed in formalin. Nuclei were stained with Hoechst and mitochondria were stained with MitoTracker Red (MTR). Images were acquired with an Olympus FSX100 microscope.

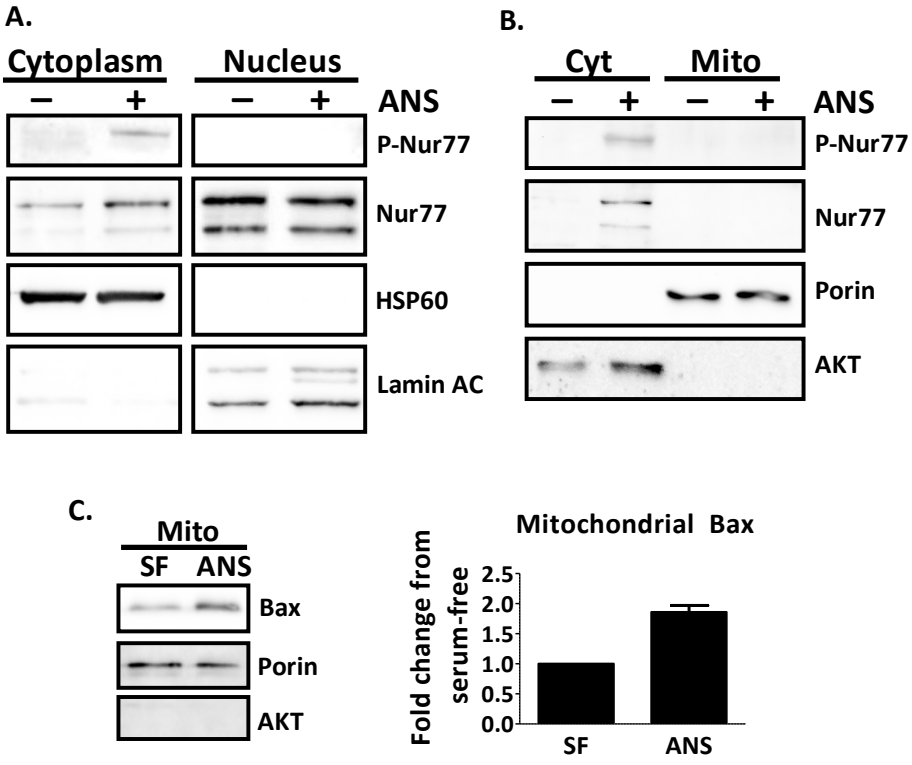

D.

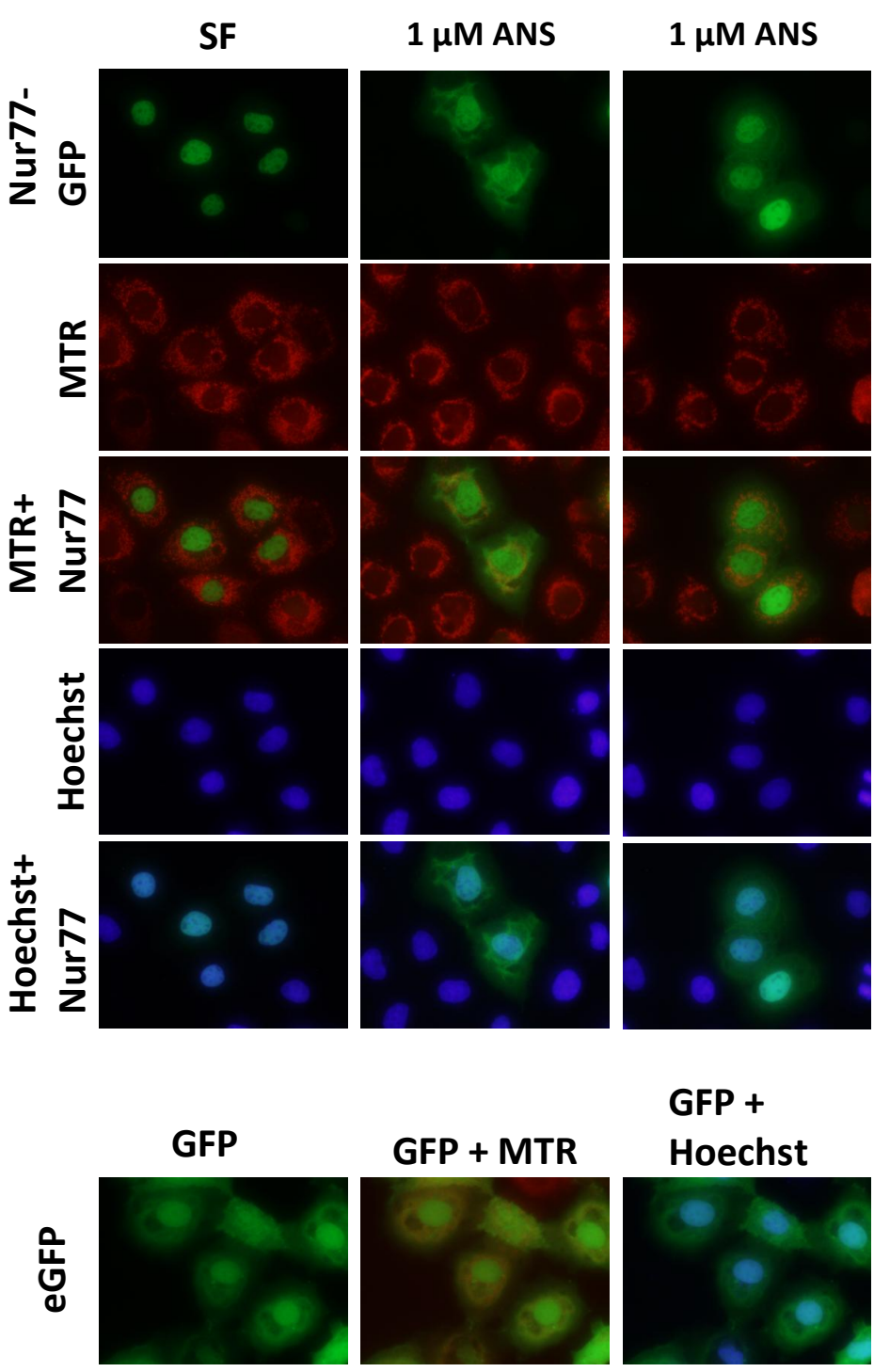
SF
1 µM ANS
1 µM ANS
Nur77-GFP
MTR
MTR+ Nur77
Hoechst
Hoechst+ Nur77
GFP
GFP + MTR
GFP + Hoechst
eGFP

IGFBP-3 and JNK2 contribute to ANS-induced phosphorylation and nuclear export of Nur77

To determine if IGFBP-3, JNK, or both are required for phosphorylation of Nur77, cells transfected with siRNA targeting IGFBP-3 or JNK2 were treated for 1 h with 1 μM ANS and whole cell lysates were collected. Fig. 5A shows that in control cells ANS-treatment induced phosphorylation of Nur77, but phosphorylation was reduced when either IGFBP-3 or JNK were knocked down. Knock-down of IGFBP-3 or JNK resulted in similar reduction of P-Nur77 (Fig. 5A), and simultaneous knock-down of both proteins did not have an additive effect (data not shown). Neither siRNA had any effect on total Nur77 protein (Fig. 5B). In addition, ANS-induced JNK phosphorylation was not reduced by IGFBP-3 knock-down (Fig. 5A and reference (66)), therefore IGFBP-3 does not mediate Nur77 phosphorylation by activating JNK.

To determine if IGFBP-3, JNK, or both modulate cellular localization of Nur77, cells were transfected with siRNA targeting IGFBP-3, treated with ANS and cellular localization of Nur77 was examined by indirect immunofluorescence. As shown in Fig. 6, ANS induced nuclear export of Nur77 and p-Nur77, and this effect was attenuated by IGFBP-3 or JNK knock-down. Knock-down of both IGFBP-3 and JNK together had the same effect as either knock-down alone.

ANS induces association of IGFBP-3 with Nur77

Having found that IGFBP-3 contributes to phosphorylation and nuclear export of Nur77, we questioned if this effect was dependent on a physical interaction between the two proteins. To test this hypothesis, IGFBP-3 was immunoprecipitated from whole cell lysates and immunoblotted for Nur77 (Fig. 7). Under basal conditions no association was detected between IGFBP-3 and Nur77, however upon ANS-treatment Nur77 co-immunoprecipitated with IGFBP-3. Interestingly, IGFBP-3 basally associates with RXRα and this association is enhanced by ANS-

treatment. Further work is needed to elucidate the role of RXRα intrinsic apoptosis of MAC-Ts and to determine the functional significance of the interaction between IGFBP-3 and RXRα.

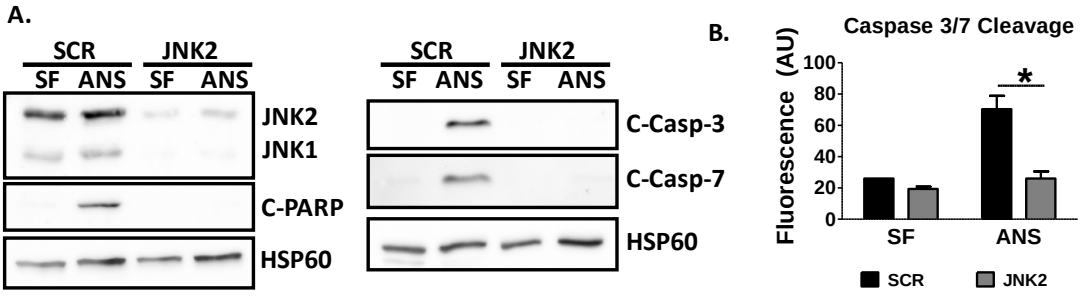

Fig. 4. siRNA knockdown of JNK2 attenuates ANS-induced apoptosis. Cells were transfected for 72 h with scramble or JNK2 siRNA, serum-starved overnight then treated ± 0.1 μM ANS for 6 h. (A) Whole cell lysates were immunobloted for total JNK and cleavage of PARP and caspases 3&7. HSP60 served as a loading control. Blots are representative of three independent experiments. (B) Caspase 3&7 cleavage was measured by the Sensolyte Homogenous AMC Caspase 3&7 Caspase Assay (AnaSpec). Bars represent mean ± SE of three experiments, with each treatment performed in triplicate within an experiment. * indicates significant difference between indicated treatments ($p < 0.05$).

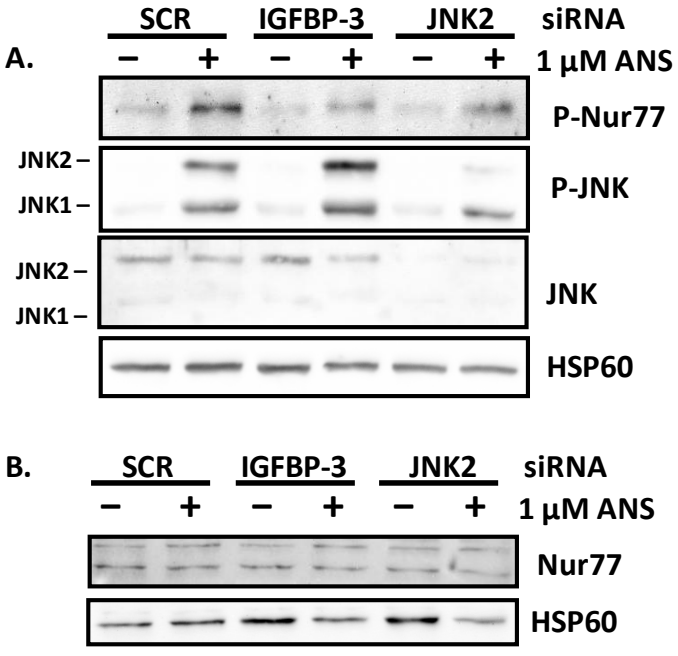

Fig. 5. IGFBP-3 and JNK2 contribute to ANS-induced phosphorylation of Nur77. Cells were serum-starved overnight then treated with 1 μM ANS for 1 h. (A) Whole cell lysates collected in complete lysis buffer were immunoblotted for phospho-Nur77, phospho-JNK, total JNK, and HSP60. (B) Whole cell lysates collected in Active Motif lysis buffer were immunoblotted for total Nur77 and HSP60. Blots are representative of three independent experiments.

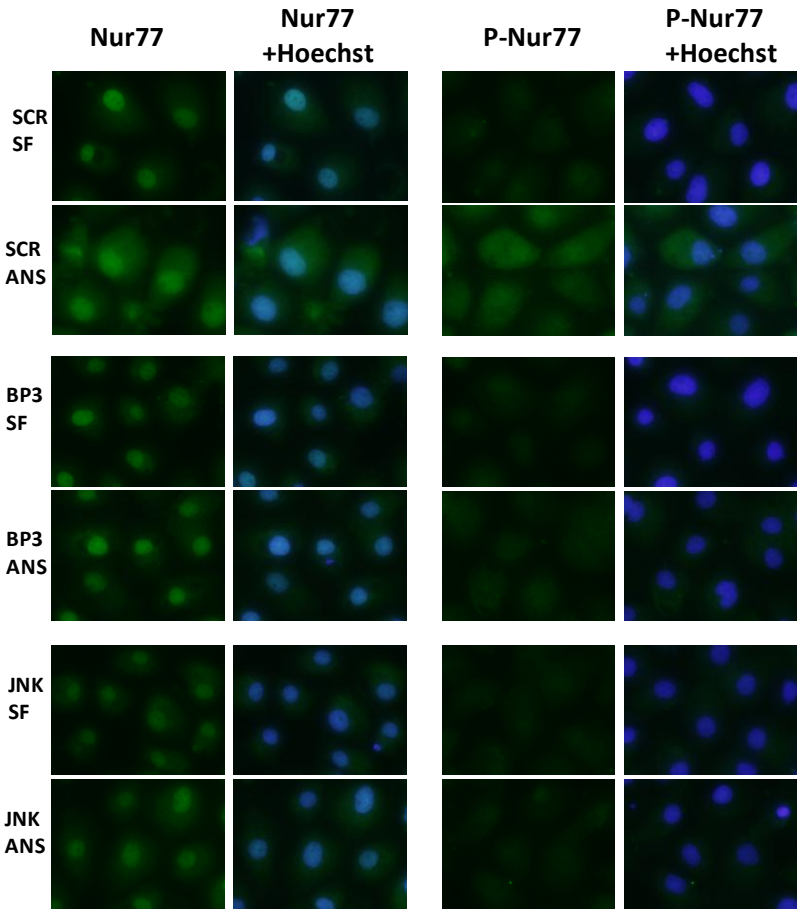

Fig. 6. Knockdown of IGFBP-3 or JNK attenuates ANS-induced Nur77 nuclear export. Cells were serum-starved overnight then treated for 1 h ± 1.0 µM ANS, then fixed, permeabilized, and incubated with antibodies recognizing Nur77 or phospho-Nur77 and a fluorescently labeled secondary antibody. Nuclei were stained with Hoechst. Images were acquired with an Olympus FSX100 microscope.

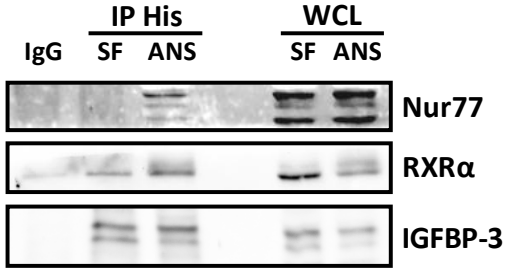

Fig. 7. ANS induces association of IGFBP-3 with Nur77 and RXRα. Cells transfected with his-IGFBP-3 were treated ± 1.0 µM ANS, collected in Active Motif lysis buffer, then 500 µg lysate was incubated with anti-His antibody (Genscript) or mouse IgG. Fifty µg whole cell lysate (WCL) was run as an input control. Samples were immunoblotted for Nur77, RXRα, and IGFBP-3.

Discussion

Nur77 is positively regulated by both mitogenic and apoptotic stimuli and has roles in both cellular survival and death. For example, Nur77 protein is induced by serum or growth factors in PC12 pheochromocytoma cells and cancers of the lung and prostate (121,177,178) and by apoptosis-inducing compounds in PC12, prostate cancer, oral cancer, neuronal, and smooth muscle cells (96,124,125,129,130,179). Nur77 is also up-regulated during differentiation of neuronal cells (180,181). In the present study, knock-down of Nur77 attenuated ANS-induced cleavage of caspases 3&7 and PARP, establishing a role for Nur77 in intrinsic apoptosis of MAC-T cells. Interestingly, in these cells Nur77 was present in detectable amounts basally and levels of total protein were unaffected by treatment. This contrasts with many of the studies cited above, where Nur77 protein was low or undetectable in untreated cells and induced by treatment. However, Nur77 is also reported to be constitutively up-regulated in some cancers, such as gastric cancer cells, therefore, expression under basal conditions is not unique to our system (182). Since total levels of Nur77 protein were unaffected by intrinsic stress, we examined phosphorylation to determine if Nur77 was subject to stress-induced post-translational modifications. Nur77 was found to be phosphorylated as early as 30 min after ANS-treatment.

Phosphorylation and cellular localization dictate whether Nur77 has a survival or apoptotic role. Nur77 acts as a nuclear transcription factor basally and phosphorylation of Nur77 reduces DNA binding and transcriptional activity to shut off its pro-survival function and promote nuclear export (121,128,131-133). In prostate cancer cells cytoplasmic Nur77 enhances apoptosis by binding Bcl-2 and converting it from a survival protein to a pro-apoptotic protein (134). Other data suggest Nur77 localizes to the mitochondria where it promotes mitochondrial

permeabilization and cytochrome c release (91,126,127,183). Dual functions in the cytoplasm and mitochondria are implicated in NIH460 lung cancer cells undergoing apoptosis as Nur77 both translocates to the mitochondria and co-localizes with Bcl-2 in these cells (125). However, in some cell types Nur77 does not localize to the mitochondria after being exported from the nucleus, indicating that mitochondrial localization is a cell-type specific event. For example, butyrate induces nuclear export of Nur77 in prostate cancer and colon cells but Nur77 localizes to the mitochondria only in the prostate cancer cells. In pancreatic cancer cells, apoptosis induced by 1,1-bis(3'-indolyl)-1-(p-anisyl) methane (DIMC-pPhOH) inactivates Nur77 transcriptional activity but does not cause nuclear export, suggesting that in these cells inhibition of nuclear Nur77 activity is enough to induce apoptosis (95). Interestingly, in our system Nur77 was not detected in the mitochondria using cellular fractionation. Since mitochondrial fractionations produce low protein yields, we also transfected cells with GFP-Nur77 to enable the use of direct fluorescence microscopy. Even with this enhanced detection technique, Nur77 was not detected in the mitochondria. It is possible that the fraction of Nur77 localizing to the mitochondria is still below the threshold of detection. However, published work demonstrating mitochondrial localization of Nur77 often shows punctuate Nur77 staining that clearly localizes to the mitochondria (91,126,134). Therefore, the absence of distinct co-localization of GFP with MitoTracker red together with the diffuse intracellular distribution of GFP makes it unlikely that Nur77 is targeted to the mitochondria in these cells.

Since phosphorylation and localization contribute to the function of Nur77 we wanted to examine the factors modulating these two events. Nur77 is reported to be phosphorylated by a number of kinases, including Jun-N-terminal kinase (JNK) (130,179). JNK is activated by ANS in multiple cell lines, including MAC-T cells, lung cancer cells, fibroblasts, macrophages, and

hepatocytes (66,130,135,173,184). Prolonged JNK activation is part of the molecular switch that tells cells to progress through apoptosis and shut off survival signals. In the present work we show that siRNA knock-down of JNK attenuated ANS-induced apoptosis and also reduced phosphorylation and nuclear export of Nur77. Our conclusions are supported by studies in cancers of the lung and breast, showing JNK phosphorylates Nur77 in response to cellular stressors including ANS (133). The requirement for JNK in modulating activation and nuclear export of Nur77 varies between cell lines. JNK activation is not required for this effect in T-cells or vascular smooth muscle cells (127,129). Thus in MAC-T cells the role of JNK more closely resembles its role in breast cancer cells than in immune or muscle cells, suggesting that the role of JNK is not dependent on classification of tissues as malignant or benign, but could be affected by tissue type.

Treatment of prostate cancer cells with IGFBP-3 induces nuclear export of Nur77 (94). This led us to investigate whether IGFBP-3 exerts its apoptotic effects through activation of the pro-apoptotic activity of Nur77. Knock-down of IGFBP-3 reduced the ability of ANS to induce phosphorylation of Nur77 in whole cell lysates. Also, cellular fractionation and immunofluorescence data indicated that IGFBP-3 was required for export of Nur77 out of the nucleus. Together, these data show that IGFBP-3 contributes to both activation and translocation of Nur77 in cells undergoing apoptosis. IGFBP-3 and JNK each contribute to both activation and nuclear export of Nur77, suggesting that they might function cooperatively to regulate the apoptotic effects of Nur77. In prostate cancer cells, treatment with IGFBP-3 directly induces JNK activation, nuclear export of Nur77, and apoptosis (91). However, we previously found that treatment of MAC-T cells with IGFBP-3 does not induce apoptosis or inhibit proliferation (46,65). Further, in the present study knock-down of IGFBP-3 did not

reduce the ability of ANS to induce JNK activation (Fig. 5). Therefore if IGFBP-3 and JNK do function cooperatively it is downstream of JNK activation, possibly at the level of nuclear Nur77 phosphorylation. For example, IGFBP-3 could bind Nur77, sequestering it from DNA to halt transcriptional activity and tethering it to facilitate phosphorylation by JNK.

To test if IGFBP-3 physically associates with Nur77 we immunoprecipitated IGFBP-3 and immunoblotted for Nur77. In the absence of treatment no association was detected, however in ANS-treated cells Nur77 co-immunoprecipitated with IGFBP-3. This interaction suggests that IGFBP-3 modulates activation of Nur77 through a physical interaction. In prostate cancer cells and prostate tumor xenografts, IGFBP-3 induces apoptosis, dependent on an association with Nur77 (94). Our work is the first to show an association between IGFBP-3 and Nur77 in normal epithelial cells. Additional work is needed to optimize IP experiments in cellular fractions to determine how the association between IGFBP-3 and Nur77 controls activation and localization of Nur77.

In conclusion, we found that Nur77 is involved in intrinsic apoptosis in MAC-T cells, and that the apoptotic effects of Nur77 are modulated by both IGFBP-3 and JNK. Further studies are required to determine how IGFBP-3 and JNK function to activate Nur77.

Chapter 4.

Mechanism for nuclear localization of IGFBP-3 in response to activation of intrinsic apoptotic stress pathways

Abstract

IGFBP-3 has both mitogenic and apoptotic functions in normal mammary epithelial cells (MEC) and breast cancer cell lines. The factors that determine whether IGFBP-3 promotes cellular survival or death are unclear. Anisomycin (ANS), an activator of the intrinsic apoptotic pathway, is a potent inducer of IGFBP-3 production in immortalized non-transformed MEC and knock-down of IGFBP-3 with siRNA attenuates the ability of ANS to activate apoptosis. Interestingly, IGFBP-3 is found in both the nucleus and the conditioned media in response to ANS indicating a potential for both intra- and extra-cellular functions. We previously established that IGFBP-3 exerts its apoptotic effects in part through modulation of activation and localization of orphan nuclear receptor Nur77. The goal of this study was to determine if ANS specifically regulates transport of IGFBP-3 to the nucleus. Transfection of cells with a plasmid expressing GFP-tagged IGFBP-3 indicated that the 64 kDa IGFBP-3-GFP resides basally in the cytosol and translocates to the nucleus in response to ANS. Since IGFBP-3-GFP is too large to passively diffuse through nuclear pores, this supports a role for active nuclear import. De-glycosylation of nuclear samples with endoglycosidase-H showed that intracellular IGFBP-3 is glycosylated, indicating it has been transported through the secretory pathway. However, inhibition of ER-to-Golgi transport with Brefeldin A inhibited secretion of IGFBP-3 and increased nuclear accumulation of IGFBP-3, indicating that secretion is not required for nuclear localization. Immunoprecipitation experiments showed that IGFBP-3 and nuclear transport protein importin-β co-precipitated in ANS-treated cells but not in un-treated controls. In addition, inhibition of importin-β with importazole reduced ANS-induced nuclear IGFBP-3, further supporting a role for importin-β in nuclear transport of IGFBP-3. In summary, these data show ANS induces nuclear import of IGFBP-3 and that this is a regulated event mediated by binding to importin-β.

Introduction

IGF binding-protein-3 (IGFBP-3) has dual roles in cellular survival and death. The molecular switch governing the cellular function of IGFBP-3 remains unknown. Circulating IGFBP-3 binds IGF-I and acts as a carrier protein, protecting IGF-I from degradation and regulating the availability of IGF-I to its IGF-I-receptor (IGF-IR). At the cell surface IGFBP-3 can either enhance or inhibit the mitogenic effects of IGF-I. Interestingly, IGFBP-3 has been found to bind the cell surface to potentiate IGF-I signaling (5,6). However, an excess of IGFBP-3 in culture medium has also been shown to inhibit IGF-I-induced proliferation (7,8). This effect was initially attributed to the ability of IGFBP-3 to bind IGF-I and sequester it from its receptor, however, mutants of IGFBP-3 that do not bind IGF-I or IGF-II retain this anti-proliferative effect (reviewed by Firth and Baxter (9)).

The discovery that IGFBP-3 can inhibit proliferation and induce apoptosis independent of IGF-I led to a search for the mechanism by which IGFBP-3 facilitates these events. While IGFBP-3 is a secreted protein it is also detected in the nucleus of multiple cell lines, suggesting it has either an autocrine or intracellular function (6,7,81). Intracellular IGFBP-3 is associated with a role in apoptosis, independent of IGF-I. Nuclear IGFBP-3 interacts with transcription factors RXRα, RAR, Nur77 and Rpb3 (89,94,185), thus a role in transcriptional regulation has been hypothesized. However, in prostate cancer cells, IGFBP-3 directly induces nuclear export of Nur77, which then localizes to the mitochondria to facilitate cytochrome c release (91). Therefore these data indicate suggest a chaperone function for IGFBP-3 in redistributing Nur77 to enhance its apoptotic function.

Conflicting data exist describing a mechanism for nuclear accumulation of IGFBP-3. Multiple groups argue that IGFBP-3 is secreted and re-internalized, then directed to the nucleus. In osteosarcoma cells IGFBP-3 added to growth medium is internalized by clathrin- and caveolin-mediated pathways (88). Additionally, in prostate cancer cells exogenous IGFBP-3 is reported to bind transferrin then get internalized as a complex with Tf and TfR (81). Both of these systems rely on exogenous IGFBP-3 so their physiological relevance remains unclear. Data in cells expressing endogenous or transfected IGFBP-3 are conflicting. When prostate cancer cells are transfected with IGFBP-3 lacking the signal peptide required for secretion, IGFBP-3 is found in the nucleus and can still induce apoptosis, suggesting that secretion is not a required event for IGFBP-3-induced apoptosis (83). In contrast, TGF-β induces production and nuclear localization of IGFBP-3, however nuclear IGFBP-3 is attenuated by the addition of an anti-IGFBP-3 antibody indicating that secretion is required (81). However, the authors did not examine production of IGFBP-3 in cells treated ± the antibody, so the absence of nuclear IGFBP-3 could be due to other mechanisms.

IGFBP-3 has a bipartite nuclear localization sequence that directs it to the nucleus in multiple cell lines (60,89,99). Binding assays show IGFBP-3 has a weak affinity for nuclear pore protein importin-α and strong affinity for importin-β, suggesting involvement of the latter protein in nuclear import (99). Knock-down of importin-β with siRNA reduces nuclear import of exogenous IGFBP-3 in osteosarcoma cells, however total endocytic activity is also decreased, making it difficult to interpret these results (88). Work in permeabilized Chinese hamster ovary (CHO) cells shows that antibody immuno-neutralization of importin-β prevents nuclear localization of exogenous IGFBP-3, indicating a potential physiological role for this interaction (99). The mechanism of nuclear import of endogenous IGFBP-3 remains unclear.

Previous work from our lab shows that IGFBP-3 plays a role in the ability of anisomycin (ANS) to induce intrinsic apoptosis in MAC-T bovine mammary epithelial cells (Chapter 2). ANS-induced production and secretion of IGFBP-3 and siRNA knockdown of IGFBP-3 attenuate the ability of ANS to induce intrinsic apoptosis. Further, IGFBP-3 is detected in the nucleus of ANS-treated cells, leading us to hypothesize that cellular localization contributes to regulation of the biological function of IGFBP-3. We have shown that in MAC-T cells undergoing apoptosis, IGFBP-3 modulates nuclear export of Nur77, establishing a nuclear function for IGFBP-3 (Chapter 3). The objective of the present study was to investigate the mechanism for nuclear import of IGFBP-3.

Materials and methods

Chemical reagents

Phenol red-free (PRF) DMEM-low glucose media, gentamycin, bovine insulin, ANS, and fetal bovine serum (FBS) were purchased from Sigma (St. Louis MO). Recombinant human IGF-I (100% identical to bovine IGF-I) was obtained from Peprotech (Princeton, NJ). DMEM-H (4.5 g/L D-glucose), penicillin and streptomycin were purchased from Invitrogen (Carlsbad, CA). Antibodies against the following proteins were purchased as indicated: HSP60 and importin-β (Abcam, Cambridge, MA), His-tag (Genscript, Piscataway, NJ), PARP (Cell Signaling Technology, Danvers MA) and lamin AC (Santa Cruz). A polyclonal antibody against bovine IGFBP-3 was kindly provided by Dr. David Clemmons, University of North Carolina at Chapel Hill (used in Fig. 2-4). The anti-bovine-IGFBP-3 antibody used in Fig. 5 was produced in-house (see Chapter 5). Endoglycosidase-H_f was purchased from New England Biolabs (Ipswich, MA). Fluorescently labeled transferrin (Tf-FITC) was purchased from Rockland Inc. (Gilberstville, PA). Custom SmartPool siRNA for bovine IGFBP-3 and scramble siRNA control were purchased from Dharmacon, Inc. (Lafayette, CO). Mirus Transit TKO transfection reagent was purchased from Stratagene (La Jolla, Ca). The following inhibitors were purchased as indicated: Importazole (Millipore, Billerica, MA), Brefeldin A (Sigma Aldrich, St Louis, MO), and Pitstop2 (Cellagen Technology, San Diego, CA). Hoechst 33342 was purchased from Invitrogen. Superfect transfection reagent was purchased from Qiagen (Valencia, CA).

Cell culture

The bovine MEC line MAC-T (Huynh et al., 1991) was routinely maintained in complete media consisting of DMEM containing 4.5 g/liter D-glucose (i.e., DMEM-H), 20 U/ml penicillin, 20 µg/ml streptomycin, 50 µg/ml gentamicin, 10% FBS, and 5 µg/ml insulin (137). For all experiments

cells were used between passages 8-22. For experiments, cells were plated and grown to confluence in phenol red-free DMEM-H containing 10% FBS and antibiotics and without insulin. Except where otherwise noted, cells were rinsed with phosphate-buffered saline (PBS), and incubated in serum-free (SF) DMEM-H with 0.2% BSA and 30 nM sodium selenite overnight prior to exposure to treatments in SF DMEM-H without additives.

Construction of His-tagged IGFBP-3 (IGFBP3-His)

A PCR reaction was used to add a 6x-His tag to the C terminus of bovine IGFBP-3. *Xho*I and *Not*I restriction sites were added to the 5' and 3' ends, respectively, to flank the IGFBP-his sequence, producing a 923 bp IGFBP3-his fragment. The 50 µl PCR reaction contained 20 ng DNA template (pRc/RSV IGFBP3, Grill and Cohick, 2000), 20 pmol forward primer 5'-ATATTACTCGAG TAATGCTGCGGGCACGCCCCGCGCTC-3', 20 pmol reverse primer 5'-ATAGTTTAGCGGCCGCTCAATGGTGATGGTGATGATGCTTGCTCTCCATGCTGTAGCAGT-3', 2 mM Mg SO_4, 0.2 mM of each dNTP, 5% DMSO and 1 unit Platinum *Taq* High Fidelity DNA Polymerase (Life Technologies, Carlsbad, CA). The cycling parameters were 94˚C 2 min; 30 cycles of 94˚C 1 min, 55˚C 1 min, 68˚C 1 min; 68˚C 10 min. The IGFBP-3-his fragment was purified using Nucleospin Gel and PCR Clean-up kit (Macherey-Nagel, Bethlehem, PA). BP3-His (insert) and pEGFP-N1 (vector) were digested with *Xho*I and *Not*I. This digestion excises EGFP from the plasmid. After vector dephosphorylation with Anarctic Phosphatase (New England Biolabs) both insert (902 bp) and vector (3945 bp) were purified as described above and ligated using T4 DNA Ligase (Invitrogen, Carlsbad, CA). The ligation reaction was used to transform One Shot TOP 10 competent cells (Invitrogen). After miniprep, colonies were screened for positive clones by restriction digestion. Bovine IGFBP3-His construction was confirmed by sequencing.

Construction of GFP-tagged IGFBP-3 (IGFBP-3-GFP)

A GFP-tag was added to IGFBP-3 as described for IGFBP-3-his, with the following changes. *Xho*I and *BamHI* restriction sites were added to the 5' and 3' ends of bovine IGFBP-3, respectively, producing a 900 bp fragment. The same forward primer was used for both IGFBP-3-his and IGFBP-3-GFP. The reverse primer used for IGFBP-3-GFP was 5'-ACAAGTGGATCCACCTTGCTCTCCATGCTGTAGCAGTC-3'. The cycling parameters were 94˚C 2 min; 30 cycles of 94˚C 1 min, 50˚C 1 min, 68˚C 1 min; 68˚C 10 min. IGFBP-3-GFP was digested with *Xho*I and *BamHI*.

Transient transfection of IGFBP-3

MAC-T cells were plated in complete media at 3.5 x 10^4 cells/cm^2. The next day subconfluent cells were transfected with a plasmid encoding cDNA for bovine IGFBP-3 (46), IGFBP-3-His, IGFBP-3-GFP, or eGFP as a control. Plasmids were prepared using the EndoFree plasmid Maxi Kit (Qiagen, Valencia CA). Cells were transfected using SuperFect combined with plasmid in a 1:5 ratio for 100 x 25mm^2 dishes and in a 1:10 ratio for 8-well μslides (Ibidi, Martinsried, Germany). The transfection mixture was prepared in DMEM-H with no additives, vortexed for 10 sec, and incubated at RT for 10 min. Spent media were removed from cells and replaced with fresh complete media and the transfection mixture. After 3 h, media were removed and replaced with fresh complete media. Following a 24 h recovery in serum-containing media, cells were rinsed twice in PBS and incubated with fresh SF DMEM-H for 30 min then treated as indicated in the figure legends.

Cell lysis and Western immunoblotting

Cytosolic extracts were obtained by lysing cells in hypertonic buffer (20 mM Hepes pH 7, 10 mM KCL, 0.1% Triton, 20% Glycerol) supplemented with protease inhibitors with 10 strokes of the dounce homogenizer followed by centrifugation for 5 min at 1000 x g. Pellets were resuspended in buffer C (20 mM Hepes pH 7.9, 0.42 M NaCl, 1.5 mM $MgCl_2$, 0.2 mM EDTA, 25% Glycerol) supplemented with protease inhibitors, incubated on ice 30 min, then centrifuged at 13,250 RPM for 10 min to obtain the nuclear fraction. Lysates were assayed for protein with the BioRad Protein Assay (BioRad, Hercules, CA). Proteins were separated by SDS–polyacrylamide gel electrophoresis (PAGE) on 12.5% or 15% gels and transferred to nitrocellulose (0.2 µm; Bio-Rad) or PVDF (0.45 µM; Millipore, Bedford, MA) membranes. Membranes were blocked for 1 h at room temperature in Tris–buffered saline + 0.05% Tween-20 (v/v) (TBS-T) and 5% non-fat dried milk (w/v), and incubated with primary antisera at 4°C overnight with gentle agitation. Membranes were then washed in TBS-T and incubated for 1 h at room temperature with appropriate HRP-conjugated secondary antibodies. Peroxidase activity was detected with ECL Prime (GE, Pittsburgh, PA). Chemiluminescence was detected with the Fluorchem FC2 (Protein Simple, Santa Clara, CA).

Fluorescence microscopy

Cells were plated on 8-well Ibidi µ-slides, transfected and treated as described above. Cells were then fixed with 10% neutral buffered formalin (Fisher Scientific, Waltham, MA). Nuclei were stained with Hoechst (Invitrogen). Cells were stored in mounting media (Ibidi) and images were acquired with an Olympus FSX100 microscope.

Results

Nuclear import of IGFBP-3 is a regulated event

In MAC-T cells, IGFBP-3 is approximately 38 kDa, just below the 45 kDa molecular weight cut-off for passive diffusion into the nucleus (186). To investigate whether IGFBP-3 is specifically targeted to the nucleus or if it diffuses through nuclear pores, cells were transfected with GFP-tagged IGFBP-3. The tagged protein has a molecular weight of approximately 64 kDa, making it too large for passive diffusion through the nuclear pores. As shown in Fig. 1, with serum-free conditions IGFBP-3-GFP was detected exclusively in the cytosol, indicating it was excluded from the nucleus in untreated cells. Treatment with ANS resulted in nuclear import of IGFBP-3-GFP, indicating that nuclear import is induced by treatment.

Nuclear IGFBP-3 is glycosylated

Glycosylation is a hallmark of the secretory pathway so we next used enzymatic digestion of cellular fractions to determine if intracellular IGFBP-3 is glycosylated. As shown in Fig. 2, nuclear and cytosolic IGFBP-3 runs as a doublet between 36-38 kDa. Digestion of either fraction with endoglycosidase-H resulted in a single faster migrating band of approximately 30 kDa, indicating that nuclear IGFBP-3 is glycosylated.

Non-secreted IGFBP-3 localizes to the nucleus

To determine if secreted IGFBP-3 is re-internalized then directed to the nucleus, Pitstop2, an inhibitor of clathrin-mediated endocytosis (CME) was used. To confirm that Pitstop2 successfully prevents endocytosis, cells were treated with fluorescently-labeled transferrin (Tf-FITC) which is known to utilize CME for cellular entry. In the absence of inhibitor, Tf-FITC was distributed throughout the cell, however treatment with Pitstop2 resulted in an absence of

intracellular Tf-FITC, demonstrating inhibition of endocytosis (Fig. 3A). Cells were then treated with ANS with or without the inhibitor. Treatment with Pitstop2 did not reduce nuclear accumulation of IGFBP-3 (Fig. 3B), indicating that nuclear IGFBP-3 is not derived from secreted protein.

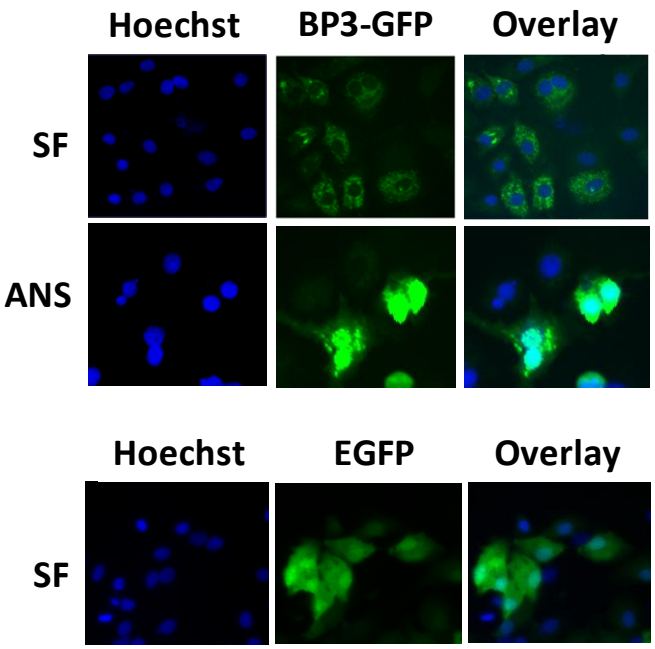

Fig. 1. ANS induces nuclear localization of IGFBP-3. MAC-T cells transfected with IGFBP-3-GFP were treated ± ANS for 2 h then fixed. Nuclei were stained with Hoechst. Cells were imaged on an FSX100 microscope. Images are representative of 2 independent experiments.

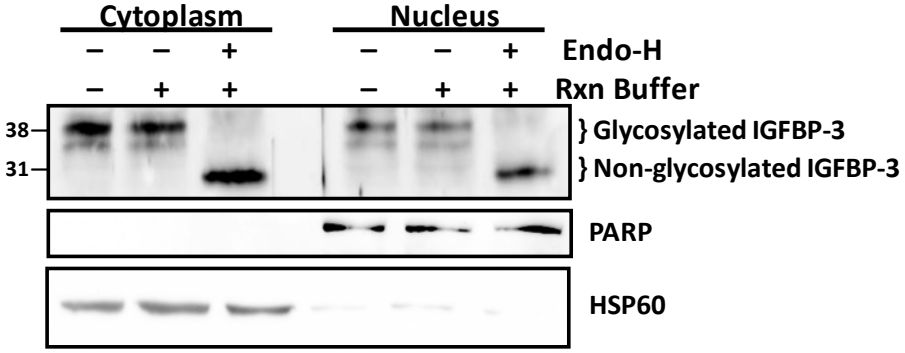

Fig. 2. Nuclear IGFBP-3 is glycosylated. Cells transfected with IGFBP-3-his were treated 6 h + ANS to induce nuclear localization of IGFBP-3 then fractionated. Lysates were treated ± Endoglycosidase-H to deglycosylate proteins, separated by SDS-PAGE and immunoblotted for IGFBP-3. PARP and HSP60 served as controls for nuclear and cytoplasmic loading, respectively. Results are representative of two independent experiments.

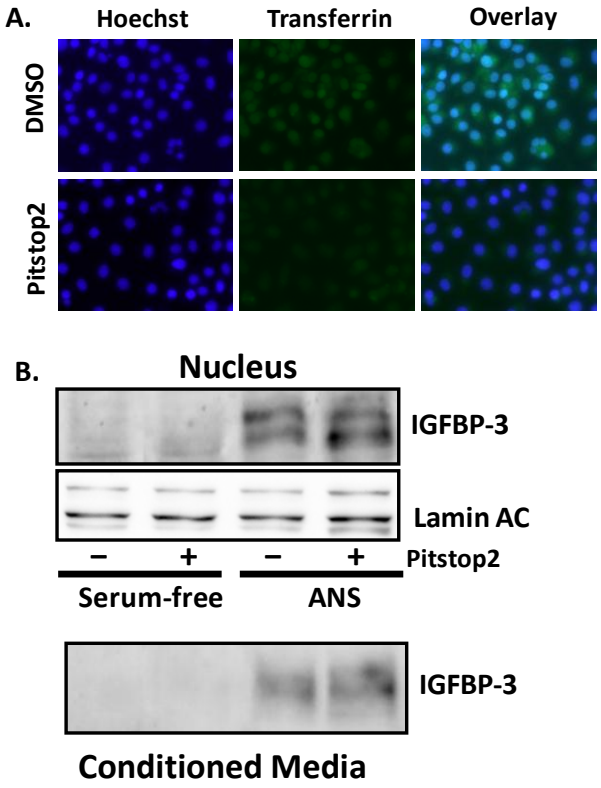

Fig. 3. Secreted IGFBP-3 is not re-internalized. (A) To confirm the Pitstop2 inhibitor blocks clathrin-mediated endocytosis cells were treated 45 min + Transferrin-FITC (25 µg/ml) ± Pitstop2. (B) Cells treated with ANS ± Pitstop2 were fractionated and Western immunoblotted for IGFBP-3 or Lamin AC. Conditioned media (CM) were collected and immunoblotted for IGFBP-3 to confirm that synthesis of IGFBP-3 was not affected. Results are representative of two (3A) or three (3B) experiments.

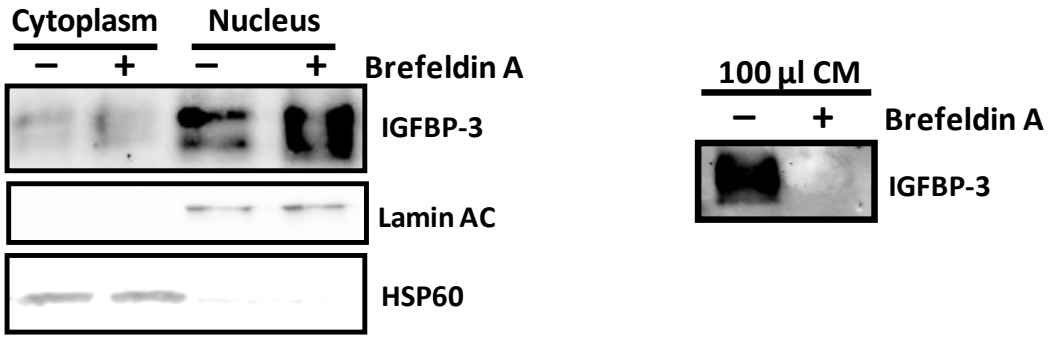

Fig. 4. Non-secreted IGFBP-3 localizes to the nucleus. Cells were treated with ANS ± Brefeldin A then conditioned media (CM) was collected and cells were fractionated. Samples were western immunblotted for IGFBP-3. Lamin AC and HSP60 served as nuclear and cytosolic loading controls, respectively. Results are representative of three independent experiments.

The Pitstop2 data showed that secreted IGFBP-3 was not reinternalized. We next wanted to confirm that non-secreted protein can localize to the nucleus. Brefeldin-A inhibits ER to golgi transport, effectively inhibiting secretion. Cells treated with ANS ± Brefeldin-A were fractionated and immunoblotted for IGFBP-3 (Fig. 4). As expected, ANS induced nuclear accumulation of IGFBP-3. Interestingly, treatment with Brefeldin-A enhanced nuclear accumulation of IGFBP-3, indicating that non-secreted protein localizes to the nucleus. Conditioned media were also collected to confirm that Brefeldin-A successfully inhibits secretion of IGFBP-3. As shown in Fig. 4, IGFBP-3 was detected in media conditioned by ANS-treated cells, but not in media conditioned by cells treated with ANS + Brefeldin-A.

Nuclear import of IGFBP-3 is dependent on importin-β

ANS induced nuclear localization of IGFBP-3-GFP (Fig. 1) indicating that nuclear import of IGFBP-3 is a regulated event. In breast cancer cells, IGFBP-3 has been reported to use importin-β for nuclear import (99). To determine if ANS promotes association between IGFBP-3 and importin-β, cells were transfected with IGFBP-His and treated ± ANS. Co-immunoprecipitation experiments indicated that IGFBP-3 and importin-β associated in ANS-treated cells but not in untreated controls (Fig. 5). To determine if nuclear import of IGFBP-3 is facilitated by importin-β we treated cells ± ANS with or without importazole, a small molecule inhibitor of importin-β. However, importazole interfered with the ability of ANS to induce IGFBP-3 production (data not shown). To avoid this issue, cells were transfected with IGFBP-3-GFP then treated ± ANS ± importazole. As shown in Fig. 6, ANS-induced nuclear localization of IGFBP-3-GFP was attenuated by importazole, indicating that IGFBP-3 does utilize importin-β for nuclear import.

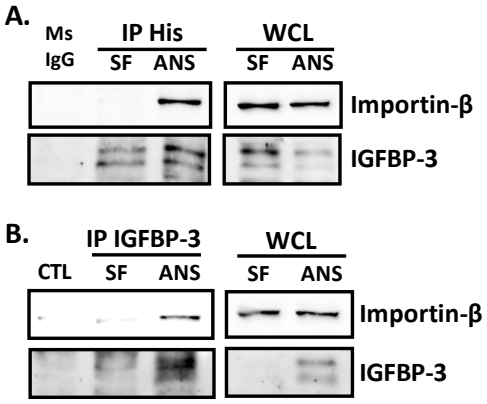

Fig. 5. IGFBP-3 associates with importin-β in response to cellular stress. (A) Cells transfected with IGFBP-3-his were treated 1 h ± 0.1 µM ANS. Whole cell lysates (WCL) were collected and IGFBP-3 was immunoprecipitated with an anti-his-tag antibody or lysates were incubated with an IgG control. IP products were immunoblotted for IGFBP-3 or importin-β. Results are representative of two independent experiments. (B) Non-transfected cells were treated 8 h ± 0.1 µM ANS. Whole cell lysates were collected and IGFBP-3 was immunoprecipitated with anti-bIGFBP-3 antibody. Non-immune serum served as a control (CTL).

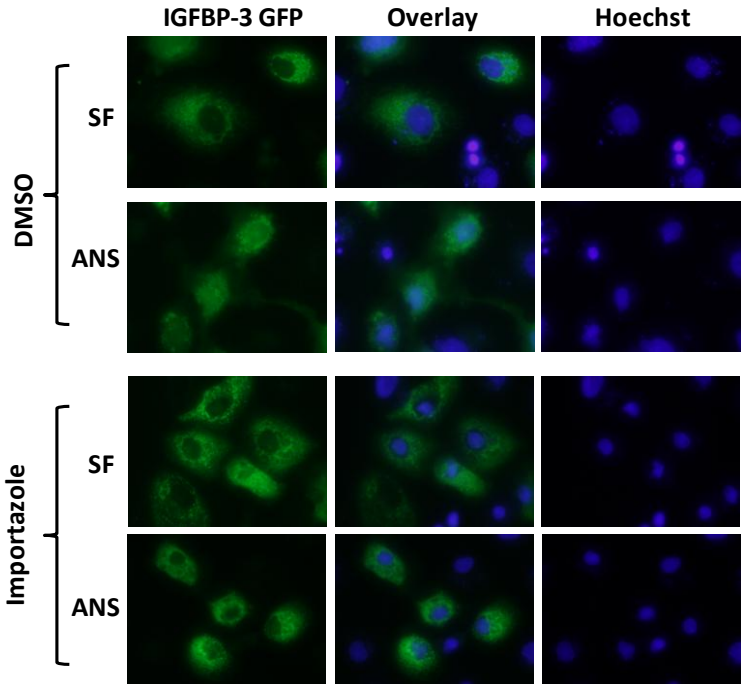

Fig. 6. Importazole reduces nuclear import of IGFBP-3-GFP. Cells transfected with IGFBP-3-GFP were treated 4 h ± 0.1 µM ANS ± 40 µM Importazole. Cells were fixed in formalin then nuclei were stained with Hoechst. Images were acquired with an Olympus FSX100 microscope. Images are representative of two independent experiments.

Discussion

IGFBP-3 is produced and secreted in response to mitogenic and apoptotic stimuli. IGF-I and epidermal growth factor (EGF) both induce accumulation of IGFBP-3 in culture media, where IGFBP-3 potentiates their mitogenic effects (5,46,51). IGFBP-3 is also produced in response to stressors including TGF-β (7,81), TNF-α (67), hypoxia (187), and ANS (Chapter 2) and potentiates their apoptotic effects. The mechanism governing the role IGFBP-3 in cell fate remains unclear, however one potential mediator of biological function is cellular localization.

Nuclear localization of IGFBP-3 is associated with its role in apoptosis. IGFBP-3 localizes to the nucleus in response to apoptotic stimuli including TGF-β (7,81) and ANS (Chapter 2). IGFBP-3 is also detected in the nucleus of cells transfected or treated with IGFBP-3, and can inhibit proliferation (50,89) or induce apoptosis in these cells (50,60,88). In addition, the absence of nuclear IGFBP-3 is associated with resistance to apoptosis in senescent fibroblasts (77). We have demonstrated that IGFBP-3 mediates ANS-induced apoptosis through activation and nuclear export of Nur77 (Chapter 3). These data established a nuclear function for IGFBP-3 in intrinsic apoptosis. We next wanted to characterize the mechanism of nuclear import of IGFBP-3 in MAC-T cells.

To determine if nuclear import of IGFBP-3 is a regulated event, MAC-T cells transfected with GFP-IGFBP-3 were treated ± ANS then cellular distribution of IGFBP-3 was examined. While endogenous IGFBP-3 is approximately 36-38 kDa, the GFP-tagged IGFBP-3 is closer to 64 kDa, making it too large for passive diffusion through the nuclear pore. We found that in the absence of treatment IGFBP-3 resided in the cytosol and that upon addition of ANS it translocated to the nucleus. Since caspases activated during apoptosis act to degrade the nuclear membrane,

another possibility is that IGFBP-3 diffuses through this leaky membrane. However, our previous work showed that the pan-caspase inhibitor z-vad-fmk does not reduce nuclear accumulation of IGFBP-3 (Chapter 2). Together, these data suggest that nuclear import of IGFBP-3 is an active process, leading us to examine a mechanism for nuclear localization of IGFBP-3.

IGFBP-3 is both a secreted and a nuclear protein. It has been proposed that IGFBP-3 is secreted, re-internalized, then directed to the nucleus (81). However, data regarding secretion and re-internalization of IGFBP-3 are conflicting. In breast and prostate cancer cells a mutation of the signal peptide required for cellular secretion of IGFBP-3 fails to block its ability to induce apoptosis suggesting that IGFBP-3 does not have to be secreted to modulate apoptosis (80,83). However another group working with PC-3 cells found that sequestering secreted IGFBP-3 with a mutant IGF-I that does not bind the IGFR prevents nuclear accumulation of IGFBP-3 and inhibits TGF-β-induced apoptosis (63), suggesting that an IGF-IGFBP-3 complex located extracellularly could be transported to the nucleus to induce apoptosis. Other data indicate that exogenous IGFBP-3 binds to the cell surface prior to cellular uptake and nuclear localization, suggesting the presence of cellular machinery controlling uptake of secreted IGFBP-3 (86). One group has identified an IGFBP-3 receptor on the cell surface of breast cancer and prostate cancer cells and shown it to be linked to the extrinsic apoptotic pathway, however the physiological significance of this putative receptor in cells endogenously expressing both IGFBP-3 and the IGFBP-3R remains unknown (82). In MAC-T cells, ANS activates the intrinsic apoptotic pathway making it unlikely that IGFBP-3 utilizes a cell-surface receptor to induce apoptosis in these cells (65).

We previously established that ANS induces production of IGFBP-3 and IGFBP-3 is subsequently found both in the culture media and in the nucleus of MAC-T cells (Chapter 2). To determine if secreted IGFBP-3 is re-internalized in MAC-T cells, cells were treated with ANS ± Pitstop2. Pitstop2 is a cell permeable inhibitor of clathrin-mediated endocytosis with reported off-target inhibitory effects on other mechanisms of endocytosis (188). These off-target effects are not a concern in this system because if IGFBP-3 is secreted and re-internalized then the chances of achieving a reduction in intracellular IGFBP-3 would be enhanced. Nuclear IGFBP-3 was unaffected by Pitstop2, indicating that secreted IGFBP-3 is not re-internalized in MAC-T cells.

Having established that secreted IGFBP-3 is not re-internalized we next wanted to confirm that non-secreted IGFBP-3 can localize to the nucleus. Brefeldin-A, an inhibitor of ER to golgi trafficking was used to inhibit secretion. Cells treated with ANS + Brefeldin-A had similar amounts of nuclear IGFBP-3 as cells treated with ANS alone, showing that in MAC-T cells non-secreted IGFBP-3 can localize to the nucleus. These data are especially interesting because nuclear IGFBP-3 is N-glycosylated, indicating it has been through at least part of the secretory pathway (Fig. 2). The presence of glycosylated IGFBP-3 in the nucleus suggests that IGFBP-3 somehow escapes the secretory pathway and gets redirected to the nucleus. Retrograde translocation is one possible mechanism, but this pathway is typically used for receptor recycling at the cell surface, trafficking of cholesterol between the plasma membrane and intracellular vesicles, or for misfolded proteins as part of the unfolded protein response. Re-internalization of IGFBP-3 from the medium would be a slow, inefficient step in the highly organized mechanism of apoptosis, so it seems logical that nuclear IGFBP-3 is derived from non-secreted protein.

Having established that nuclear import of IGFBP-3 is a regulated event, not a result of passive diffusion, we next examined a role for importin-β in nuclear transport of IGFBP-3. In cells with a permeabilized cell membrane, exogenous IGFBP-3 utilizes its NLS to bind importin-β to gain nuclear entry (99). In vitro experiments also show that NLS of IGFBP-3 has a stronger affinity for importin-β than importin-α (99,100). To determine if IGFBP-3 utilizes importin-β for nuclear import in MAC-T cells we treated ± ANS then immunoprecipitated (IP) IGFBP-3 and immunoblotted the IP product for importin-β. In untreated cells, no association was detected between IGFBP-3 and importin-β, however, upon ANS-treatment these proteins co-precipitated. The IP data indicate a regulated association between IGFBP-3 and importin-β so we next tested the effect of importazole, a chemical inhibitor of importin-β, on the ability of ANS to induce nuclear localization of IGFBP-3. Importazole successfully reduced nuclear import of IGFBP-3-GFP, indicating a role for importin-β in nuclear transport of IGFBP-3.

An understanding of the mechanism for nuclear import of IGFBP-3 is important in establishing how IGFBP-3 exerts its apoptotic effects. While IGFBP-3 is a secreted protein, its presence in the nucleus indicates it has either autocrine or intracrine effects. Since non-secreted IGFBP-3 can localize to the nucleus in MAC-T cells and other cell lines it is likely that intracrine effects play a role in IGFBP-3-mediated apoptosis (83). We and others have identified a role for IGFBP-3 in modulating activation and nuclear localization of Nur77 during apoptosis (Chapter 3 and (91)). Further work will determine the nature of the interaction between IGFBP-3 and Nur77 in MAC-T cells to better understand the role of nuclear IGFBP-3 in apoptosis.

Chapter 5.

Expression and purification of IGFBP-3 and production of a polyclonal antibody

Abstract

An understanding of the molecular mechanisms governing milk production in the bovine mammary gland will enhance the development of technologies to increase total lactational yield. At the cellular level, the IGF system affects mammary gland development and milk production, however, the molecular tools available for studying the IGF family of proteins in the bovine system remain limited. The commercially available IGFBP-3 antibodies are designed for human or rodent systems and do not recognize the bovine proteins. The aim of this work was to develop a polyclonal antibody specific for bovine IGFBP-3. To obtain IGFBP-3 for use as an antigen, MAC-T cells were transfected with a DNA plasmid encoding histidine (his)-tagged bovine IGFBP-3. Since IGFBP-3 is a secreted protein, it was collected from conditioned media and purified with a nickel affinity column. Pure protein was separated on an acrylamide gel then silver stained to confirm absence of contaminants. New Zealand white rabbits were immunized with IGFBP-3 three times over the course of 5 months. Western immunoblot data showed that the resulting serum contained anti-IGFBP-3 antibodies that recognized purified IGFBP-3-his as well as IGFBP-3 in biological samples. Serum from multiple species was immunoblotted with anti-bIGFBP-3 antibody. The antibody failed to recognize rat and murine IGFBP-3 in serum while it had some sensitivity for human, equine and porcine IGFBP-3. Finally, the bIGFBP-3 antibody was successfully used to immunoprecipitate endogenous IGFBP-3 from non-transfected cells. In conclusion, we successfully generated an antibody specific to bovine IGFBP-3 that can be used for Western immunoblot and co-immunoprecipitation experiments.

Introduction

Apoptosis in the mammary gland is of special significance in the lactating dairy cow. Milk production gradually increases for 6-8 weeks after calving until peak yield is reached. This increase in milk yield is attributed to an increase in secretory capacity of milk-secreting cells (1). After peak yield is reached milk output gradually declines. Secretory capacity remains unchanged after peak yield is reached so the decline in milk production is attributed to loss of milk secreting cells through apoptosis (1,189). IGFBP-3 has an established role in apoptosis in a number of cell types, including MAC-T bovine mammary epithelial cells (MEC) (6,65,190).

IGFBP-3 functions in both cellular survival and death. Circulating IGFBP-3 acts to enhance IGF-signaling by prolonging the half-life of circulating IGF-I. At the cell surface IGFBP-3 potentiates mitogenic signaling by IGF-I or EGF (107). However, IGFBP-3 can also inhibit proliferation by sequestering IGF-I from its receptor. Interestingly, IGFBP-3 has effects independent of IGF-I. IGFBP-3 can inhibit proliferation and induce apoptosis in a number of cell types, either directly or by modulating the effects of external stressors (107). IGFBP-3 is produced in response to intrinsic stressors, and functions to enhance the apoptotic stimulus (67,187,191).

IGFBP-3 produced locally in the mammary gland is thought to contribute to the intrinsic apoptotic response in MAC-T cells. We previously established that IGFBP-3 is produced in response to the intrinsic stressor anisomycin (ANS) and that IGFBP-3 knock-down attenuates ANS-induced apoptosis of MAC-T cells (Chapter 2). Cellular fractionation data show that ANS directs IGFBP-3 to the nucleus where it facilitates nuclear export of orphan nuclear receptor Nur77 (Chapter 3). Antibodies made against human, rat or porcine IGFBP-3 have limited cross-

reactivity with bovine IGFBP-3. Our lab has been using a polyclonal antibody produced against glycosylated full-length IGFBP-3 by Dr. David Clemmons at UNC Chapel Hill in the 1990s. This antibody has been depleted by our laboratory. Therefore, to continue our investigations on the role of intracellular IGFBP-3 in bovine mammary gland physiology it was necessary to develop an antibody specific for the bovine protein to replace this antibody. The primary objective of this work was to express bovine IGFBP-3, purify it from culture medium, then use the pure protein as an antigen for antibody production.

Materials and methods

Chemical reagents

Phenol red-free (PRF) DMEM-low glucose media, gentamycin, bovine insulin, anisomycin (ANS), and fetal bovine serum (FBS) were purchased from Sigma (St. Louis MO). Recombinant human IGF-I (100% identical to bovine IGF-I) was obtained from Peprotech (Princeton, NJ). DMEM with high glucose, penicillin and streptomycin were purchased from Invitrogen (Carlsbad, CA). ANS was purchased from Sigma Aldrich (Saint Louis, MO). Antibodies against the following proteins were purchased as indicated: HSP60 (Abcam, Cambridge, MA), human IGFBP-3 (Millipore, Billerica, MA) and Lamin A/C (Santa Cruz). Endoglycosidase-H_f was purchased from New England Biolabs (Ipswich, MA). Custom SmartPool siRNA for bovine IGFBP-3 and scramble siRNA control were purchased from Dharmacon, Inc (Lafayette, CO). Mirus Transit TKO transfection reagent was purchased from Stratagene (La Jolla, CA). Silver stain kit was purchased from BioRad (Hercules, CA).

Cell culture

The bovine MEC line MAC-T (137) or primary bovine MECs (138) were routinely maintained in complete media consisting of DMEM containing 4.5 g/ liter D-glucose (i.e., DMEM-H), 20 U/ml penicillin, 20 μg/ml streptomycin, 50 μg/ml gentamicin, 10% FBS, and 5 μg/ml insulin. For experiments, cells were plated and grown to confluence in phenol red-free DMEM-H containing 10% FBS and antibiotics and without insulin. Except where otherwise noted, cells were rinsed with phosphate-buffered saline (PBS), and incubated in serum-free (SF) DMEM-H with 0.2% BSA and 30 nM sodium selenite overnight prior to exposure to treatments in SF DMEM-H without additives.

Construction of His-tagged IGFBP-3 (BP3-His)

A PCR reaction was used to add a 6x-His tag to the C terminus of bovine IGFBP-3. *Xho*I and *Not*I restriction sites were added to the 5' and 3' ends, respectively, to flank the IGFBP-His sequence, producing a 923 bp IGFBP3-his fragment. The 50 µl PCR reaction contained 20 ng DNA template (pRc/RSV IGFBP3, Grill and Cohick, 2000), 20 pmol forward primer 5'-ATATTACTCGAG TAATGCTGCGGGCACGCCCCGCGCTC-3', 20 pmol reverse primer 5'-ATAGTTTAGCGGCCGCTCAATGGTGATGGTGATGATGCTTGCTCTCCAT-GCTGTAGCAGT-3', 2 mM Mg SO_4, 0.2 mM of each dNTP, 5% DMSO and 1 unit Platinum *Taq* High Fidelity DNA Polymerase (Life Technologies, Carlsbad, CA). The cycling parameters were 94˚C 2 min; 30 cycles of 94˚C 1 min, 55˚C 1 min, 68˚C 1 min; 68˚C 10 min. The IGFBP-3-His fragment was purified using Nucleospin Gel and PCR Clean-up kit (Macherey-Nagel, Bethlehem, PA). BP3-His (insert) and pEGFP-N1 (vector) were digested with *Xho*I and *Not*I. This digestion excises EGFP from the plasmid. After vector dephosphorylation with Anarctic Phosphatase (New England Biolabs) both insert (902 bp) and vector (3945 bp) were purified as described above and ligated using T4 DNA Ligase (Invitrogen, Carlsbad, CA). The ligation reaction was used to transform One Shot TOP 10 competent cells (Invitrogen). After miniprep, colonies were screened for positive clones by restriction digestion. Bovine IGFBP3-His construction was confirmed by sequencing.

Transient transfection and purification of IGFBP-3

MAC-T cells were plated in complete media at $3.5x10^4$ cells/cm^2. The next day sub-confluent cells were transfected with a plasmid encoding cDNA for bovine IGFBP-3-His. Plasmids were prepared using the EndoFree plasmid Maxi Kit (Qiagen, Valencia CA). Cells were transfected using SuperFect (Qiagen) combined with plasmid in a 1:5 ratio for 100 mm^2 dishes. The

transfection mixture was prepared in DMEM-H with no additives, vortexed for 10 sec, and incubated at RT for 10 min. Spent media were removed from cells and replaced with fresh complete media and the transfection mixture. After 3 h, media were removed and replaced with fresh complete media. Following a 24 h recovery in serum-containing media, cells were rinsed twice in PBS and incubated with fresh SF DMEM-H (5 ml per plate) for 72 h. All media were collected and filtered through a 0.45 µM bottle top filter (Corning, Tewksbury, MA) to remove dead cells and debris, then stored at 4°C until use. Chromatography columns (BioRad) were each loaded with 1 ml of Ni-NTA slurry, supernatant was allowed to flow through then beads were re-suspended in 4 ml bind buffer (300 mM NaCl, 50 mM Na_3HPO_4, 10 mM imidazole, pH 8). Supernatant was allowed to flow through then discarded. 10 ml media was added per column and incubated 2 h at 4°C on a rotating platform then beads were allowed to settle by gravity and media allowed to flow through. Columns were washed 3x with wash buffer (300 mM NaCl, 50 mM Na_3HPO_4, 20 mM imidazole, pH 8). Bound protein was eluted with 3x 1ml volumes of elution buffer (300 mM NaCl, 50 mM Na_3HPO_4, 250 mM imidazole, pH 8). Primary elutions were saved for use as antigen. As shown in Table 1 (p. 107), media typically contained over 3 µg IGFBP-3 per ml of conditioned media. Addition of BSA (200 µg/ml) to serum-free medium increased stability of secreted IGFBP-3, evidenced by the reduced concentration of IGFBP-3 in media used for Antigen #3.

Antigen preparation and serum collection

Primary elutions containing IGFBP-3 were concentrated in Amicon Ultra YM10 Centrifugal concentrators (Millipore). At the same time buffer exchange was used to dilute the elution buffer to achieve an imidazole concentration below 50 mM. Concentrated IGFBP-3 was

sterilized by passage through a syringe filter (Machery-Nagel, Duren, GE). Samples were then stored overnight at -20°C or used as an antigen on the same day.

Two naive New Zealand white rabbits each received three subcutaneous doses of IGFBP-3 according to the schedule described in Table 1. Non-immune serum was collected prior to the first dose and tested for cross-reactivity with IGFBP-3. The initial dose of IGFBP-3 was mixed with an equal volume of Freund's complete adjuvant. Subsequent doses were mixed with Freund's incomplete adjuvant. All doses were administered at four subcutaneous injection sites. Serum was drawn according to the schedule presented in table 2. Animals were housed at the Rutgers University Laboratory Animal Facility.

Antigen #	µg IGFBP-3	# 100 cm^2 plates	mL media	µg IGFBP-3 per ml media	Media containing serum	Media containing BSA
1-1	500	30	150	3.3	No	Yes
1-2	500	30	150	3.3	Yes	No
2	400	22	110	3.6	No	Yes
3	100	22	110	1	No	No
Total:	**1500**	**104**	**520**	**Ave: 2.9**		

Table 1. Expression of IGFBP-3 for use as an antigen. Pure IGFBP-3 from multiple purification experiments was combined for use as an antigen. For the initial dose of IGFBP-3, antigen was prepared for each rabbit separately. Rabbit #104 received IGFBP-3 purified from serum-free medium (Antigen 1-1), rabbit #109 received IGFBP-3 purified from serum-containing media (Antigen 1-2). Antigen #2 was equally divided between the two rabbits. Antigen #3 was administered to rabbit #109 only, since rabbit #104 was removed from study. In initial purification experiments bovine serum albumin (BSA) was added to serum-free medium to enhance stability of secreted IGFBP-3. IGFBP-3 was purified from serum-free medium unless otherwise noted.

Week	Date	Bleed # / Boost #
Week 0, Day 0	5-23-13	Pre-Immune Serum Initial immunization (500µg/animal)
Week 4	6-16-13	Bleed 1 (1 ml serum/animal)
Week 5	6-26-13	Bleed 2 (1 ml/animal) Boost 1 (200 µg/animal)
Week 7	7-10-13	Bleed 3 (1ml/animal)
Week 9	7-26-13	Bleed 4 (15ml/animal)
Week 14	8-20-13	Bleed 5 (15 ml) Boost 2 (100 µg) Rabbit#104 removed from study
Week 18	9-20-13	Bleed 6 (15 ml)
Week 22	10-9-13	Bleed 7/Exsanguination (40 ml)

Table 2. Antibody production time line. Dates of injections and bleeds are detailed with the ng amount of IGFBP-3 administered or ml volume of serum collected. Rabbit #104 was removed from study at week 14 due to poor production of anti-IGFBP-3 antibodies.

Western immunoblotting

Whole cell lysates were collected in lysis buffer (1% Triton-X 100, 50 mM HEPES, 80 mM β-glycerophosphate, 2 mM EDTA, 2 mM EGTA, 10 mM NaF, 0.1% SDS, supplemented with 0.1 mM PMSF, 1 µg/ml each of aprotinin, leupeptin, and trypsin inhibitor, 10 mM NaF and 2 mM NaO), incubated 30 min on ice then centrifuged 13,000xg for 15 min. For nuclear extraction, cytosolic extracts were obtained by lysing cells in hypertonic buffer (20 mM Hepes pH 7, 10 mM KCL, 0.1% Triton, 20% glycerol supplemented with 1 mM DTT, 1 mM PMSF, 1 µg/ml each of aprotinin, leupeptin, and trypsin inhibitor, 10 mM NaF and 2 mM NaO) with 10 strokes of the dounce homogenizer followed by centrifugation for 5 min 1000xg. Pellets were resuspended in buffer C

(20 mM Hepes pH 7.9, 0.42M NaCl, 1.5mM MgCl2, 0.2mM EDTA, 25% glycerol, supplemented with 0.1 mM DTT, 0.1 mM PMSF, 1 µg/ml each of aprotinin, leupeptin, and trypsin inhibitor, 10 mM NaF and 2 mM NaO), incubated on ice 30 min, then centrifuged at 13,250 RPM for 10 min and the supernatant was saved as the nuclear fraction. Lysates were assayed for protein with the BioRad Protein Assay (BioRad, Hercules, Ca). Proteins were separated by SDS polyacrylamide gel electrophoresis (PAGE) under non-reducing non-denaturing conditions on 10 or 15% gels and transferred to nitrocellulose (0.2 µM; Bio-Rad) or PVDF (0.45 µM; Millipore) membranes. Membranes were blocked for 1 h at room temperature in Tris–buffered saline + 0.05% Tween-20 (v/v) (TBS-T) and 5% non-fat dried milk (w/v), and incubated with primary antisera at 4°C overnight with gentle agitation. Membranes were then washed in TBS-T and incubated for 1 h at room temperature with appropriate HRP-conjugated secondary antibodies. Peroxidase activity was detected with ECL Prime (GE, Pittsburgh, PA). Chemiluminescence was detected with the Fluorchem FC2 (Protein Simple, Santa Clara, CA).

Silver staining

For silver staining, 30 µl of primary elutions were run under reducing and denaturing conditions on a 12.5% polyacrylamide gel. The gel was then fixed and stained using a silver stain kit according to manufacturer-s instructions (BioRad).

siRNA experiments

MAC-T cells were plated in complete media at $3x10^4$ cells/cm^2. The following day, subconfluent cells were transfected with 50 nM IGFBP-3 siRNA oligos or a corresponding concentration of scrambled control siRNA using Mirus Transit TKO Transfection Reagent according to

manufacturer's instructions. After 48 h, cells were washed with PBS and incubated overnight in serum-free DMEM-H media, then treated for analysis of gene knock-down. Gene knock-down of IGFBP-3 was verified by Western immunoblotting as described above.

Deglycosylation of proteins

Whole cell lysates (50 µg) were incubated with denaturing buffer for 10 min at 100°C. Then reducing buffer ± 5000 units Endoglycosidase H_f was added and samples were incubated at 37°C for 2 h. Samples were mixed with Laemmli loading buffer, heated 10 min at 60°C then loaded on a 12.5% SDS PAGE gel for Western immunoblot analysis.

Immunoprecipitation

Whole cell lysates were collected in Active Motif lysis buffer AM1 according to manufacturer's instructions (Active Motif, Carlbad, CA). Five-hundred µg whole cell lysate was incubated overnight at 4° C with 2 µl serum containing anti-IGFBP-3 antibodies or non-immune serum. Twenty µl protein-G bead slurry (Millipore) was added and washed 3x with PBS then mixed with lysates for 2 h at 4° C. Beads were then pelleted, washed 3x with PBS, then resuspended in 40 µl 2x Laemmli loading buffer, and boiled for 5 min to elute bound proteins. Beads were then pelleted and supernatant was loaded onto a 10% SDS PAGE gel.

Results

Purified IGFBP-3 is free of contaminants

To examine the purity of the primary elutions, samples were run by SDS PAGE and silver stained (Fig. 1). IGFBP-3-his-IGFBP-3 was detected as a block running between the 38-52 kDa molecular weight markers, which is consistent with the literature (60,101). No other bands were detected on the silver stain, indicating that the nickel affinity column was successful in removing only IGFBP-3 from the conditioned media. IGFBP-3 detected by immunoblotting was detected at the same molecular weight as IGFBP-3 detected with the silver stain (Fig. 1).

Detection of IGFBP-3 in serum

IGFBP-3 is the most abundant IGFBP in serum so we tested the ability of our antibody to detect IGFBP-3 in serum collected from a range of species. As shown in Fig. 2, our antibody detected IGFBP-3 in bovine serum, with weaker affinity for human, porcine and equine IGFBP-3. A commercial anti-IGFBP-3 antibody (Millipore) recognized IGFBP-3 in human and porcine serum, with limited affinity for bovine, porcine and equine IGFBP-3. Previous work in our lab found that IGFBP-3 was readily detected in 0.5 µl serum, so that is the volume that was used to test cross-reactivity with the species shown. However, it is possible that detection of IGFBP-3 in other species would be enhanced by running larger volumes of serum.

Detection of IGFBP-3 in biological samples

To confirm that the IGFBP-3 signal detected in cell lysates was specific to IGFBP-3, we used siRNA to knock-down expression of IGFBP-3 then collected conditioned media and cellular fractions from cells treated ± ANS (Fig. 3A). Endogenous IGFBP-3 was undetectable basally, but

increased in media and cellular fractions following 6 h ANS-treatment as expected. Knockdown of IGFBP-3 with siRNA attenuated IGFBP-3 in media and fractions.

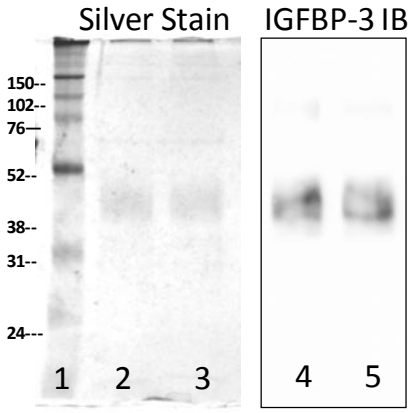

Fig. 1. Purity of primary elution of IGFBP-3. Primary elution of pure IGFBP-3 was run by SDS-PAGE and analyzed by Silver stain (Lanes 2-3; 30 µl primary elution from two separate columns) or Western blot (Lanes 3-4; 15 µl of primary elution from each column). Lane 1 represents molecular weight ladder.

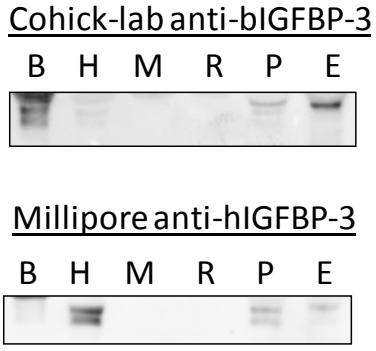

Fig. 2. Detection of IGFBP-3 in serum. Bovine (B), human (H), murine (M), rat (R), porcine (P), or equine (E) serum (0.5 µl per lane) was immunoblotted for IGFBP-3 with our anti-bovine-IGFBP-3 antibody or a commercial antibody against human IGFBP-3 (Millipore).

Since we purified IGFBP-3 protein from mammalian cells, the antigen consisted of glycosylated IGFBP-3. This led us to ask if the antibody also recognizes non-glycosylated IGFBP-3. Lysates from MAC-T cells treated 8 h ± ANS were incubated ± Endoglycosidase H_f (Endo-H) to remove carbohydrate groups. As shown in Fig. 3B, glycosylated IGFBP-3 was detected as a doublet in whole cell lysates running at approximately 36-38 kDa. Upon incubation with Endo-H this doublet was reduced to a single, faster migrating band of approximately 29 kDa which corresponds with the molecular weight of non-glycosylated IGFBP-3. These data indicate that both glycosylated and non-glycosylated IGFBP-3 are readily detected with the bIGFBP-3 antibody.

The IGFBP-3 antibody will be used to examine IGFBP-3 in both immortalized and primary cells. To determine if the antibody recognizes IGFBP-3 produced by primary cells, primary bovine MECS were treated ± ANS, IGF-I, or ANS+IGF-I and conditioned media were collected. Fig. 3C shows that both ANS and IGF-I induced expression and secretion of IGFBP-3, supporting similar results obtained in MAC-T cells (65). The bIGFBP-3 antibody recognized IGFBP-3 secreted in response to each of these treatments. Interestingly, IGFBP-3 runs at a lower molecular weight in media of cells treated with IGF-I, compared to the IGFBP-3 secreted in response to ANS or ANS+IGF-I.

Co-immunoprecipitation of IGFBP-3

To determine if the antibody could be used for immunoprecipitation, cells transfected with IGFBP-3-his were lysed and IGFBP-3 was immunoprecipitated (IP) from whole cell lysates using

the bovine IGFBP-3 antibody. As shown in Fig. 4, IP of bovine IGFBP-3 from cell lysates was successful.

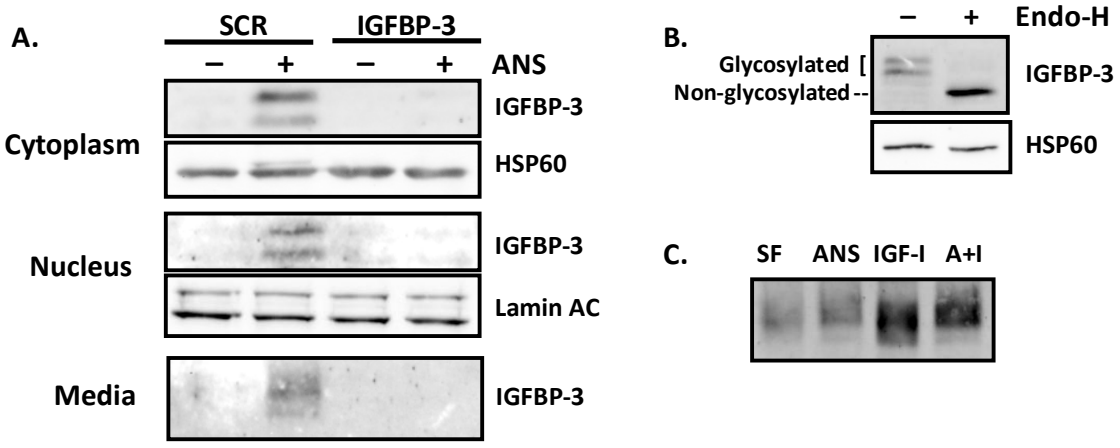

Fig. 3. Detection of endogenous IGFBP-3 in biological samples. (A) MAC-T cells were transfected with 50 nM IGFBP-3 or scramble siRNA for 48 h, serum-starved overnight, and treated 6 h ± 0.1 µM ANS. Cellular fractions and conditioned media (100 µl) were immunoblotted for IGFBP-3. Lamin AC and HSP60 served as nuclear and cytoplasmic markers, respectively. (B) Whole cell lysates from cells treated 8 h + 0.1 µM ANS were incubated ± Endo-glycosidase-H_f (Endo-H) then immunoblotted for IGFBP-3. HSP60 served as a loading control. (C) Primary bovine MECs were treated 24 h ± 0.1 µM ANS, 100 ng/ml IGF-I or ANS+IGF-I (A+I). 200 µl media were concentrated and immunoblotted for IGFBP-3.

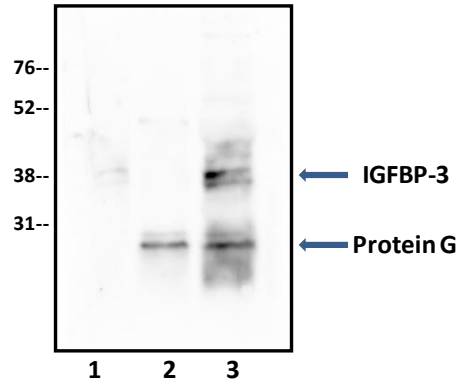

Fig. 4. Immunoprecipitation of IGFBP-3. MAC-T cells transfected with IGFBP-3-his were collected in Active Motif lysis buffer. 50 µg WCL was run as input control (lane 1). 0.5 mg cell lysate was incubated with rabbit IgG (lane 2) or bIGFBP-3 antibody (lane 3).

Discussion

The overall goal of this work was to express and purify IGFBP-3 to produce an antibody that recognizes bovine IGFBP-3. We first needed to identify the appropriate expression conditions to produce recombinant IGFBP-3. Recombinant proteins can be expressed in bacteria, insect cells, or mammalian cells. Bacteria synthesize recombinant proteins without post-translational modifications such as glycosylation while insect and mammalian cells retain the ability to glycosylate proteins (192). However, insect systems do not always result in glycosylation patterns with the same pattern as in mammalian cells. Additionally, an extra secretion signal must be added to achieve secretion from insect cells. This secretion signal gets cleaved off as part of the secretory process in insect cells so it likely would not affect the final sequence of secreted IGFBP-3, however addition of the insect secretion signal might affect intracellular processing such as protein folding and availability of glycosylation sites (192). IGFBP-3 has three glycosylation sites and both intracellular and secreted IGFBP-3 are glycosylated, making glycosylated IGFBP-3 the optimal antigen to recognize IGFBP-3 in biological samples (101). We chose to express IGFBP-3-his in mammalian cells because they retain the ability to glycosylate and secrete recombinant proteins without any extra modifications.

IGFBP-3 has been purified using multiple affinity column techniques. IGFBP-3 has affinities for heparin and IGF-I, facilitating purification of IGFBP-3 using custom affinity columns with immobilized heparin or IGF-I (193-195). Alternatively, addition of a tag allows for use of commercially available products to assemble nickel affinity columns. We found nickel affinity purification to be more economical than assembly of custom affinity columns. To facilitate nickel affinity purification, a 6xHis-tag was added to the C-terminus of IGFBP-3. Affinity tags can

be cleaved off when incorporated with a peptidase site, however the his-tag is small so we chose not to remove it (196). The secretion signal is at the N-terminus of IGFBP-3 so we chose to add the tag to the C-terminus. IGFBP-3 is a secreted protein, facilitating purification from conditioned media.

Fig. 1 shows successful expression and purification of bIGFBP-3. Detection of IGFBP-3 was optimal with serum from bleed 5 (data not shown) so all immunoblots used bleed 5 serum diluted in TBS-T+5% milk. To determine if the antibody recognizes IGFBP-3 from other species, serum from 6 species was immunoblotted with anti-bIGFBP-3 antibody (i.e. Cohick) or a commercial antibody against human IGFBP-3 (Millipore). Fig. 2 shows the drastic difference in sensitivity of Millipore antibody for human vs. bovine IGFBP-3 and demonstrates the need for a more sensitive antibody for bovine IGFBP-3. Both the Millipore and Cohick antibodies only recognized the most glycosylated form of equine IGFBP-3. Longer exposures with the Cohick antibody showed weak detection of human IGFBP-3. It is interesting that the Cohick and Millipore antibodies detect IGFBP-3 from their target species so well but detect IGFBP-3 from human and bovine IGFBP-3 respectively, so poorly. IGFBP-3 from both species runs at the same molecular weight so no obvious changes in post-translational modifications exist. Differences in protein folding or location of glycosylation sites could contribute to the poor species cross-reactivity of the antibodies. Human and bovine IGFBP-3 have only 83% protein sequence homology. When the full length protein is used as an antigen for polyclonal antibody production, as was done for the Millipore and Cohick antibodies, the antibodies generated could recognize sequences that are not conserved across species.

To further characterize the differences between the Cohick and Millipore antibodies we were interested in comparing their sensitivity for bovine IGFBP-3, however, the Cohick antibody is not purified so we could not match their concentrations. However, there are a few approaches we can use to troubleshoot this issue. First, we can isolate the IgG from the rabbit serum. This would precipitate all of the antibodies in the serum and serve as a crude purification step. Ammonium sulfate precipitation works to separate IgG from other serum proteins due to the low salt concentration needed to precipitate IgG relative to other circulating proteins (197). This isolated IgG can then be used directly as a primary antibody or can be further purified with commercial IgG purification columns. Alternatively, we could specifically purify the anti-IGFBP-3 antibodies. To accomplish this we can immobilize bIGFBP-3 on resin beads and incubate the beads+bIGFBP-3 with the serum containing anti-bIGFBP-3 antibodies. Only anti-bIGFBP-3 IgG will adhere to the column. Unbound proteins would be washed off, then the bound IgG would be eluted and used as a purified IGFBP-3 antibody. The final IgG product could be quantified with a Nano-drop using the settings for measuring IgG concentration.

Fig. 2 demonstrated detection of bovine IGFBP-3 in serum; however, serum contains large amounts of IGFBP-3 and does not reflect amounts of IGFBP-3 in biological samples. To determine if the bIGFBP-3 antibody recognized IGFBP-3 in biological samples we ran nuclear and cytoplasmic fractions and conditioned media. As shown in Fig 3A, the antibody detected IGFBP-3 produced by MAC-T cells treated with ANS. Knock-down of IGFBP-3 attenuated detection of intracellular or secreted IGFBP-3 supporting the conclusion that the antibody is specific to IGFBP-3. Sensitive detection of IGFBP-3 in biological samples is especially important for work with primary mammary epithelial cells. Cross reactivity with IGFBP-3 produced by primary cells

was examined in Fig 3C. These data show that ANS and IGF-I induce production and secretion of IGFBP-3, supporting our findings in MAC-T cells and demonstrating that the antibody detects IGFBP-3 produced by primary cells. Interestingly, IGFBP-3 produced in response to IGF-I runs at a lower molecular weight than IGFBP-3 produced in response to ANS. These results are consistent with results in MAC-T cells (65). This shift in molecular weight could be due to differential glycosylation patterns or phosphorylation of IGFBP-3 in cells treated with ANS but not with IGF-I. Alternatively, the rate of passage of IGFBP-3 out of the cell could be faster in IGF-I-treated cells, leaving less time for additional glycosylation as IGFBP-3 passes through the secretory pathway.

The antigen consisted of glycosylated IGFBP-3 so we wanted to determine if the antibody also detects non-glycosylated IGFBP-3. Proteins in whole cell lysates were deglycosylated with Endo-H then immunoblotted for IGFBP-3. The two bands detected in whole cell lysates were reduced to a single, lower molecular weight band upon Endo-H-treatment. Detection of all three bands of IGFBP-3 demonstrated that the antibody recognizes both glycosylated and non-glycosylated IGFBP-3.

Finally, we wanted to determine if the Cohick antibody works for IP experiments. Fig. 4 shows successful IP of IGFBP-3 from cells transfected with IGFBP-3-His. Data in Chapter 4 demonstrated IP of endogenous IGFBP-3 from MAC-T whole cell lysates. These data are especially exciting because we are the first group to show that *endogenous* IGFBP-3 associates with importin-β in mammalian cells. All previous work has relied on over-expression of IGFBP-3 or use of purified proteins.

Future work will determine optimal storage conditions for pure IGFBP-3 and biological activity of the pure protein. We previously found that over-expression of IGFBP-3 does not induce apoptosis in MAC-T cells. However, we have not examined the effect of exogenous IGFBP-3 on apoptosis (Chapter 2). To determine if exogenous IGFBP-3 affects ANS-induced apoptosis we can treat cells ± IGFBP-3 ± ANS then measure caspase activation over time. This will determine if exogenous IGFBP-3 directly induces apoptosis or if it enhances ANS-induced apoptosis. We can also knock-down IGFBP-3 then treat cells with ANS ± IGFBP-3 to determine if the exogenous protein can restore sensitivity to ANS-induced apoptosis. Finally, to determine if IGFBP-3 binds IGF-I we can treat cells ± IGF-I ± IGFBP-3. Cells treated with IGF-I should have increased phosphorylated AKT, and if IGFBP-3 attenuates phosphorylation of AKT in IGF-I-treated cells then we can conclude that pure IGFBP-3 binds IGF-I.

Chapter 6.

General conclusions and future directions

Modulation of death signals in the mammary gland can be used to prolong lactation persistency in the dairy cow. Current approaches to increase milk yield include increased milking frequency, formulation of total mixed rations, and optimization of length of milking and dry periods (142,144,146). Recombinant bovine somatotropin (rBST) successfully increases milk yield by preserving the number of milk secreting cells and delaying the decline in milk yield (1). However, consumer concerns over milk from rBST-treated cows have created a demand for non-hormonal methods to enhance milk output. In order to target apoptosis in the mammary gland a better understanding of the molecular mechanisms regulating cellular survival and death are needed.

While a role for IGFBP-3 in apoptosis is well-established in breast cancer cells, our work is the first to show that IGFBP-3 also plays a role in apoptosis of non-transformed bovine MECs (58,80). We found in MAC-T cells that siRNA knock-down of IGFBP-3 attenuated ANS-induced intrinsic apoptosis (Chapter 2). In many cell systems IGFBP-3 directly induces apoptosis, however we found that over-expression of IGFBP-3 did not induce MAC-T cell death (Chapter 2). This indicates that the biological function of IGFBP-3 is modulated by extracellular environment in MAC-T cells, and that the apoptotic functions of IGFBP-3 are not simply due to elevated levels of intra- or extracellular IGFBP-3. An important goal of future studies will be to determine if nuclear IGFBP-3 increases in mammary tissue during late lactation in vivo. Due to the lack of sensitive antibodies that recognize the bovine protein, the studies that have examined expression of IGFBP-3 in tissue from lactating cows during late lactation have looked at mRNA levels only (198-200). Therefore, it remains possible that a decline in growth factor signaling paired with an increase in apoptotic signals alters the cellular localization of IGFBP-3 which has

more impact on protein function than changes in mRNA expression. Interestingly, IGFBP-3 produced in the mammary gland is synthesized primarily by the milk-secreting alveolar cells rather than the stromal cells, further supporting a role for endogenous IGFBP-3 in local control of MEC apoptosis (198). Alteration of biological function at the local level, as opposed to altered production of IGFBP-3, would also suggest intracrine or paracrine action of locally produced IGFBP-3. The Cohick anti-bovine-IGFBP-3 antibody will be tested for application in immunohistochemistry. If successful, we can then use immunohistochemistry to examine localization of IGFBP-3 in mammary gland tissue isolated from dairy cows at various stages of lactation.

Cellular fractionation data indicated that IGFBP-3 localizes to the nucleus in ANS-treated MAC-T cells (Chapter 2). Therefore, it is possible that direction of IGFBP-3 to the nucleus by ANS activates the apoptotic role of IGFBP-3. Knock-down experiments showed that IGFBP-3 modulated ANS-induced phosphorylation and nuclear export of Nur77 (Chapter 3). The nature of the interplay between IGFBP-3, Nur77, and JNK remains unclear. Immunoprecipitation experiments established that IGFBP-3 binds Nur77 in ANS-treated cells, however the functional significance of this interaction requires further investigation. We hypothesize that IGFBP-3 anchors Nur77 in the nucleus so that JNK can phosphorylate Nur77, then phospho-Nur77 translocates out of the nucleus to the cytoplasm. If this hypothesis is true then co-immunoprecipitation experiments will show that Nur77 and IGFBP-3 associate in the nucleus basally and that ANS-treatment induces phosphorylation of Nur77 by JNK, followed by dissociation of Nur77 and IGFBP-3 and nuclear export of Nur77. JNK knock-down should then prevent phosphorylation of Nur77 and preserve the association between Nur77 and IGFBP-3. Alternatively, IGFBP-3 has been shown in prostate cancer cells to associate with cytoplasmic

Nur77, indicating that it chaperones Nur77 out of the nucleus (94). If this is true in MAC-T cells then JNK knock-down should prevent nuclear export of both IGFBP-3 and Nur77 as a complex. Efforts to immunoprecipitate Nur77 from fractions have been unsuccessful to date, however further work to optimize fractionation conditions for IP will elucidate the sequence of nuclear import of IGFBP-3 and binding of IGFBP-3 to Nur77.

Mitochondrial Nur77 is reported to induce a conformational change in Bcl-2, converting it from a survival to an apoptotic protein (124,134). However, in our system, cytoplasmic Nur77 did not clearly localize to the mitochondria. To examine if Nur77 binds Bcl-2 in ANS-treated MAC-T cells we will immunoprecipitate Nur77 and immunoblot for Bcl-2. In this scenario, binding of IGFBP-3 to Nur77 could dissociate nuclear Nur77 from the DNA to promote phosphorylation of Nur77 by active JNK, followed by nuclear export of phospho-Nur77. The cytoplasmic Nur77 would then be available to interact with Bcl-2. This data would connect IGFBP-3 to indirect initiation of MOMP. Alternatively, if no association between Nur77 and Bcl-2 is detected the cytoplasmic IGFBP-3 could associate with Bcl-2 to directly influence MOMP.

The mechanism for nuclear import of IGFBP-3 remains controversial. The immunoprecipitation data showed transport into the nucleus was mediated by importin-β. However, we also needed to address if secreted IGFBP-3 was re-internalized and directed to the nucleus. Treatment with ANS induced accumulation of IGFBP-3 in both conditioned media and inside the cell. In MAC-T cells, nuclear IGFBP-3 was glycosylated, indicating that it had passed through the secretory machinery prior to nuclear import. Inhibition of clathrin-mediated endocytosis did not affect detection of IGFBP-3 in the nucleus, showing that secreted IGFBP-3 was not re-internalized

(Chapter 4). Further, inhibition of secretion with brefeldin-A enhanced nuclear localization of IGFBP-3. These data establish that secretion is not a required step for direction of IGFBP-3 to the nucleus (Chapter 4). The specific signal targeting IGFBP-3 to the media or the nucleus remains elusive. In prostate cancer cells, IGFBP-3 lacking the signal peptide for secretion localizes to the nucleus but does not get glycosylated, indicating it does not pass through the ER prior to nuclear import (83). This supports our conclusion that non-secreted IGFBP-3 enters the nucleus, however, in MAC-T cells, nuclear IGFBP-3 was glycosylated, suggesting that transit through the ER is a required step in our system. The secretion signal is not inactivated by getting cleaved from IGFBP-3. If this occurred then we would be unable to detect IGFBP-3-GFP in the nucleus, since the GFP-tag was added to the N-terminus of IGFBP-3, which is where the secretion signal is located. It is possible that endogenous IGFBP-3 produced in response to ANS gets sent to the ER where its secretion signal gets modified and turned off and the NLS gets activated, resulting in nuclear localization of IGFBP-3. However, this still does not address why some IGFBP-3 is sent to the nucleus while the rest gets secreted into the culture media.

Low basal levels of IGFBP-3 presents a challenge in elucidating the role of endogenous IGFBP-3 in the early stages of apoptosis and limits our ability to detect IGFBP-3 in lysates. In MAC-T cells, low levels of IGFBP-3 were constitutively produced and secreted (Chapter 2). Basal levels of IGFBP-3 were below the limit of detection and it takes ~ 3 h of treatment to induce IGFBP-3 to detectable intracellular levels. However, nuclear export of Nur77 was an early event, occurring by 1 h after treatment. Interestingly, induction of IGFBP-3 was not required for nuclear export of Nur77. Translocation of Nur77 occurs before induction of IGFBP-3 protein was detected, therefore the low levels of IGFBP-3 expressed basally are sufficient for nuclear export of Nur77. Over-expression of IGFBP-3-his greatly enhanced our ability to detect intracellular binding

partners for IGFBP-3. However, continued optimization of the Cohick-lab IGFBP-3 antibody for immunoprecipitation of endogenous IGFBP-3 should enhance our ability to detect intracellular IGFBP-3 at the same time points we detect Nur77 translocation.

The role of *nuclear* IGFBP-3 in apoptosis remains unanswered. An interaction between IGFBP-3 and Nur77 in whole cell lysates paired with the effect of IGFBP-3 knock-down on phosphorylation and nuclear export of Nur77 suggests that nuclear IGFBP-3 modulates activation of the apoptotic functions of Nur77. However, to directly address this question we need to knock-down endogenous IGFBP-3, express IGFBP-3 with a mutated NLS (IGFBP-3-mNLS), then measure ANS-induced Nur77 translocation. Perhaps more importantly, we could knock-down endogenous IGFBP-3 then test if the IGFBP-3-mNLS restores sensitivity of MAC-T cells to ANS-induced apoptosis. Expression of IGFBP-3 with a mutated NLS induces apoptosis in breast and prostate cancer cells, implying that nuclear IGFBP-3 is not essential for apoptosis (80,83). However, the fact that nuclear import of IGFBP-3 was regulated by ANS-treatment in MAC-T cells suggests a nuclear function for IGFBP-3 in apoptosis. In addition, we showed that the low basal levels of IGFBP-3 are sufficient for Nur77 translocation, however ANS induces dramatic increases in nuclear IGFBP-3. IGFBP-3 has a relatively long half-life (14-18 h), and mRNA expression is not up-regulated until 3 h of ANS-treatment in MAC-T cells (201). This raises the possibility that basal IGFBP-3 rapidly translocates to the nucleus to facilitate Nur77 translocation, then the newly synthesized protein has another unidentified function in later stages of apoptosis.

Another observation worthy of further investigation is the inverse relationship between expression of IGFBP-3 and IGFBP-2 in ANS-treated cells. Interestingly, IGF-I induced expression of both proteins, however, in ANS-treated cells IGFBP-3 expression increased while IGFBP-2 expression was inhibited (Chapter 2). The alteration of the ratio between the two IGFBPs could contribute to regulation of their biological function. IGFBP-2 has an anti-apoptotic effect in lung adenocarcinoma cells, and knock-down of IGFBP-2 enhances apoptosis induced by camptothecin (168). Thus, both IGFBP-2 and IGFBP-3 have roles in modulation of apoptosis. However, the interaction between IGFBP-3 and IGFBP-2 in apoptosis is not addressed in the current literature. A number of studies address the IGF-independent effects of individual binding proteins, however the interplay between the binding proteins presents an unexplored avenue for further investigation.

Finally, the mechanism used by IGF-I to attenuate ANS-induced apoptosis may help elucidate how MECs respond to concurrent survival and death signals, and how the balance between these signals determines cellular fate. Interestingly, IGF-I completely abrogated the ability of ANS to induce caspase activation without affecting nuclear accumulation of IGFBP-3 (Chapter 2). Unpublished data from our lab show that IGF-I attenuated ANS-induced cytochrome c release. The ability of IGF-I to attenuate apoptosis without affecting nuclear localization of IGFBP-3, paired with inhibition of mitochondrial release of cytochrome c, suggests that IGF-I acts downstream of nuclear IGFBP-3. To test if IGF-I attenuates the apoptotic actions of IGFBP-3 we can use fractionation experiments to determine if IGF-I attenuates ANS-induced Nur77 nuclear export.

Dairy cows are unlikely to encounter ANS under typical *in vivo* conditions. However, up-regulation of IGFBP-3 expression and induction of the intrinsic apoptotic response by ANS enhances our *in vitro* system for studying the role of endogenous IGFBP-3 in intrinsic apoptosis in MECs. Growth factor withdrawal is one contributor to intrinsic apoptosis, and changes in the IGF-IR are detected over the lactation period (38,202). ANS and growth factor withdrawal activate the same apoptotic pathway, however, ANS induces a greater response more rapidly than growth factor withdrawal. This magnified response enables increased detection of changes in apoptotic proteins in cultured cells. In addition, MAC-T cells do not produce IGF-I and all experiments were done in serum-free medium lacking IGF-I. Under *in vivo* conditions it is unlikely that there is ever a complete absence of IGF-I signaling. It is more probable that apoptosis is induced when the balance between survival signals, including IGF-I, and apoptotic signals changes to favor cell death.

An understanding of how MECs receive and respond to conflicting cellular signals, i.e. survival and apoptotic, will enhance technology and management practices that promote survival of MECs to increase persistency or increase peak yield. The current data present novel findings addressing the role of *endogenous* IGFBP-3 in apoptosis of *normal* MECs.

Literature cited

1. Capuco AV, Wood DL, Baldwin R, McLeod K, Paape MJ. Mammary cell number, proliferation, and apoptosis during a bovine lactation: relation to milk production and effect of bST. *Journal of dairy science.* 2001;84(10):2177-2187.

2. DeChiara TM, Efstratiadis A, Robertson EJ. A growth-deficiency phenotype in heterozygous mice carrying an insulin-like growth factor II gene disrupted by targeting. *Nature.* 1990;345(6270):78-80.

3. Baker J, Liu JP, Robertson EJ, Efstratiadis A. Role of insulin-like growth factors in embryonic and postnatal growth. *Cell.* 1993;75(1):73-82.

4. LeRoith D, Werner H, Beitner-Johnson D, Roberts CT, Jr. Molecular and cellular aspects of the insulin-like growth factor I receptor. *Endocrine reviews.* 1995;16(2):143-163.

5. Martin JL, Lin MZ, McGowan EM, Baxter RC. Potentiation of growth factor signaling by insulin-like growth factor-binding protein-3 in breast epithelial cells requires sphingosine kinase activity. *The Journal of biological chemistry.* 2009;284(38):25542-25552.

6. Granata R, Trovato L, Garbarino G, Taliano M, Ponti R, Sala G, Ghidoni R, Ghigo E. Dual effects of IGFBP-3 on endothelial cell apoptosis and survival: involvement of the sphingolipid signaling pathways. *FASEB journal : official publication of the Federation of American Societies for Experimental Biology.* 2004;18(12):1456-1458.

7. Xi G, Hathaway MR, White ME, Dayton WR. Localization of insulin-like growth factor (IGFBP)-3 in cultured porcine embryonic myogenic cells before and after TGF-beta1 treatment. *Domestic animal endocrinology.* 2007;33(4):422-429.

8. Payet LD, Wang XH, Baxter RC, Firth SM. Amino- and carboxyl-terminal fragments of insulin-like growth factor (IGF) binding protein-3 cooperate to bind IGFs with high affinity and inhibit IGF receptor interactions. *Endocrinology.* 2003;144(7):2797-2806.

9. Firth SM, Baxter RC. Cellular actions of the insulin-like growth factor binding proteins. *Endocrine reviews.* 2002;23(6):824-854.

10. Czabotar PE, Lessene G, Strasser A, Adams JM. Control of apoptosis by the BCL-2 protein family: implications for physiology and therapy. *Nature reviews Molecular cell biology.* 2013;15(1):49-63.

11. Jin Z, El-Deiry WS. Overview of cell death signaling pathways. *Cancer biology & therapy.* 2005;4(2):139-163.

12. Weinlich R, Dillon CP, Green DR. Ripped to death. *Trends in cell biology.* 2011;21(11):630-637.

13. Parsons MJ, Green DR. Mitochondria in cell death. *Essays in biochemistry.* 2010;47:99-114.

14. Elmore S. Apoptosis: a review of programmed cell death. *Toxicologic pathology.* 2007;35(4):495-516.

15. Tait SW, Green DR. Mitochondria and cell death: outer membrane permeabilization and beyond. *Nature reviews Molecular cell biology.* 2010;11(9):621-632.

16. Youle RJ, Strasser A. The BCL-2 protein family: opposing activities that mediate cell death. *Nature reviews Molecular cell biology.* 2008;9(1):47-59.

17. Hilmi C, Larribere L, Giuliano S, Bille K, Ortonne JP, Ballotti R, Bertolotto C. IGF1 promotes resistance to apoptosis in melanoma cells through an increased expression of BCL2, BCL-X(L), and survivin. *The Journal of investigative dermatology.* 2008;128(6):1499-1505.

18. Chand HS, Harris JF, Mebratu Y, Chen Y, Wright PS, Randell SH, Tesfaigzi Y. Intracellular insulin-like growth factor-1 induces Bcl-2 expression in airway epithelial cells. *Journal of immunology.* 2012;188(9):4581-4589.

19. Kurmasheva RT, Houghton PJ. IGF-I mediated survival pathways in normal and malignant cells. *Biochimica et biophysica acta.* 2006;1766(1):1-22.

20. van Golen CM, Castle VP, Feldman EL. IGF-I receptor activation and BCL-2 overexpression prevent early apoptotic events in human neuroblastoma. *Cell death and differentiation.* 2000;7(7):654-665.

21. Singh SK, Moretta D, Almaguel F, De Leon M, De Leon DD. Precursor IGF-II (proIGF-II) and mature IGF-II (mIGF-II) induce Bcl-2 And Bcl-X L expression through different signaling pathways in breast cancer cells. *Growth factors.* 2008;26(2):92-103.

22. Muscarella DE, Bloom SE. The contribution of c-Jun N-terminal kinase activation and subsequent Bcl-2 phosphorylation to apoptosis induction in human B-cells is dependent on the mode of action of specific stresses. *Toxicology and applied pharmacology.* 2008;228(1):93-104.

23. Deng X, Xiao L, Lang W, Gao F, Ruvolo P, May WS, Jr. Novel role for JNK as a stress-activated Bcl2 kinase. *The Journal of biological chemistry.* 2001;276(26):23681-23688.

24. Torocsik B, Szeberenyi J. Anisomycin affects both pro- and antiapoptotic mechanisms in PC12 cells. *Biochemical and biophysical research communications.* 2000;278(3):550-556.

25. Xia S, Li Y, Rosen EM, Laterra J. Ribotoxic stress sensitizes glioblastoma cells to death receptor induced apoptosis: requirements for c-Jun NH2-terminal kinase and Bim. *Molecular cancer research : MCR.* 2007;5(8):783-792.

26. Pucci B, Indelicato M, Paradisi V, Reali V, Pellegrini L, Aventaggiato M, Karpinich NO, Fini M, Russo MA, Farber JL, Tafani M. ERK-1 MAP kinase prevents TNF-induced apoptosis through bad phosphorylation and inhibition of Bax translocation in HeLa Cells. *Journal of cellular biochemistry.* 2009;108(5):1166-1174.

27. Putcha GV, Le S, Frank S, Besirli CG, Clark K, Chu B, Alix S, Youle RJ, LaMarche A, Maroney AC, Johnson EM, Jr. JNK-mediated BIM phosphorylation potentiates BAX-dependent apoptosis. *Neuron.* 2003;38(6):899-914.

28. Ghibelli L, Diederich M. Multistep and multitask Bax activation. *Mitochondrion.* 2010;10(6):604-613.

29. Du C, Fang M, Li Y, Li L, Wang X. Smac, a mitochondrial protein that promotes cytochrome c-dependent caspase activation by eliminating IAP inhibition. *Cell.* 2000;102(1):33-42.

30. Zimmermann KC, Green DR. How cells die: apoptosis pathways. *The Journal of allergy and clinical immunology.* 2001;108(4 Suppl):S99-103.

31. Zimmermann KC, Bonzon C, Green DR. The machinery of programmed cell death. *Pharmacology & therapeutics.* 2001;92(1):57-70.

32. Riedl SJ, Salvesen GS. The apoptosome: signalling platform of cell death. *Nature reviews Molecular cell biology.* 2007;8(5):405-413.

33. Earnshaw WC, Martins LM, Kaufmann SH. Mammalian caspases: structure, activation, substrates, and functions during apoptosis. *Annual review of biochemistry.* 1999;68:383-424.

34. Guicciardi ME, Gores GJ. Life and death by death receptors. *FASEB journal : official publication of the Federation of American Societies for Experimental Biology.* 2009;23(6):1625-1637.

35. Thorburn A. Death receptor-induced cell killing. *Cellular signalling.* 2004;16(2):139-144.

36. Deng Y, Lin Y, Wu X. TRAIL-induced apoptosis requires Bax-dependent mitochondrial release of Smac/DIABLO. *Genes & development.* 2002;16(1):33-45.

37. Marti A, Feng Z, Altermatt HJ, Jaggi R. Milk accumulation triggers apoptosis of mammary epithelial cells. *European journal of cell biology.* 1997;73(2):158-165.

38. Zarzynska J, Motyl T. Apoptosis and autophagy in involuting bovine mammary gland. *Journal of physiology and pharmacology : an official journal of the Polish Physiological Society.* 2008;59 Suppl 9:275-288.

39. Watson CJ, Kreuzaler PA. Remodeling mechanisms of the mammary gland during involution. *The International journal of developmental biology.* 2011;55(7-9):757-762.

40. Zarzynska J, Gajkowska B, Wojewodzka U, Dymnicki E, Motyl T. Apoptosis and autophagy in involuting bovine mammary gland is accompanied by up-regulation of TGF-beta1 and suppression of somatotropic pathway. *Polish journal of veterinary sciences.* 2007;10(1):1-9.

41. Monks J, Henson PM. Differentiation of the mammary epithelial cell during involution: implications for breast cancer. *Journal of mammary gland biology and neoplasia.* 2009;14(2):159-170.

42. Li M, Liu X, Robinson G, Bar-Peled U, Wagner KU, Young WS, Hennighausen L, Furth PA. Mammary-derived signals activate programmed cell death during the first stage of mammary gland involution. *Proceedings of the National Academy of Sciences of the United States of America.* 1997;94(7):3425-3430.

43. Walton KD, Wagner KU, Rucker EB, 3rd, Shillingford JM, Miyoshi K, Hennighausen L. Conditional deletion of the bcl-x gene from mouse mammary epithelium results in accelerated apoptosis during involution but does not compromise cell function during lactation. *Mechanisms of development.* 2001;109(2):281-293.

44. Wareski P, Motyl T, Ryniewicz Z, Orzechowski A, Gajkowska B, Wojewodzka U, Ploszaj T. Expression of apoptosis-related proteins in mammary gland of goat. *Small ruminant research : the journal of the International Goat Association.* 2001;40(3):279-289.

45. Motyl T, Gajkowska B, Wojewodzka U, Wareski P, Rekiel A, Ploszaj T. Expression of apoptosis-related proteins in involuting mammary gland of sow. *Comparative biochemistry and physiology Part B, Biochemistry & molecular biology.* 2001;128(4):635-646.

46. Grill CJ, Cohick WS. Insulin-like growth factor binding protein-3 mediates IGF-I action in a bovine mammary epithelial cell line independent of an IGF interaction. *Journal of cellular physiology.* 2000;183(2):273-283.

47. Grill CJ, Sivaprasad U, Cohick WS. Constitutive expression of IGF-binding protein-3 by mammary epithelial cells alters signaling through Akt and p70S6 kinase. *Journal of molecular endocrinology.* 2002;29(1):153-162.

48. Mishra S, Murphy LJ. Phosphorylation of insulin-like growth factor (IGF) binding protein-3 by breast cancer cell membranes enhances IGF-I binding. *Endocrinology.* 2003;144(9):4042-4050.

49. Granata R, Trovato L, Lupia E, Sala G, Settanni F, Camussi G, Ghidoni R, Ghigo E. Insulin-like growth factor binding protein-3 induces angiogenesis through IGF-I- and SphK1-dependent mechanisms. *Journal of thrombosis and haemostasis : JTH.* 2007;5(4):835-845.

50. Burrows C, Holly JM, Laurence NJ, Vernon EG, Carter JV, Clark MA, McIntosh J, McCaig C, Winters ZE, Perks CM. Insulin-like growth factor binding protein 3 has opposing actions on malignant and nonmalignant breast epithelial cells that are each reversible and dependent upon cholesterol-stabilized integrin receptor complexes. *Endocrinology.* 2006;147(7):3484-3500.

51. Martin JL, Weenink SM, Baxter RC. Insulin-like growth factor-binding protein-3 potentiates epidermal growth factor action in MCF-10A mammary epithelial cells. Involvement of p44/42 and p38 mitogen-activated protein kinases. *The Journal of biological chemistry.* 2003;278(5):2969-2976.

52. Franklin SL, Ferry RJ, Jr., Cohen P. Rapid insulin-like growth factor (IGF)-independent effects of IGF binding protein-3 on endothelial cell survival. *The Journal of clinical endocrinology and metabolism.* 2003;88(2):900-907.

53. Brosseau C, Pirianov G, Colston KW. Role of insulin-like growth factor binding protein-3 in 1, 25-dihydroxyvitamin-d 3 -induced breast cancer cell apoptosis. *International journal of cell biology.* 2013;2013:960378.

54. Levitt RJ, Buckley J, Blouin MJ, Schaub B, Triche TJ, Pollak M. Growth inhibition of breast epithelial cells by celecoxib is associated with upregulation of insulin-like growth factor binding protein-3 expression. *Biochemical and biophysical research communications.* 2004;316(2):421-428.

55. Sakamoto K, Yano T, Kobayashi T, Hagino A, Aso H, Obara Y. Growth hormone suppresses the expression of IGFBP-5, and promotes the IGF-I-induced phosphorylation of Akt in bovine mammary epithelial cells. *Domestic animal endocrinology.* 2007;32(4):260-272.

56. Silha JV, Sheppard PC, Mishra S, Gui Y, Schwartz J, Dodd JG, Murphy LJ. Insulin-like growth factor (IGF) binding protein-3 attenuates prostate tumor growth by IGF-dependent and IGF-independent mechanisms. *Endocrinology.* 2006;147(5):2112-2121.

57. Lee HY, Chun KH, Liu B, Wiehle SA, Cristiano RJ, Hong WK, Cohen P, Kurie JM. Insulin-like growth factor binding protein-3 inhibits the growth of non-small cell lung cancer. *Cancer research.* 2002;62(12):3530-3537.

58. Schedlich LJ, Graham LD. Role of insulin-like growth factor binding protein-3 in breast cancer cell growth. *Microscopy research and technique.* 2002;59(1):12-22.

59. Butt AJ, Dickson KA, Jambazov S, Baxter RC. Enhancement of tumor necrosis factor-alpha-induced growth inhibition by insulin-like growth factor-binding protein-5 (IGFBP-5), but not IGFBP-3 in human breast cancer cells. *Endocrinology.* 2005;146(7):3113-3122.

60. Santer FR, Bacher N, Moser B, Morandell D, Ressler S, Firth SM, Spoden GA, Sergi C, Baxter RC, Jansen-Durr P, Zwerschke W. Nuclear insulin-like growth factor binding protein-3 induces apoptosis and is targeted to ubiquitin/proteasome-dependent proteolysis. *Cancer research.* 2006;66(6):3024-3033.

61. Kim HS, Ingermann AR, Tsubaki J, Twigg SM, Walker GE, Oh Y. Insulin-like growth factor-binding protein 3 induces caspase-dependent apoptosis through a death receptor-

mediated pathway in MCF-7 human breast cancer cells. *Cancer research.* 2004;64(6):2229-2237.

62. Bernard L, Babajko S, Binoux M, Ricort JM. The amino-terminal region of insulin-like growth factor binding protein-3, (1-95)IGFBP-3, induces apoptosis of MCF-7 breast carcinoma cells. *Biochemical and biophysical research communications.* 2002;293(1):55-60.

63. Hong J, Zhang G, Dong F, Rechler MM. Insulin-like growth factor (IGF)-binding protein-3 mutants that do not bind IGF-I or IGF-II stimulate apoptosis in human prostate cancer cells. *The Journal of biological chemistry.* 2002;277(12):10489-10497.

64. Rajah R, Valentinis B, Cohen P. Insulin-like growth factor (IGF)-binding protein-3 induces apoptosis and mediates the effects of transforming growth factor-beta1 on programmed cell death through a p53- and IGF-independent mechanism. *The Journal of biological chemistry.* 1997;272(18):12181-12188.

65. Leibowitz BJ, Agostini-Dreyer A, Jetzt AE, Krumm CS, Cohick WS. IGF binding protein-3 mediates stress-induced apoptosis in non-transformed mammary epithelial cells. *Journal of cellular physiology.* 2013;228(4):734-742.

66. Leibowitz BJ, Cohick WS. Endogenous IGFBP-3 is required for both growth factor-stimulated cell proliferation and cytokine-induced apoptosis in mammary epithelial cells. *Journal of cellular physiology.* 2009;220(1):182-188.

67. Rajah R, Lee KW, Cohen P. Insulin-like growth factor binding protein-3 mediates tumor necrosis factor-alpha-induced apoptosis: role of Bcl-2 phosphorylation. *Cell growth & differentiation : the molecular biology journal of the American Association for Cancer Research.* 2002;13(4):163-171.

68. Perks CM, McCaig C, Clarke JB, Clemmons DR, Holly JM. A non-IGF binding mutant of IGFBP-3 modulates cell function in breast epithelial cells. *Biochemical and biophysical research communications.* 2002;294(5):988-994.

69. Li C, Harada A, Oh Y. IGFBP-3 sensitizes antiestrogen-resistant breast cancer cells through interaction with GRP78. *Cancer letters.* 2012;325(2):200-206.

70. Dokmanovic M, Shen Y, Bonacci TM, Hirsch DS, Wu WJ. Trastuzumab regulates IGFBP-2 and IGFBP-3 to mediate growth inhibition: implications for the development of predictive biomarkers for trastuzumab resistance. *Molecular cancer therapeutics.* 2011;10(6):917-928.

71. Schedlich LJ, Yenson VM, Baxter RC. TGF-beta-induced expression of IGFBP-3 regulates IGF1R signaling in human osteosarcoma cells. *Molecular and cellular endocrinology.* 2013;377(1-2):56-64.

72. Han J, Jogie-Brahim S, Harada A, Oh Y. Insulin-like growth factor-binding protein-3 suppresses tumor growth via activation of caspase-dependent apoptosis and cross-talk with NF-kappaB signaling. *Cancer letters.* 2011;307(2):200-210.

73. Cheung SCK, Long XH, Liu LZ, Liu QQ, Lan LL, Tong PCY, Sun SSM. Inhibition of Human MCF-7 Breast Cancer Cells and HT-29 Colon Cancer Cells by Rice-Produced Recombinant Human Insulin-Like Growth Binding Protein-3 (rhIGFBP-3). *PloS one.* 2013;8(10).

74. Perks CM, Holly JM. IGF binding proteins (IGFBPs) and regulation of breast cancer biology. *Journal of mammary gland biology and neoplasia.* 2008;13(4):455-469.

75. Zhao L, He LR, Zhang R, Cai MY, Liao YJ, Qian D, Xi M, Zeng YX, Xie D, Liu MZ. Low expression of IGFBP-3 predicts poor prognosis in patients with esophageal squamous cell carcinoma. *Medical oncology.* 2012;29(4):2669-2676.

76. Zhao L, Li QQ, Zhang R, Xi M, Liao YJ, Qian D, He LR, Zeng YX, Xie D, Liu MZ. The overexpression of IGFBP-3 is involved in the chemosensitivity of esophageal squamous cell carcinoma cells to nimotuzumab combined with cisplatin. *Tumour biology : the journal of the International Society for Oncodevelopmental Biology and Medicine.* 2012;33(4):1115-1123.

77. Hampel B, Wagner M, Teis D, Zwerschke W, Huber LA, Jansen-Durr P. Apoptosis resistance of senescent human fibroblasts is correlated with the absence of nuclear IGFBP-3. *Aging cell.* 2005;4(6):325-330.

78. Kim SR, Lee KS, Lee KB, Lee YC. Recombinant IGFBP-3 inhibits allergic lung inflammation, VEGF production, and vascular leak in a mouse model of asthma. *Allergy.* 2012;67(7):869-877.

79. Lee YC, Jogie-Brahim S, Lee DY, Han J, Harada A, Murphy LJ, Oh Y. Insulin-like growth factor-binding protein-3 (IGFBP-3) blocks the effects of asthma by negatively regulating NF-kappaB signaling through IGFBP-3R-mediated activation of caspases. *The Journal of biological chemistry.* 2011;286(20):17898-17909.

80. Butt AJ, Fraley KA, Firth SM, Baxter RC. IGF-binding protein-3-induced growth inhibition and apoptosis do not require cell surface binding and nuclear translocation in human breast cancer cells. *Endocrinology.* 2002;143(7):2693-2699.

81. Lee KW, Liu B, Ma L, Li H, Bang P, Koeffler HP, Cohen P. Cellular internalization of insulin-like growth factor binding protein-3: distinct endocytic pathways facilitate re-uptake and nuclear localization. *The Journal of biological chemistry.* 2004;279(1):469-476.

82. Ingermann AR, Yang YF, Han J, Mikami A, Garza AE, Mohanraj L, Fan L, Idowu M, Ware JL, Kim HS, Lee DY, Oh Y. Identification of a novel cell death receptor mediating IGFBP-3-induced anti-tumor effects in breast and prostate cancer. *The Journal of biological chemistry.* 2010;285(39):30233-30246.

83. Bhattacharyya N, Pechhold K, Shahjee H, Zappala G, Elbi C, Raaka B, Wiench M, Hong J, Rechler MM. Nonsecreted insulin-like growth factor binding protein-3 (IGFBP-3) can induce apoptosis in human prostate cancer cells by IGF-independent mechanisms without being concentrated in the nucleus. *The Journal of biological chemistry.* 2006;281(34):24588-24601.

84. Butt AJ, Firth SM, King MA, Baxter RC. Insulin-like growth factor-binding protein-3 modulates expression of Bax and Bcl-2 and potentiates p53-independent radiation-induced apoptosis in human breast cancer cells. *The Journal of biological chemistry.* 2000;275(50):39174-39181.

85. Jia Y, Lee KW, Swerdloff R, Hwang D, Cobb LJ, Sinha Hikim A, Lue YH, Cohen P, Wang C. Interaction of insulin-like growth factor-binding protein-3 and BAX in mitochondria promotes male germ cell apoptosis. *The Journal of biological chemistry.* 2010;285(3):1726-1732.

86. Schedlich LJ, Young TF, Firth SM, Baxter RC. Insulin-like growth factor-binding protein (IGFBP)-3 and IGFBP-5 share a common nuclear transport pathway in T47D human breast carcinoma cells. *The Journal of biological chemistry.* 1998;273(29):18347-18352.

87. Li W, Fawcett J, Widmer HR, Fielder PJ, Rabkin R, Keller GA. Nuclear transport of insulin-like growth factor-I and insulin-like growth factor binding protein-3 in opossum kidney cells. *Endocrinology.* 1997;138(4):1763-1766.

88. Micutkova L, Hermann M, Offterdinger M, Hess MW, Matscheski A, Pircher H, Muck C, Ebner HL, Laich A, Ferrando-May E, Zwerschke W, Huber LA, Jansen-Durr P. Analysis of the cellular uptake and nuclear delivery of insulin-like growth factor binding protein-3 in human osteosarcoma cells. *International journal of cancer Journal international du cancer.* 2012;130(7):1544-1557.

89. Oufattole M, Lin SW, Liu B, Mascarenhas D, Cohen P, Rodgers BD. Ribonucleic acid polymerase II binding subunit 3 (Rpb3), a potential nuclear target of insulin-like growth factor binding protein-3. *Endocrinology.* 2006;147(5):2138-2146.

90. Zappala G, Elbi C, Edwards J, Gorenstein J, Rechler MM, Bhattacharyya N. Induction of apoptosis in human prostate cancer cells by insulin-like growth factor binding protein-3 does not require binding to retinoid X receptor-alpha. *Endocrinology.* 2008;149(4):1802-1812.

91. Lee KW, Ma L, Yan X, Liu B, Zhang XK, Cohen P. Rapid apoptosis induction by IGFBP-3 involves an insulin-like growth factor-independent nucleomitochondrial translocation of RXRalpha/Nur77. *The Journal of biological chemistry.* 2005;280(17):16942-16948.

92. Cao X, Liu W, Lin F, Li H, Kolluri SK, Lin B, Han YH, Dawson MI, Zhang XK. Retinoid X receptor regulates Nur77/TR3-dependent apoptosis [corrected] by modulating its nuclear export and mitochondrial targeting. *Molecular and cellular biology.* 2004;24(22):9705-9725.

93. Paharkova-Vatchkova V, Lee KW. Nuclear export and mitochondrial and endoplasmic reticulum localization of IGF-binding protein 3 regulate its apoptotic properties. *Endocrine-related cancer.* 2010;17(2):293-302.

94. Lee KW, Cobb LJ, Paharkova-Vatchkova V, Liu B, Milbrandt J, Cohen P. Contribution of the orphan nuclear receptor Nur77 to the apoptotic action of IGFBP-3. *Carcinogenesis.* 2007;28(8):1653-1658.

95. Lee SO, Abdelrahim M, Yoon K, Chintharlapalli S, Papineni S, Kim K, Wang H, Safe S. Inactivation of the orphan nuclear receptor TR3/Nur77 inhibits pancreatic cancer cell and tumor growth. *Cancer research.* 2010;70(17):6824-6836.

96. No H, Bang Y, Lim J, Kim SS, Choi HS, Choi HJ. Involvement of induction and mitochondrial targeting of orphan nuclear receptor Nur77 in 6-OHDA-induced SH-SY5Y cell death. *Neurochemistry international.* 2010;56(4):620-626.

97. Singh B, Charkowicz D, Mascarenhas D. Insulin-like growth factor-independent effects mediated by a C-terminal metal-binding domain of insulin-like growth factor binding protein-3. *The Journal of biological chemistry.* 2004;279(1):477-487.

98. Huq A, Singh B, Meeker T, Mascarenhas D. The metal-binding domain of IGFBP-3 selectively delivers therapeutic molecules into cancer cells. *Anti-cancer drugs.* 2009;20(1):21-31.

99. Schedlich LJ, Le Page SL, Firth SM, Briggs LJ, Jans DA, Baxter RC. Nuclear import of insulin-like growth factor-binding protein-3 and -5 is mediated by the importin beta subunit. *The Journal of biological chemistry.* 2000;275(31):23462-23470.

100. Iosef C, Gkourasas T, Jia CY, Li SS, Han VK. A functional nuclear localization signal in insulin-like growth factor binding protein-6 mediates its nuclear import. *Endocrinology.* 2008;149(3):1214-1226.

101. Firth SM, Baxter RC. Characterisation of recombinant glycosylation variants of insulin-like growth factor binding protein-3. *The Journal of endocrinology.* 1999;160(3):379-387.

102. Yan X, Payet LD, Baxter RC, Firth SM. Activity of human pregnancy insulin-like growth factor binding protein-3: determination by reconstituting recombinant complexes. *Endocrinology.* 2009;150(11):4968-4976.

103. Sommer A, Spratt SK, Tatsuno GP, Tressel T, Lee R, Maack CA. Properties of glycosylated and non-glycosylated human recombinant IGF binding protein-3 (IGFBP-3). *Growth regulation.* 1993;3(1):46-49.

104. Conover CA. Glycosylation of insulin-like growth factor binding protein-3 (IGFBP-3) is not required for potentiation of IGF-I action: evidence for processing of cell-bound IGFBP-3. *Endocrinology.* 1991;129(6):3259-3268.

105. Miyamoto S, Yano K, Sugimoto S, Ishii G, Hasebe T, Endoh Y, Kodama K, Goya M, Chiba T, Ochiai A. Matrix metalloproteinase-7 facilitates insulin-like growth factor bioavailability through its proteinase activity on insulin-like growth factor binding protein 3. *Cancer research.* 2004;64(2):665-671.

106. Maile LA, Gill ZP, Perks CM, Holly JM. The role of cell surface attachment and proteolysis in the insulin-like growth factor (IGF)-independent effects of IGF-binding protein-3 on apoptosis in breast epithelial cells. *Endocrinology.* 1999;140(9):4040-4045.

107. Baxter RC. Insulin-like growth factor binding protein-3 (IGFBP-3): Novel ligands mediate unexpected functions. *Journal of cell communication and signaling.* 2013;7(3):179-189.

108. Grkovic S, O'Reilly VC, Han S, Hong M, Baxter RC, Firth SM. IGFBP-3 binds GRP78, stimulates autophagy and promotes the survival of breast cancer cells exposed to adverse microenvironments. *Oncogene.* 2013;32(19):2412-2420.

109. Pattison ST, Fanayan S, Martin JL. Insulin-like growth factor binding protein-3 is secreted as a phosphoprotein by human breast cancer cells. *Molecular and cellular endocrinology.* 1999;156(1-2):131-139.

110. Battistutta R. Protein kinase CK2 in health and disease: Structural bases of protein kinase CK2 inhibition. *Cellular and molecular life sciences : CMLS.* 2009;66(11-12):1868-1889.

111. Cobb LJ, Mehta H, Cohen P. Enhancing the apoptotic potential of insulin-like growth factor-binding protein-3 in prostate cancer by modulation of CK2 phosphorylation. *Molecular endocrinology.* 2009;23(10):1624-1633.

112. Coverley JA, Martin JL, Baxter RC. The effect of phosphorylation by casein kinase 2 on the activity of insulin-like growth factor-binding protein-3. *Endocrinology.* 2000;141(2):564-570.

113. Cobb LJ, Liu B, Lee KW, Cohen P. Phosphorylation by DNA-dependent protein kinase is critical for apoptosis induction by insulin-like growth factor binding protein-3. *Cancer research.* 2006;66(22):10878-10884.

114. Schedlich LJ, Nilsen T, John AP, Jans DA, Baxter RC. Phosphorylation of insulin-like growth factor binding protein-3 by deoxyribonucleic acid-dependent protein kinase reduces ligand binding and enhances nuclear accumulation. *Endocrinology.* 2003;144(5):1984-1993.

115. Neal JA, Meek K. Choosing the right path: does DNA-PK help make the decision? *Mutation research.* 2011;711(1-2):73-86.

116. Hill R, Lee PW. The DNA-dependent protein kinase (DNA-PK): More than just a case of making ends meet? *Cell cycle.* 2010;9(17):3460-3469.

117. Shahjee H, Bhattacharyya N, Zappala G, Wiench M, Prakash S, Rechler MM. An N-terminal fragment of insulin-like growth factor binding protein-3 (IGFBP-3) induces apoptosis in human prostate cancer cells in an IGF-independent manner. *Growth hormone & IGF research : official journal of the Growth Hormone Research Society and the International IGF Research Society.* 2008;18(3):188-197.

118. Mohanraj L, Kim HS, Li W, Cai Q, Kim KE, Shin HJ, Lee YJ, Lee WJ, Kim JH, Oh Y. IGFBP-3 inhibits cytokine-induced insulin resistance and early manifestations of atherosclerosis. *PloS one.* 2013;8(1):e55084.

119. Moll UM, Marchenko N, Zhang XK. p53 and Nur77/TR3 - transcription factors that directly target mitochondria for cell death induction. *Oncogene.* 2006;25(34):4725-4743.

120. Mohan HM, Aherne CM, Rogers AC, Baird AW, Winter DC, Murphy EP. Molecular pathways: the role of NR4A orphan nuclear receptors in cancer. *Clinical cancer research : an official journal of the American Association for Cancer Research.* 2012;18(12):3223-3228.

121. Kolluri SK, Bruey-Sedano N, Cao X, Lin B, Lin F, Han YH, Dawson MI, Zhang XK. Mitogenic effect of orphan receptor TR3 and its regulation by MEKK1 in lung cancer cells. *Molecular and cellular biology.* 2003;23(23):8651-8667.

122. Zhang XK. Targeting Nur77 translocation. *Expert opinion on therapeutic targets.* 2007;11(1):69-79.

123. Sohn SJ, Thompson J, Winoto A. Apoptosis during negative selection of autoreactive thymocytes. *Current opinion in immunology.* 2007;19(5):510-515.

124. Thompson J, Winoto A. During negative selection, Nur77 family proteins translocate to mitochondria where they associate with Bcl-2 and expose its proapoptotic BH3 domain. *The Journal of experimental medicine.* 2008;205(5):1029-1036.

125. Liu J, Zhou W, Li SS, Sun Z, Lin B, Lang YY, He JY, Cao X, Yan T, Wang L, Lu J, Han YH, Cao Y, Zhang XK, Zeng JZ. Modulation of orphan nuclear receptor Nur77-mediated apoptotic pathway by acetylshikonin and analogues. *Cancer research.* 2008;68(21):8871-8880.

126. Wilson AJ, Arango D, Mariadason JM, Heerdt BG, Augenlicht LH. TR3/Nur77 in colon cancer cell apoptosis. *Cancer research.* 2003;63(17):5401-5407.

127. Wang A, Rud J, Olson CM, Jr., Anguita J, Osborne BA. Phosphorylation of Nur77 by the MEK-ERK-RSK cascade induces mitochondrial translocation and apoptosis in T cells. *Journal of immunology.* 2009;183(5):3268-3277.

128. Katagiri Y, Hirata Y, Milbrandt J, Guroff G. Differential regulation of the transcriptional activity of the orphan nuclear receptor NGFI-B by membrane depolarization and nerve growth factor. *The Journal of biological chemistry.* 1997;272(50):31278-31284.

129. Kim HJ, Kim JY, Lee SJ, Kim HJ, Oh CJ, Choi YK, Lee HJ, Do JY, Kim SY, Kwon TK, Choi HS, Lee MO, Park IS, Park KG, Lee KU, Lee IK. alpha-Lipoic acid prevents neointimal hyperplasia via induction of p38 mitogen-activated protein kinase/Nur77-mediated apoptosis of vascular smooth muscle cells and accelerates postinjury reendothelialization. *Arteriosclerosis, thrombosis, and vascular biology.* 2010;30(11):2164-2172.

130. Han YH, Cao X, Lin B, Lin F, Kolluri SK, Stebbins J, Reed JC, Dawson MI, Zhang XK. Regulation of Nur77 nuclear export by c-Jun N-terminal kinase and Akt. *Oncogene.* 2006;25(21):2974-2986.

131. Masuyama N, Oishi K, Mori Y, Ueno T, Takahama Y, Gotoh Y. Akt inhibits the orphan nuclear receptor Nur77 and T-cell apoptosis. *The Journal of biological chemistry.* 2001;276(35):32799-32805.

132. Pekarsky Y, Hallas C, Palamarchuk A, Koval A, Bullrich F, Hirata Y, Bichi R, Letofsky J, Croce CM. Akt phosphorylates and regulates the orphan nuclear receptor Nur77. *Proceedings of the National Academy of Sciences of the United States of America.* 2001;98(7):3690-3694.

133. Liu B, Wu JF, Zhan YY, Chen HZ, Zhang XY, Wu Q. Regulation of the orphan receptor TR3 nuclear functions by c-Jun N terminal kinase phosphorylation. *Endocrinology.* 2007;148(1):34-44.

134. Lin B, Kolluri SK, Lin F, Liu W, Han YH, Cao X, Dawson MI, Reed JC, Zhang XK. Conversion of Bcl-2 from protector to killer by interaction with nuclear orphan receptor Nur77/TR3. *Cell.* 2004;116(4):527-540.

135. Hoshikawa Y, Kanki K, Ashla AA, Arakaki Y, Azumi J, Yasui T, Tezuka Y, Matsumi Y, Tsuchiya H, Kurimasa A, Hisatome I, Hirano T, Fujimoto J, Kagechika H, Shomori K, Ito H, Shiota G. c-Jun N-terminal kinase activation by oxidative stress suppresses retinoid signaling through proteasomal degradation of retinoic acid receptor alpha protein in hepatic cells. *Cancer science.* 2011;102(5):934-941.

136. Bruck N, Bastien J, Bour G, Tarrade A, Plassat JL, Bauer A, Adam-Stitah S, Rochette-Egly C. Phosphorylation of the retinoid x receptor at the omega loop, modulates the expression of retinoic-acid-target genes with a promoter context specificity. *Cellular signalling.* 2005;17(10):1229-1239.

137. Huynh HT, Robitaille G, Turner JD. Establishment of bovine mammary epithelial cells (MAC-T): an in vitro model for bovine lactation. *Experimental cell research.* 1991;197(2):191-199.

138. Fleming JM, Leibowitz BJ, Kerr DE, Cohick WS. IGF-I differentially regulates IGF-binding protein expression in primary mammary fibroblasts and epithelial cells. *The Journal of endocrinology.* 2005;186(1):165-178.

139. Dong F, Wu HB, Hong J, Rechler MM. Insulin-like growth factor binding protein-2 mediates the inhibition of DNA synthesis by transforming growth factor-beta in mink lung epithelial cells. *Journal of cellular physiology.* 2002;190(1):63-73.

140. Kim HS, Lee WJ, Lee SW, Chae HW, Kim DH, Oh Y. Insulin-like growth factor binding protein-3 induces G1 cell cycle arrest with inhibition of cyclin-dependent kinase 2 and 4 in MCF-7 human breast cancer cells. *Hormone and metabolic research = Hormon- und Stoffwechselforschung = Hormones et metabolisme.* 2010;42(3):165-172.

141. Boutinaud M, Guinard-Flamenta J, Jammes H. The number and activity of mammary epithelial cells, determining factors for milk production. *Reprod Nutr Dev.* 2004;44(5):499-508.

142. Capuco AV, Ellis SE, Hale SA, Long E, Erdman RA, Zhao X, Paape MJ. Lactation persistency: insights from mammary cell proliferation studies. *Journal of animal science.* 2003;81 Suppl 3:18-31.

143. Annen EL, Fitzgerald AC, Gentry PC, McGuire MA, Capuco AV, Baumgard LH, Collier RJ. Effect of continuous milking and bovine somatotropin supplementation on mammary epithelial cell turnover. *J Dairy Sci.* 2007;90:165-183.

144. Hale SA, Capuco AV, Erdman RA. Milk yield and mammary growth effects due to increased milking frequency during early lactation. *Journal of dairy science.* 2003;86(6):2061-2071.

145. Fitzgerald AC, Annen-Dawson EL, Baumgard LH, Collier RJ. Evaluation of continuous lactation and increased milking frequency on milk production and mammary cell turnover in primiparous Holstein cows. *J Dairy Sci.* 2007;90(12):5483-5489.

146. Dahl GE. Effects of short day photoperiod on prolactin signaling in dry cows: a common mechanism among tissues and environments? *Journal of animal science.* 2008;86(13 Suppl):10-14.

147. Jogie-Brahim S, Feldman D, Oh Y. Unraveling insulin-like growth factor binding protein-3 actions in human disease. *Endocr Rev.* 2009;30(5):417-437.

148. Kooijman R. Regulation of apoptosis by insulin-like growth factor (IGF)-I. *Cytokine Growth Factor Rev.* 2006;17(4):305-323.

149. Cohen P. Insulin-like growth factor binding protein-3: insulin-like growth factor independence comes of age. *Endocrinology.* 2006;147(5):2109-2111.

150. Bhattacharyya N, Pechhold K, Shahjee H, Zappala G, Elbi C, Raaka B, Wiench M, Hong J, Rechler MM. Nonsecreted insulin-like growth factor binding protein-3 (IGFBP-3) can induce apoptosis in human prostate cancer cells by IGF-independent mechanisms without being concentrated in the nucleus. *J Biol Chem.* 2006;281:24588-24601.

151. Liu B, Lee HY, Weinzimer SA, Powell DR, Clifford JL, Kurie JM, Cohen P. Direct functional interactions between insulin-like growth factor-binding protein-3 and retinoid X receptor-alpha regulate transcriptional signaling and apoptosis. *J Biol Chem.* 2000;275(43):33607-33613.

152. Cohick WS, Turner JD. Regulation of insulin-like growth factor binding protein synthesis by a bovine mammary epithelial cell line. *J Endocrinol.* 1998;157:327-336.

153. Fleming J, Leibowitz BJ, Kerr DE, Cohick WS. IGF-I differentially regulates IGF binding protein expression in primary mammary fibroblasts and epithelial cells. *J Endocrinol.* 2005;186:165-178.

154. Leibowitz B, Cohick W. Endogenous IGFBP-3 is required for both growth factor-stimulated cell proliferation and cytokine-induced apoptosis in mammary epithelial cells. *J Cell Physiol.* 2009;220:182-188.

155. Hori T, Kondo T, Tabuchi Y, Takasaki I, Zhao QL, Kanamori M, Yasuda T, Kimura T. Molecular mechanism of apoptosis and gene expressions in human lymphoma U937 cells treated with anisomycin. *Chem Biol Interact.* 2008;172(2):125-140.

156. Huynh HT, Robitaille G, Turner JD. Establishment of bovine mammary epithelial cells (MAC-T): an in vitro model for bovine lactation. *Exp Cell Res.* 1991;197:191-199.

157. Grill CJ, Cohick WS. Insulin-like growth factor binding protein-3 mediates IGF-I action in a bovine mammary epithelial cell line independent of an IGF interaction. *J Cell Physiol.* 2000;183:273-283.

158. Zi X, Zhang J, Agarwal R, Pollak M. Silibinin up-regulates insulin-like growth factor-binding protein 3 expression and inhibits proliferation of androgen-independent prostate cancer cells. *Cancer Res.* 2000;60(20):5617-5620.

159. Rajah R, Valentinis B, Cohen P. Insulin-like growth factor (IGF)-binding protein-3 induces apoptosis and mediates the effects of transforming growth factor-B1 on programmed cell death through a p53-and IGF-independent mechanism. *J Biol Chem.* 1997;272:12181-12188.

160. Shim ML, Levitt Katz LE, Davis J, Dotzler WC, Cohen P, Ferry RJ, Jr. Insulin-like growth factor binding protein-3 is a novel mediator of apoptosis in insulin-secreting cells. *Growth Horm IGF Res.* 2004;14(3):216-225.

161. Jaques G, Noll K, Wegmann B, Witten S, Kogan E, Radulescu RT, Havemann K. Nuclear localization of insulin-like growth factor binding protein-3 in a lung cancer cell line. *Endocrinology.* 1997;138(4):1767-1770.

162. Wraight CJ, Liepe IJ, White PJ, Hibbs AR, Werther GA. Intranuclear localization of insulin-like growth factor binding protein-3 (IGFBP-3) during cell division in human keratinocytes. *J Invest Dermatol.* 1998;111(2):239-242.

163. Curtin JF, Cotter TG. Anisomycin activates JNK and sensitises DU 145 prostate carcinoma cells to Fas mediated apoptosis. *Br J Cancer.* 2002;87(10):1188-1194.

164. Dhanasekaran DN, Reddy EP. JNK signaling in apoptosis. *Oncogene.* 2008;27(48):6245-6251.

165. Baker NL, Carlo Russo V, Bernard O, D'Ercole AJ, Werther GA. Interactions between bcl-2 and the IGF system control apoptosis in the developing mouse brain. *Brain Res Dev Brain Res.* 1999;118:109-118.

166. Linseman DA, Phelps RA, Bouchard RJ, Le SS, Laessig TA, McClure ML, Heidenreich KA. Insulin-like growth factor-I blocks Bcl-2 interacting mediator of cell death (Bim) induction and intrinsic death signaling in cerebellar granule neurons. *J Neurosci.* 2002;22(21):9287-9297.

167. Ness JK, Scaduto RC, Jr., Wood TL. IGF-I prevents glutamate-mediated bax translocation and cytochrome C release in O4+ oligodendrocyte progenitors. *Glia.* 2004;46(2):183-194.

168. Hoeflich A, Reisinger R, Lahm H, Kiess W, Blum WF, Kolb HJ, Weber MM, Wolf E. Insulin-like growth factor-binding protein 2 in tumorigenesis: protector or promoter? *Cancer research.* 2001;61(24):8601-8610.

169. Migita T, Narita T, Asaka R, Miyagi E, Nagano H, Nomura K, Matsuura M, Satoh Y, Okumura S, Nakagawa K, Seimiya H, Ishikawa Y. Role of insulin-like growth factor binding protein 2 in lung adenocarcinoma: IGF-independent antiapoptotic effect via caspase-3. *Am J Pathol.* 2010;176(4):1756-1766.

170. Micutkova L, Hermann M, Offterdinger M, Hess MW, Matscheski A, Pircher H, Muck C, Ebner HL, Laich A, Ferrando-May E, Zwerschke W, Huber LA, Jansen-Durr P. Analysis of the cellular uptake and nuclear delivery of insulin-like growth factor binding protein-3 in human osteosarcoma cells. *Int J Cancer.* 2011;130(7):1544-1557.

171. Schedlich LJ, Graham LD, O'Han MK, Muthukaruppan A, Yan X, Firth SM, Baxter RC. Molecular basis of the interaction between IGFBP-3 and retinoid X receptor: role in modulation of RAR-signaling. *Archives of biochemistry and biophysics.* 2007;465(2):359-369.

172. Yu J, Zhang L. PUMA, a potent killer with or without p53. *Oncogene.* 2008;27 Suppl 1:S71-83.

173. Chung KC, Kim SM, Rhang S, Lau LF, Gomes I, Ahn YS. Expression of immediate early gene pip92 during anisomycin-induced cell death is mediated by the JNK- and p38-dependent activation of Elk1. *European journal of biochemistry / FEBS.* 2000;267(15):4676-4684.

174. Kim BJ, Ryu SW, Song BJ. JNK- and p38 kinase-mediated phosphorylation of Bax leads to its activation and mitochondrial translocation and to apoptosis of human hepatoma HepG2 cells. *The Journal of biological chemistry.* 2006;281(30):21256-21265.

175. Tsuruta F, Sunayama J, Mori Y, Hattori S, Shimizu S, Tsujimoto Y, Yoshioka K, Masuyama N, Gotoh Y. JNK promotes Bax translocation to mitochondria through phosphorylation of 14-3-3 proteins. *The EMBO journal.* 2004;23(8):1889-1899.

176. Ganju N, Eastman A. Bcl-X(L) and calyculin A prevent translocation of Bax to mitochondria during apoptosis. *Biochemical and biophysical research communications.* 2002;291(5):1258-1264.

177. Katagiri Y, Takeda K, Yu ZX, Ferrans VJ, Ozato K, Guroff G. Modulation of retinoid signalling through NGF-induced nuclear export of NGFI-B. *Nature cell biology.* 2000;2(7):435-440.

178. Li H, Kolluri SK, Gu J, Dawson MI, Cao X, Hobbs PD, Lin B, Chen G, Lu J, Lin F, Xie Z, Fontana JA, Reed JC, Zhang X. Cytochrome c release and apoptosis induced by mitochondrial targeting of nuclear orphan receptor TR3. *Science.* 2000;289(5482):1159-1164.

179. Liu PY, Sheu JJ, Lin PC, Lin CT, Liu YJ, Ho LI, Chang LF, Wu WC, Chen SR, Chen J, Harn YC, Lin SZ, Tsai CH, Chiou TW, Harn HJ. Expression of Nur77 induced by an n-butylidenephthalide derivative promotes apoptosis and inhibits cell growth in oral squamous cell carcinoma. *Investigational new drugs.* 2012;30(1):79-89.

180. Maruoka H, Sasaya H, Shimamura Y, Nakatani Y, Shimoke K, Ikeuchi T. Dibutyryl-cAMP up-regulates nur77 expression via histone modification during neurite outgrowth in PC12 cells. *Journal of biochemistry.* 2010;148(1):93-101.

181. Lee YW, Stachowiak EK, Birkaya B, Terranova C, Capacchietti M, Claus P, Aletta JM, Stachowiak MK. NGF-induced cell differentiation and gene activation is mediated by integrative nuclear FGFR1 signaling (INFS). *PloS one.* 2013;8(7):e68931.

182. Lin XF, Zhao BX, Chen HZ, Ye XF, Yang CY, Zhou HY, Zhang MQ, Lin SC, Wu Q. RXRalpha acts as a carrier for TR3 nuclear export in a 9-cis retinoic acid-dependent manner in gastric cancer cells. *Journal of cell science.* 2004;117(Pt 23):5609-5621.

183. Cheng Z, Volkers M, Din S, Avitabile D, Khan M, Gude N, Mohsin S, Bo T, Truffa S, Alvarez R, Mason M, Fischer KM, Konstandin MH, Zhang XK, Heller Brown J, Sussman MA. Mitochondrial translocation of Nur77 mediates cardiomyocyte apoptosis. *European heart journal.* 2011;32(17):2179-2188.

184. He K, Zhou HR, Pestka JJ. Mechanisms for ribotoxin-induced ribosomal RNA cleavage. *Toxicology and applied pharmacology.* 2012;265(1):10-18.

185. Schedlich LJ, O'Han MK, Leong GM, Baxter RC. Insulin-like growth factor binding protein-3 prevents retinoid receptor heterodimerization: implications for retinoic acid-sensitivity

in human breast cancer cells. *Biochemical and biophysical research communications.* 2004;314(1):83-88.

186. Hoelz A, Debler EW, Blobel G. The structure of the nuclear pore complex. *Annual review of biochemistry.* 2011;80:613-643.

187. Natsuizaka M, Naganuma S, Kagawa S, Ohashi S, Ahmadi A, Subramanian H, Chang S, Nakagawa KJ, Ji X, Liebhaber SA, Klein-Szanto AJ, Nakagawa H. Hypoxia induces IGFBP3 in esophageal squamous cancer cells through HIF-1alpha-mediated mRNA transcription and continuous protein synthesis. *FASEB journal : official publication of the Federation of American Societies for Experimental Biology.* 2012;26(6):2620-2630.

188. Dutta D, Williamson CD, Cole NB, Donaldson JG. Pitstop 2 is a potent inhibitor of clathrin-independent endocytosis. *PloS one.* 2012;7(9):e45799.

189. Colitti M. BCL-2 family of proteins and mammary cellular fate. *Anatomia, histologia, embryologia.* 2012;41(4):237-247.

190. Butt AJ, Martin JL, Dickson KA, McDougall F, Firth SM, Baxter RC. Insulin-like growth factor binding protein-3 expression is associated with growth stimulation of T47D human breast cancer cells: the role of altered epidermal growth factor signaling. *The Journal of clinical endocrinology and metabolism.* 2004;89(4):1950-1956.

191. Vasylyeva TL, Chen X, Ferry RJ, Jr. Insulin-like growth factor binding protein-3 mediates cytokine-induced mesangial cell apoptosis. *Growth hormone & IGF research : official journal of the Growth Hormone Research Society and the International IGF Research Society.* 2005;15(3):207-214.

192. Hartley JL. Cloning technologies for protein expression and purification. *Current opinion in biotechnology.* 2006;17(4):359-366.

193. Pircher H, Matscheski A, Laich A, Hermann M, Moser B, Viertler HP, Micutkova L, Lindner H, Sarg B, Zwerschke W, Jansen-Durr P. A new method for the purification of bioactive insulin-like growth factor-binding protein-3. *Protein expression and purification.* 2010;71(2):160-167.

194. Pampusch MS, Kamanga-Sollo E, White ME, Hathaway MR, Dayton WR. Effect of recombinant porcine IGF-binding protein-3 on proliferation of embryonic porcine myogenic cell cultures in the presence and absence of IGF-I. *The Journal of endocrinology.* 2003;176(2):227-235.

195. Firth SM, Ganeshprasad U, Poronnik P, Cook DI, Baxter RC. Adenoviral-mediated expression of human insulin-like growth factor-binding protein-3. *Protein expression and purification.* 1999;16(1):202-211.

196. Waugh DS. An overview of enzymatic reagents for the removal of affinity tags. *Protein expression and purification.* 2011;80(2):283-293.

197. Gagnon P. Technology trends in antibody purification. *Journal of chromatography A.* 2012;1221:57-70.

198. Plath-Gabler A, Gabler C, Sinowatz F, Berisha B, Schams D. The expression of the IGF family and GH receptor in the bovine mammary gland. *The Journal of endocrinology.* 2001;168(1):39-48.

199. Gibson CA, Staley MD, Baumrucker CR. Identification of IGF binding proteins in bovine milk and the demonstration of IGFBP-3 synthesis and release by bovine mammary epithelial cells. *Journal of animal science.* 1999;77(6):1547-1557.

200. Piantoni P, Wang P, Drackley JK, Hurley WL, Loor JJ. Expression of metabolic, tissue remodeling, oxidative stress, and inflammatory pathways in mammary tissue during involution in lactating dairy cows. *Bioinformatics and biology insights.* 2010;4:85-97.

201. Yamada PM, Lee KW. Perspectives in mammalian IGFBP-3 biology: local vs. systemic action. *American journal of physiology Cell physiology.* 2009;296(5):C954-976.

202. Baumrucker CR, Erondu NE. Insulin-like growth factor (IGF) system in the bovine mammary gland and milk. *Journal of mammary gland biology and neoplasia.* 2000;5(1):53-64.